RESPOSTAS MORFOFISIOLÓGICAS E BIOQUÍMICAS DE ESPÉCIES DO GÊNERO *Psidium* À INFECÇÃO POR *Meloidogyne enterolobii*

SARA NÁLLIA DE OLIVEIRA COSTA

UNIVERSIDADE ESTADUAL DO NORTE FLUMINENSE DARCY RIBEIRO

CAMPOS DOS GOYTACAZES
OUTUBRO – 2025

RESPOSTAS MORFOFISIOLÓGICAS E BIOQUÍMICAS DE ESPÉCIES DO GÊNERO *Psidium* À INFECÇÃO POR *Meloidogyne enterolobii*

SARA NÁLLIA DE OLIVEIRA COSTA

Tese apresentada ao Centro de Biociências e Biotecnologia da Universidade Estadual do Norte Fluminense Darcy Ribeiro, como parte das exigências para obtenção do título de Doutora em Biociências e Biotecnologia.

Orientadora: Profa. Dra. Kátia Valevski Sales Fernandes

Coorientadora: Dra. Juliana Martins Ribeiro
(Empresa Brasileira de Pesquisa Agropecuária – Embrapa
Centro de Pesquisa Agropecuária do Trópico Semiárido –
Embrapa Semiárido)

UNIVERSIDADE ESTADUAL DO NORTE FLUMINENSE DARCY RIBEIRO

CAMPOS DOS GOYTACAZES
OUTUBRO – 2025

FICHA CATALOGRÁFICA
UENF - Bibliotecas
Elaborada com os dados fornecidos pela autora.

C837 Costa, Sara Nállia de Oliveira.

Respostas morfofisiológicas e bioquímicas de espécies do gênero *Psidium* à infecção por *Meloidogyne enterolobii* / Sara Nállia de Oliveira Costa. - Campos dos Goytacazes, RJ, 2025.

160 f. : il.
Inclui bibliografia.

Tese (Doutorado em Biociências e Biotecnologia) - Universidade Estadual do Norte Fluminense Darcy Ribeiro, Centro de Biociências e Biotecnologia, 2025.
Orientadora: Katia Valevski Sales Fernandes.
Coorientadora: Juliana Martins Ribeiro.

1. Meloidogyne enterolobii. 2. Goiabeira. 3. Resistência genética. 4. Abordagens ômicas. 5. Manejo integrado. I. Universidade Estadual do Norte Fluminense Darcy Ribeiro. II. Título.

CDD - 570

RESPOSTAS MORFOFISIOLÓGICAS E BIOQUÍMICAS DE ESPÉCIES DO GÊNERO *Psidium* À INFECÇÃO POR *Meloidogyne enterolobii*

SARA NÁLLIA DE OLIVEIRA COSTA

Tese apresentada ao Centro de Biociências e Biotecnologia da Universidade Estadual do Norte Fluminense Darcy Ribeiro, como parte das exigências para obtenção do título de Doutora em Biociências e Biotecnologia.

Aprovada em 27 de agosto de 2025.

Comissão Examinadora:

Profa. Dra. Ana Eliza Zeraik (Membro interno - UENF)

Prof. Dr. Felipe Astolpho de Almeida (Membro interno - UENF)

Prof. Dr. Daniel Basílio Zandonadi (Membro externo - UFRJ)

Profa. Dra. Kátia Valevski Sales Fernandes – Orientadora (UENF)

Dra. Juliana Martins Ribeiro – Coorientadora (Embrapa Semiárido)

Dedicatória

À minha filha Maria,
meu amor mais bonito.

Agradecimentos

À força maior que rege o universo, por permitir meus erros, aprendizados e crescimento. Pela condução silenciosa, mas constante, por meio de lições de compreensão, tolerância e por manter acesa em mim a chama da fé, mesmo nos momentos mais desafiadores.

Ao Programa de Pós-Graduação em Biociências e Biotecnologia da Universidade Estadual do Norte Fluminense Darcy Ribeiro, por oferecer um ambiente fértil, instigante e acolhedor para o desenvolvimento científico e pessoal.

À Professora Kátia, minha orientadora, por sua condução segura, marcada por competência, profissionalismo e dedicação inestimável.

À Pesquisadora Juliana, minha coorientadora, por sua presença afetuosa, empática e acolhedora, que me inspirou com sua sororidade e sensibilidade científica.

Aos pesquisadores que colaboraram nos trabalhos desenvolvidos ao longo desta jornada, pelo comprometimento e pelas valiosas trocas de conhecimento.

Aos membros da banca examinadora, por gentilmente aceitarem o convite e por contribuírem com suas críticas construtivas que enriqueceram este trabalho.

À minha família, pelo amor incondicional, paciência e apoio contínuo, mesmo nos momentos em que estive ausente em presença e palavras.

Aos colegas de laboratório, pela parceria, pelas conversas que aliviaram o peso da rotina e pelo compartilhamento de experiências e aprendizados.

Aos meus amigos por caminharem ao meu lado em todos os momentos. Vocês foram meu alicerce, minha alegria e meu refúgio nessa jornada.

O presente trabalho foi realizado com apoio da Coordenação de Aperfeiçoamento de Pessoal de Nível Superior – Brasil (CAPES) – Código de Financiamento 001.

Epígrafe

"(...) estrada de fazer o sonho acontecer."
(Milton Nascimento)

RESUMO

A goiabeira (*Psidium guajava* L.) possui grande importância econômica e nutricional no Brasil, mas seu cultivo tem sido prejudicado pelo nematoide-das-galhas *Meloidogyne enterolobii*, um patógeno altamente agressivo. Esta tese investigou os mecanismos de defesa de diferentes espécies do gênero *Psidium* frente à infecção por esse nematoide, utilizando análises histológicas, proteômicas e transcriptômicas. Foram comparadas *P. guajava* (suscetível), *P. guineense* e *P. friedrichsthalianum* (resistentes), visando identificar alterações morfofisiológicas e bioquímicas associadas à resistência. As abordagens integradas revelaram modificações específicas nas raízes infectadas, além da expressão diferencial de proteínas ligadas a vias metabólicas de defesa. Destaca-se o papel do estresse oxidativo como resposta inicial à infecção, com a rápida produção de espécies reativas de oxigênio (EROs), que atuam como sinalizadores para mecanismos como reforço da parede celular, morte celular programada e indução de compostos secundários. Esses achados contribuem significativamente para a compreensão dos mecanismos de resistência em *Psidium*, oferecendo subsídios para o desenvolvimento de cultivares resistentes e para o uso de estratégias biotecnológicas voltadas a uma fruticultura mais sustentável.

Palavras-chave: *Meloidogyne enterolobii*; Goiabeira; Resistência genética; Abordagens ômicas; Manejo integrado.

ABSTRACT

The guava tree (*Psidium guajava* L.) holds significant economic and nutritional importance in Brazil, but its cultivation has been hindered by the root-knot nematode *Meloidogyne enterolobii*, a highly aggressive pathogen. This thesis investigated the defense mechanisms of different *Psidium* species against infection by this nematode, using histological, proteomic, and transcriptomic analyses. *P. guajava* (susceptible), *P. guineense*, and *P. friedrichsthalianum* (resistant) were compared to identify morphophysiological and biochemical changes associated with resistance. The integrated approaches revealed specific modifications in infected roots, as well as differential expression of proteins linked to defense-related metabolic pathways. Oxidative stress emerged as a key early response to infection, with the rapid production of reactive oxygen species (ROS), which act as signals for mechanisms such as cell wall reinforcement, programmed cell death, and the induction of secondary metabolites. These findings significantly advance the understanding of resistance mechanisms in *Psidium*, providing valuable insights for the development of resistant cultivars and the application of biotechnological strategies aimed at more sustainable fruit production.

Keywords: *Meloidogyne enterolobii*; Guava; Genetic resistance; Omics approaches; Integrated management.

LISTA DE FIGURAS

Capítulo 1 - Artigo "Tackling the plant parasitic nematode *Meloidogyne enterolobii*: Challenges and strategies for control in relevant crops"

Capítulo 2 - Artigo "*Psidium* defenses against *Meloidogyne enterolobii*: proteomic and microscopic analysis of this plant-predator association"

Capítulo 3 - Artigo "Transcriptomic analysis reveals systemic leaf responses underlying resistance *of P. friedrichsthalianium* to *Meloidogyne enterolobii*"

LISTA DE TABELAS

LISTA DE ABREVIATURAS E SIGLAS

ANPs	Fitoquímicos Antinematoides (Anti-Nematode Phytochemicals)
AMF	Fungos Micorrízicos Arbusculares (Arbuscular Mycorrhizal Fungi)
BRS	Brasil (Registro de Cultivares)
CNs	Nematoides de Cisto (Cyst Nematodes)
CRISPR/Cas9	Clustered Regularly Interspaced Short Palindromic Repeats / CRISPR-associated protein 9
DAI	Days After Inoculation
ddPCR	Droplet Digital PCR
ET	Etileno (Ethylene)
ETS	Suscetibilidade Induzida por Efetores (Effector-Triggered Susceptibility)
GC	Células Gigantes (Giant Cells)
GAs	Glicoalcaloides (Glycoalkaloids)
HR	Resposta Hipersensível (Hypersensitive Response)
INM	Manejo Integrado de Nematoides (Integrated Nematode Management)
ITS-PCR-RFLP	Internal Transcribed Spacer Polymerase Chain Reaction – Restriction Fragment Length Polymorphism
JA	Ácido Jasmônico (Jasmonic Acid)
LC-MS	Cromatografia Líquida acoplada à Espectrometria de Massas (Liquid Chromatography–Mass Spectrometry)
LAMP	Loop-mediated Isothermal Amplification
MAS	Seleção Assistida por Marcadores (Marker-Assisted Selection)
Mi	Gene de resistência a nematoides em tomate (*Meloidogyne incognita*)
NAMP	Padrão Molecular Associado ao Nematoide (Nematode-Associated Molecular Pattern)

PAMP	Padrão Molecular Associado a Patógenos (Pathogen-Associated Molecular Pattern)
PCR	Reação em Cadeia da Polimerase (Polymerase Chain Reaction)
PR Proteins	Proteínas Relacionadas à Patogênese (Pathogenesis-Related Proteins)
PTI	Imunidade Induzida por Padrões (Pattern-Triggered Immunity)
qPCR	Quantitative PCR
RKN	Nematoide-das-Galhas (Root-Knot Nematode)
RNA-Seq	Sequenciamento de RNA
ROS	Espécies Reativas de Oxigênio (Reactive Oxygen Species)
SAR	Resistência Sistêmica Adquirida (Systemic Acquired Resistance)
SCAR	Sequence Characterized Amplified Region
SNP	Polimorfismo de Nucleotídeo Único (Single Nucleotide Polymorphism)

SUMÁRIO

1. INTRODUÇÃO

A goiabeira (*Psidium guajava* L.), espécie nativa do continente americano, possui ampla distribuição que se estende do México ao Peru e Brasil, sendo cultivada extensivamente em regiões tropicais e subtropicais. Trata-se de uma frutífera de significativa importância econômica e nutricional, cujo fruto é rico em vitaminas A, B e C, (USMAN *et al.*, 2022), sendo consumido tanto na forma *in natura* quanto como produto industrializado.

De acordo com a Organização das Nações Unidas para a Alimentação e a Agricultura (FAO), a produção mundial de goiaba foi estimada em 2,3 milhões de toneladas em 2023 (FAO, 2023). No Brasil, segundo os dados da plataforma SIDRA/IBGE, a produção alcançou 582.832 toneladas em 2023, sendo a maior parte proveniente das regiões Nordeste (285.234 t) e Sudeste (226.608 t). O valor bruto dessa produção totalizou R$ 1.306.013 mil, destacando-se o Nordeste com R$ 619.949 mil e o Sudeste com R$ 434.917 mil (IBGE, 2023).

As folhas *de P. guajava* apresentam elevada concentração de compostos bioativos, como flavonoides, terpenoides, taninos, alcaloides e polifenóis, responsáveis por propriedades antioxidantes, anti-inflamatórias e outras atividades farmacológicas relevantes, como ação anticancerígena, antibacteriana, analgésica e anti-hiperglicêmica (HUYNH *et al.*, 2025; PARK *et al.*, 2024). Estudos indicam que as folhas possuem maior potencial antioxidante que os frutos, atribuído à presença de metabólitos secundários como antocianinas, cumarinas, glicosídeos e vitamina C, o que tem despertado crescente interesse científico na caracterização química, eficácia terapêutica e segurança desses compostos (LIU; JULLIAN; CHASSAGNE, 2024).

No entanto, a cultura da goiaba enfrenta sérios desafios fitossanitários. Entre eles, destaca-se a infecção por fitonematoides do gênero *Meloidogyne*, responsáveis por expressivas perdas de produtividade. A espécie *Meloidogyne enterolobii*, em particular, é considerada uma das mais agressivas, causando a doença conhecida como “doença das galhas” (KHAN *et al.*, 2022). Esses nematoides invadem o sistema radicular, induzindo a formação de galhas hipertrofiadas que comprometem a absorção de água e nutrientes, levando a sintomas como clorose, murcha, atraso no desenvolvimento e declínio da planta (SIKANDAR *et al.*, 2023).

A resposta da goiabeira à infecção por *M. enterolobii* pode variar entre

resistência e suscetibilidade, sendo esse um aspecto crucial para o manejo integrado da doença. Plantas resistentes ativam mecanismos de defesa que dificultam a penetração e o desenvolvimento do nematoide, ao passo que as suscetíveis estão sujeitas a maior colonização e danos (PHILBRICK *et al.*, 2020).

O manejo integrado de nematoides busca reduzir populações e danos econômicos por meio de práticas complementares. O controle cultural envolve rotação de culturas, uso de plantas antagonistas e práticas que aumentam a supressividade do solo. O químico, embora eficaz a curto prazo, deve ser usado com cautela devido a custos e impactos ambientais. O biológico utiliza microrganismos que atacam nematoides ou estimulam resistência nas plantas. Já o genético emprega cultivares resistentes ou tolerantes, obtidas por melhoramento ou biotecnologia. A integração dessas estratégias, ajustada às condições locais, é fundamental para uma produção agrícola sustentável (COSTA *et. al*, 2025).

Vale destacar que, segundo dados da Embrapa (2021), o uso global de agrotóxicos atinge cerca de 2,5 milhões de toneladas por ano. No Brasil, o consumo anual de produtos comerciais ultrapassa 300 mil toneladas, o que corresponde a aproximadamente 130 mil toneladas de ingrediente ativo (i.a.). Esse crescimento representa um aumento de 700% no uso de agrotóxicos nas últimas quatro décadas, enquanto a expansão da área agrícola no mesmo período foi de apenas 78%.

Durante o ciclo de vida, as plantas são constantemente expostas a estresses bióticos e abióticos, exigindo respostas adaptativas complexas nos níveis transcriptômico, proteômico e metabolômico. Essa plasticidade celular depende da integração entre diferentes vias de sinalização e compartimentalização subcelular (SCHOLZ *et al.*, 2025). Entender as bases moleculares dessas respostas diferenciais é fundamental para o desenvolvimento de estratégias biotecnológicas e programas de melhoramento genético voltados à resistência. Nesse contexto, as abordagens multi-ômicas têm revolucionado o entendimento das interações planta-patógeno. No caso da goiabeira, essas ferramentas têm permitido a investigação detalhada dos mecanismos moleculares envolvidos na resposta à infecção por *M. enterolobii*.

A identidade celular vegetal, nesse contexto, passou a ser entendida como resultado da expressão gênica espaço-temporal, sendo o transcriptoma uma representação molecular do estado funcional da célula, refletindo sua fase de desenvolvimento ou resposta a estímulos (SEYFFERTH *et al.*, 2021). A transcriptômica, fortalecida pelos avanços da era pós-genômica, destaca-se como

uma ferramenta poderosa para estudar a expressão gênica, especialmente em espécies cujo genoma ainda não foi completamente elucidado (TYAGI *et al.*, 2020). Através de abordagens como microarranjos de DNA e RNA-Seq, é possível obter um panorama detalhado da regulação gênica em diferentes condições fisiológicas e ambientais (SHAW; TIAN; XU, 2020).

Complementando esses dados, a proteômica permite compreender os mecanismos moleculares que controlam os fenótipos vegetais. As proteínas atuam em praticamente todos os processos celulares, e o estudo de sua expressão, modificações pós-traducionais e interações é crucial. A espectrometria de massas tem sido amplamente empregada para a identificação e quantificação de milhares de proteínas, fornecendo informações sobre sua localização, função e participação em redes regulatórias (MERGNER; KUSTER, 2022). Essa abordagem é essencial para elucidar vias metabólicas, identificar biomarcadores e compreender as respostas das plantas a estresses diversos (YAN *et al.*, 2022).

A metabolômica, por sua vez, surge como uma ferramenta abrangente e sensível para análise da composição metabólica das plantas. Os metabólitos desempenham papéis fundamentais na adaptação ao estresse, atuando como osmólitos, antioxidantes ou sinalizadores. Metabólitos primários, como aminoácidos e açúcares, estão associados diretamente à fisiologia do estresse, enquanto metabólitos secundários, como fenóis, terpenoides e alcaloides, conferem resistência a patógenos e pragas, além de atenuar os efeitos de fatores abióticos (SALAM *et al.*, 2023). A metabolômica também oferece subsídios valiosos à fenotipagem e à engenharia metabólica, possibilitando o desenvolvimento de cultivares com maior tolerância a condições adversas (PATEL *et al.*, 2021).

Tais avanços têm potencial para elevar a produtividade agrícola de forma sustentável, contribuindo para a segurança alimentar diante do crescimento populacional global (KUMAR *et al.*, 2021). A integração dos dados oriundos das abordagens ômicas, por meio da biologia de sistemas e modelagem computacional, tem permitido a construção de redes regulatórias complexas que descrevem, de forma integrada, os mecanismos de defesa vegetal. Esse conhecimento é fundamental para o desenvolvimento de estratégias de melhoramento genético, seja por métodos convencionais ou por tecnologias como a edição gênica via CRISPR/Cas9.

O CRISPR/Cas9 permite modificações genéticas precisas por meio da formação de um complexo entre a nuclease Cas9 e um RNA guia simples (sgRNA),

que direciona o corte em locais específicos do genoma. Essa abordagem é mais rápida e específica do que os métodos convencionais de melhoramento, tornando-se uma ferramenta poderosa para a melhoria de culturas (SON; PARK, 2022). Sua ampla acessibilidade também ampliou as aplicações de pesquisa na agricultura e na biotecnologia. As tecnologias de edição genômica mostram grande potencial para o tratamento de doenças genéticas e não genéticas (GUO et al., 2023).

O presente documento de tese está estruturado na forma de capítulos que refletem a estratégia de divulgação dos estudos teóricos e práticos realizados ao longo do meu período de doutorado, através de artigos de revisão e de pesquisa, alguns já publicados, outros em processo de publicação ou preparação.

O **Capítulo 1** aborda os principais desafios e estratégias de manejo do nematoide formador de galhas *Meloidogyne enterolobii*, um patógeno altamente agressivo e amplamente distribuído, que causa prejuízos significativos a diversas culturas agrícolas de relevância econômica. São discutidos aspectos relacionados ao ciclo de vida do patógeno, seus mecanismos de infecção, critérios de identificação taxonômica e as respostas de defesa desencadeadas pelas plantas hospedeiras. O capítulo também explora diferentes métodos de controle, químico, cultural, biológico e genético, além de destacar estratégias inovadoras baseadas em biotecnologia, como o uso de bioinsumos, técnicas de edição gênica e a seleção assistida por marcadores moleculares. Corresponde ao artigo “Tackling the plant parasitic nematode *Meloidogyne enterolobii*: challenges and strategies for control in relevant crops”, publicado em 2025 na revista Tropical Plant Pathology (Springer Nature - https://doi.org/10.1007/s40858-025-00734-z).

O **Capítulo 2** investiga os mecanismos de defesa ativados por duas espécies do gênero *Psidium*, *P. guajava* (susceptível) e *P. guineense* (resistente), frente à infecção pelo nematoide fitoparasita *M. enterolobii*. A pesquisa integra abordagens proteômicas do tipo *shotgun* com análises microscópicas e histoquímicas das raízes, visando elucidar as respostas celulares, bioquímicas e moleculares associadas aos fenótipos de resistência e suscetibilidade. Está sendo divulgado no artigo científico intitulado “*Psidium* defenses against *Meloidogyne enterolobii*: proteomic and microscopic analysis of this plant-predator association*”,* na revista Proteomics (Wiley Online Library).

O **Capítulo 3** apresenta uma análise comparativa entre *Psidium guajava* (espécie suscetível) e *Psidium friedrichsthalianum* (espécie resistente) à infecção por

M. enterolobii. A partir de uma abordagem transcriptômica, foram investigadas as respostas ao estresse biótico em ambas as espécies, identificando genes diferencialmente expressos, vias metabólicas envolvidas na resposta de defesa, potencialmente relacionadas à resistência ao patógeno. Sob o título "Transcriptomic analysis reveals systemic leaf responses underlying resistance *of P. friedrichsthalianium* to *Meloidogyne enterolobii*", o trabalho está em construção para submissão.

O **Capítulo 4** apresenta o protocolo para clonagem da proteína homóloga da catalase do tomate usando CRISPR, após investigação de sua relação com a susceptibilidade de *Psidium* ao nematoide *Meloidogyne enterolobii*. Desenvolvido sob supervisão do DSc. Shahid Siddique, na UC Davis, detalha a identificação de sequências, desenho de RNAs guias, extração, digestão, purificação e ligação de plasmídeos em *E. coli*, além da transformação bacteriana e confirmação por PCR. Também aborda a eletroporação em *Agrobacterium tumefaciens* para futura transformação vegetal, garantindo a construção molecular para o estudo da resistência ao nematoide.

Ao final do documento, anexamos também um trabalho desenvolvido durante o mestrado e publicado no doutorado, que abordou a resistência de espécies do gênero *Psidium* ao nematoide *Meloidogyne enterolobii*. Por meio de análises metabolômicas, o estudo identificou que *P. guineense* e *P. cattleianum*, espécies resistentes ou imunes, produzem metabólitos secundários como taninos, lignanas e terpenos, os quais podem atuar como repelentes ou antioxidantes durante a infecção.

2. OBJETIVOS

2.1 Objetivo Geral

Investigar, por meio de abordagens integradas e multidisciplinares, os mecanismos morfofisiológicos, bioquímicos e moleculares envolvidos na resistência e suscetibilidade de espécies do gênero *Psidium* ao nematoide *Meloidogyne enterolobii*, visando o desenvolvimento de estratégias biotecnológicas sustentáveis para o seu manejo, com ênfase nas análises transcriptômica e proteômica.

2.2 Objetivos específicos

- Realizar uma revisão exploratória sobre os aspectos biológicos e ecológicos do nematoide *Meloidogyne enterolobii*, avaliando seu ciclo de vida, mecanismos de infecção e fatores ambientais associados à sua patogenicidade, além de analisar e comparar estratégias de controle químico, cultural, biológico e genético, com ênfase nos avanços biotecnológicos e genômicos voltados ao desenvolvimento de cultivares resistentes e bioinsumos inovadores para o manejo sustentável do patógeno;
- Investigar as respostas morfológicas, histológicas e moleculares de *Psidium guajava* e *P. guineense* à infecção por *Meloidogyne enterolobii*, por meio da caracterização de alterações radiculares, análises proteômicas e comparação entre espécies suscetíveis e resistentes, visando a identificação de possíveis vias bioquímicas associadas à resistência e suscetibilidade ao nematoide e;
- Investigar a expressão gênica diferencial em folhas de espécies de *Psidium* inoculadas e não inoculadas com *Meloidogyne enterolobii* por meio de RNA-Seq, visando identificar genes e vias metabólicas relacionados à resposta de defesa, com ênfase no mapeamento dos processos biológicos associados à resistência.

3. CAPÍTULOS

3.1 Tackling the plant parasitic nematode *Meloidogyne enterolobii*: Challenges and strategies for control in relevant crops

Sara Nállia de Oliveira Costa[1]; Juliana Martins Ribeiro[2];
José Mauro da Cunha e Castro[2] e Kátia Valevski Sales Fernandes[1]

[1] Laboratório de Química e Função de Proteínas e Peptídeos, Universidade Estadual Do Norte Fluminense Darcy Ribeiro, Campos Dos Goytacazes, Rio de Janeiro, Brazil
[2] Empresa Brasileira de Pesquisa Agropecuária Semiárido, Petrolina, Pernambuco, Brazil

Published in Tropical Plant Pathology (2025) - doi.org/10.1007/s40858-025-00734-z

Abstract

Nematodes are vital in terrestrial ecosystems, shaping global food chains and soil nutrient cycling. Root-knot nematodes, however, such as *Meloidogyne enterolobii*, pose a great threat as plant parasites, afecting diverse plant species. This review explores essential environmental factors and tactics for handling *M. enterolobii*. The infuences of climate and soil composition on the pathogen life cycle and on its global distribution will be highlighted. We also discuss molecular and imaging techniques for nematode identifcation, and on diferent control strategies, such as chemical, cultural and biological. Features such as plant genetic resistance and the chemical basis of susceptibility and resistance to these phytopathogens are covered together with important advances on marker-assisted selection, genetic modifcation of plants with resistance genes and suppression of specifc nematode efector-coding genes. Despite the progress in this feld, the control of *M. enterolobii* remains a challenge, requiring additional research eforts. From a biotechnological perspective, the development of biological inputs for this nematode control holds promise. These bioinputs ofer advantages beyond their direct efects, promoting sustainability, reducing environmental impacts, reducing costs associated with intensive pesticide and fertilizer applications, and increasing productivity while maintaining food security.

Keywords: Agriculture; Control; Crops; Integrated management; Resistance; Root-knot nematodes.

3.1.1 Introduction

Nematodes comprise about 80% of subterranean life, occupying key roles in soil trophic levels through their infuence on nutrient cycles, microbial populations, and carbon dynamics (van den Hoogen et al. 2019). Among them, 4,100 species are plant-parasitic nematodes (PPNs), which cause plant diseases and serious economic losses (Poveda et al. 2020). PPNs are categorized as ectoparasites, semi-endoparasites, or endoparasites. Sedentary endoparasites, such as root-knot nematodes (RKNs) and cyst nematodes (CNs), are particularly destructive and pathogenic (Sato et al. 2019; Sikandar et al. 2023b).

RKNs are recognized as one of the most destructive pests of plants, and their economic impact is signifcant. *M. enterolobii* nematode is a RKN, belonging to the class Chromadorea, family Meloidogynidae, that holds a leading position amongst the top 10 phytonematodes (Jones et al. 2013; Przybylska and Stęplowska 2020). The genus *Meloidogyne* comprises approximately 100 species (Diyapoglu et al. 2022). *M. enterolobii* has become one of the most threatening pathogenic nematodes in both tropical and subtropical regions of the world, with estimated potential yield loss of 20%. Additionally, the recent identifcation of this species in Europe is thus a major concern (Koutsovoulos et al. 2020).

In 1983, *M. enterolobii* was frst identifed as *M. incognita* on the Chinese pacara tree (Enterolobium contortisiliquum) (Yang and Eisenback 1988). In 1988, it was recognized as a new species in Puerto Rico and named *M. mayaguensis* (Rammah and Hirschmann 1988) but both cases were reviewed and now it is recognized as *M. enterolobii*. It is widely referred to as the "guava root-knot nematode" due to the signifcant damages caused to guava trees (*Psidium guajava* L.) in South America (Brida et al. 2018).

In Brazil, the species *M. enterolobii* caused a 70% reduction in guava yield over seven years, resulting in an estimated direct loss of US$ 61 million (Sikandar et al. 2023b). Furthermore, it has been observed that varieties of important economic crops and rootstocks, such as tomato, banana, cherry, grape, fig, and melon, are excellent hosts for *M. enterolobii* (Liang et al. 2020; Sikandar et al. 2023b, a). It is important to

note that nematodes, including *M. enterolobii*, can exhibit different genetic lineages within a species, which can affect their virulence on different potential hosts (Schwarz et al. 2020).

Meloidogyne enterolobii predominantly thrives in tropical and subtropical regions but also occurs in temperate zones across Africa, the Americas, Asia, Europe, and Oceania (Sikandar et al. 2023b). Pan et al. (2023) highlight its varying distribution: high suitability in West, Central, and Southern Africa; widespread presence in South America, particularly Brazil, Argentina, and neighboring countries; notable regions in East, South, and Southeast Asia; and in North and Central America, including the southeastern U.S. and parts of Mexico. In Oceania, key areas are in northern and eastern Australia. Europe shows limited suitability, except for parts of France, Portugal, and Italy. Climate, especially temperature, significantly influences its distribution and lifecycle (Velloso et al. 2022). It is an obligate biotrophic endoparasite that feeds and develops entirely within the tissue of the host plant until reaching the adult stage of life (Philbrick et al. 2020). Root-knot nematodes (RKNs) are already notorious for their detrimental effects on plants. *M. enterolobii*, especially, poses an even more serious global threat due to its broad host range and the ability to infest tomato genotypes bearing Mi resistance genes. These genes are effective against some of the 100 known *Meloidogyne* species, such as *M. incognita*, *M. arenaria*, *M. javanica*, *M. luci* and *M. ethiopica*, but not against *M. enterolobii* (Philbrick et al. 2020; Santos et al. 2020).

Recent studies have focused on the discovery of new sources of genetic resistance against root-knot plant diseases caused by *M. enterolobii* nematodes. Overcoming the challenges posed by nematode reproduction in crops with established resistance genes is crucial. The combination of natural resistance strategies and genetic engineering holds promise for the effective management of nematode infections in agriculture (Sikandar et al. 2023b).

This work explores these challenges, as well as recent Integrated Nematode Management (INM) strategies to control *M. enterolobii* in relevant crops. We covered chemical, cultural, and biological control strategies, as well as genetic resistance, along with recommendations for future research to combat this agricultural pathogen.

3.1.2 Life cycle, infection mechanism and taxonomic complexity of *Meloidogyne enterolobii*

Meloidogyne spp. nematodes, stemming from a theoretical amphimictic ancestor, employ diverse reproductive strategies including sexual reproduction (amphimixis), asexual reproduction with genetic recombination (facultative meiotic parthenogenesis), and asexual reproduction without genetic recombination (apomixis) (CastagnoneSereno 2006; Bellé et al. 2019). *M. enterolobii* reproduces exclusively through obligatory mitotic parthenogenesis (apomixis), without male participation. This suggests that genetic variability might be linked to epigenetic modifcations, prompting inquiries about genome plasticity, which in turn could drive genetic diversity and adaptive evolution in these organisms (Castagnone-Sereno 2006; Bellé et al. 2019). That is probably the reason for its much greater ability to fnd diferent hosts in diverse environmental conditions.

The nematode life cycle progresses from egg to juvenile stages (J1–J4) and culminates in the adult stage, with a chromosome number of 2n = 44/46 (Khan et al. 2022). *Meloidogyne enterolobii* reproduces similarly to destructive root-knot nematodes (*M. incognita*, *M. javanica*, and *M. arenaria*) (Koutsovoulos et al. 2020). Embryogenesis involves molting from J1 to J2, where the motile juveniles migrate toward host roots, attracted by exudates. J2 initiates giant cell (GC) formation, inducing hyperplasia in surrounding cells, leading to gall formation (Ibrahima et al. 2019; Przybylska and Stęplowska 2020). Sedentary J3 and J4 stages establish themselves in the vascular cylinder, developing into reproductive females under favorable conditions (20–35 °C). Females produce up to 600 eggs in ~ 30–35 days (Philbrick et al. 2020). Environmental stress can trigger male development, contributing to soil biomes (Ibrahima et al. 2019).

Figures 1 and 2 show, respectively, microscopic images of the stages of *M. enterolobii* individuals extracted from the roots of *Psidium* spp. in Casa Nova, Bahia, Brazil, and a schematic representation of a plant attacked a RKN species of the genus *Meloidogyne*, such as *M. enterolobii*, showing some plant physiological responses to its invasion.

Environmental conditions can significantly impact the life cycle of *M. enterolobii*. In a study with tomato, cucumber, and pepper, gall symptoms appeared between 25 to 33 °C at 21 days after inoculation (DAI), with egg masses present at 28 DAI in all

cultivars (Salazar-Mesta et al. 2023). In South Africa, where temperatures reached 32 °C, *M. enterolobii* infected tomato, soybean, and corn, with mature females and eggs observed at 15 DAI and mobile J2 of the second generation at 20 DAI. Nematode degree-days (DD) were recorded as 216 for tomato, 195 for soybean, and 232 for corn (Collett et al. 2023). Additionally, Velloso et al. (2022) found that root infection in tomato seedlings was 33% higher at 30 °C than at 25 °C, with faster development from J2 to reproductive stage. The life cycle was completed in 23 days and 506.9 DD at 30 °C, with lower temperatures delaying development.

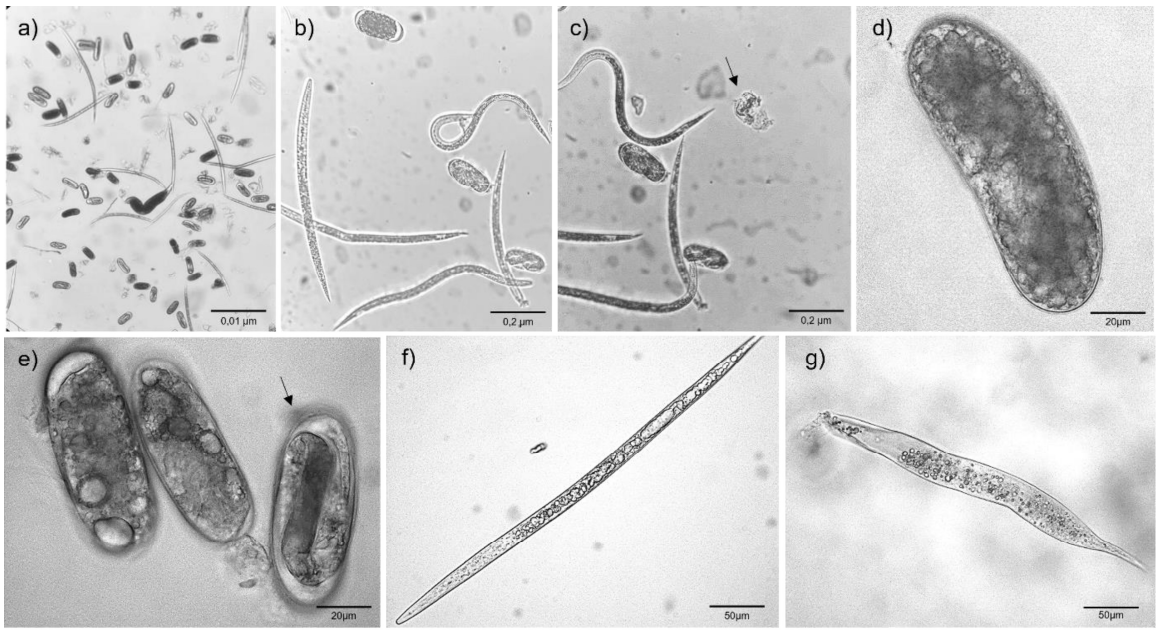

Figure 1 - Microscopic images of diferent life cycle stages of *M. enterolobii*, extracted from the roots of *Psidium* spp. in Casa Nova, Bahia, Brazil: a), b) and c) eggs and juveniles are shown, indicating diferent stages of the pathogen; c) remaining eggshells (pointed by arrow); d) egg; e) eggs with vacuolar sacs and a J1 egg about to hatch (pointed by arrow); f) and g) infective juvenile.

The diversity of terrestrial nematodes is often underreported, with many species still unclassifed. Nematode taxonomy is largely based on morphology, which is crucial for classifcation (Nisa et al. 2022). Second-stage juveniles of *M. enterolobii* are worm-like and ringed, measuring 250 to 700 µm in length and 12 to 18 µm in width. Their tail length ranges from 15 to 100 µm, with the hyaline part 5 to 30 µm long (Rammah and Hirschmann 1988; Yang and Eisenback 1988). Females are globular, pear-shaped, sedentary, and pearly white, measuring 400 to 1300 µm in length and 300 to 700 µm in width. Males are worm-like, measuring 700 to 2000 µm in length and 25 to 45 µm in width (EPPO 2016, 2024). *M. enterolobii* is highly similar with other tropical RKN like

M. incognita, *M. arenaria*, and *M. javanica*. However, it can be distinguished from these species by its perineal pattern, male and female stylet morphology, male morphology, body length, lip region, tail, and hyaline tail part in second-stage juveniles (EPPO 2016). Yet, morphometric and morphological tools alone can incorrectly identify *M. enterolobii* as *M. incognita* (Collett et al. 2021). Traditional morphological methods that rely on the female perineal pattern, morphology of the lip region, stylet, basal swellings of males, as well as the morphometrics of second-stage juveniles, are often challenging and subjective. Therefore, identifcation is typically complemented by electrophoretic and molecular techniques (Ye et al. 2021).

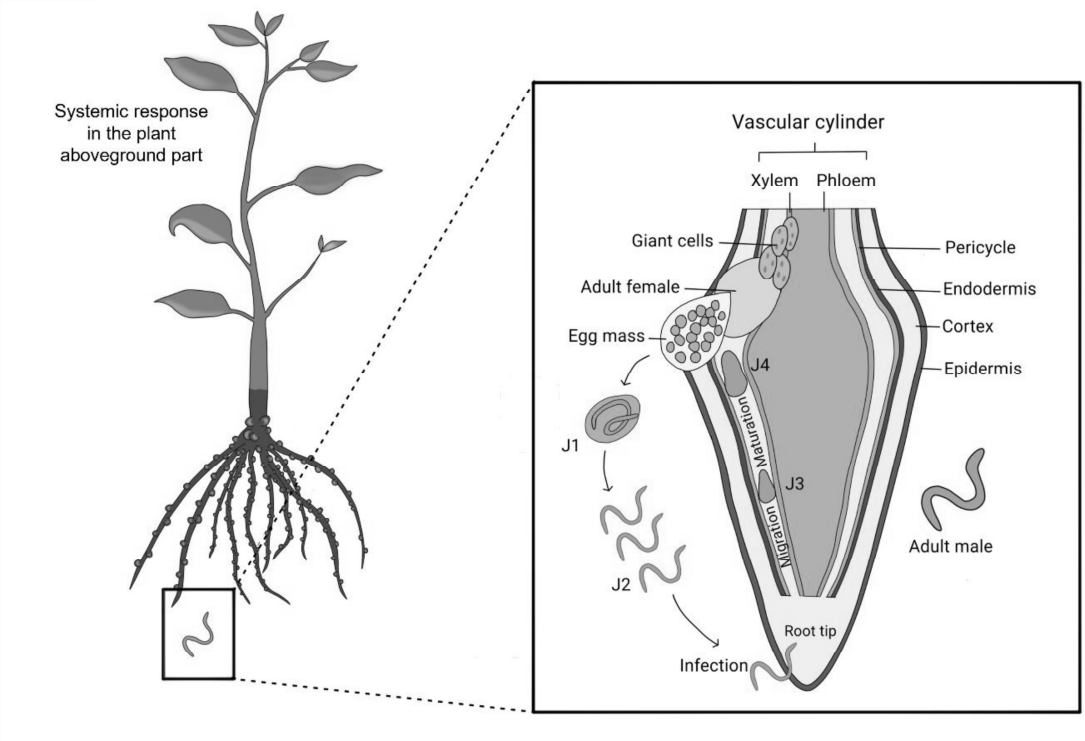

Figure 2 - Schematic representation of a plant with roots infected by *M. enterolobii*, showing how the pathogen establishes itself and completes its developmental cycle. SA – Salicylic acid; ET – ethylene; JA – Jasmonic acid; PR proteins – Pathogenesis-related proteins.

The identifcation of *Meloidogyne* species is more accurately performed through PCR and DNA analyses. These techniques reveal specifc genetic markers, diferentiating closely related species and exploring genetic diversity and virulence potential (Schwarz et al. 2020). CoxII-16S has emerged as a valuable marker for distinguishing *Meloidogyne* species (Ye et al. 2021). Quantitative PCR (qPCR) efectively detects various nematode species and provides nematode density estimates that strongly approximate those traditional counts from soil samples (Hodson et al.

2023). Droplet Digital PCR (ddPCR) ofers high sensitivity, even at low DNA concentrations, without pre-enrichment (Shao et al. 2023).

Biochemical analyses, like non-specifc esterase (EST) electrophoresis, combined with molecular techniques such as internal transcribed spacer PCR–RFLP (ITS-PCR–RFLP), sequence characterized amplifed region (SCAR) markers, real-time PCR, and loop-mediated isothermal amplifcation (LAMP), help to identify economically relevant *Meloidogyne* species (Rusinque et al. 2023). The LAMP assay, targeting the 5S rDNA-IGS2 region, is increasingly popular for point-of-service detection due to its speed and simplicity. RPA (Recombinase Polymerase Amplifcation), another isothermal technique, amplifes minimal DNA samples in minutes, targeting rDNA IGS and SCAR markers (Shao et al. 2023).

Field applications require integrating detection processes with practical solutions. For example, NemaNet, a machine learning tool, simplifes soybean nematode identifcation using a convolutional neural network trained on an extensive image dataset (Abade et al. 2022). In a comparative analysis of published works (Table 1S – supplementary materials), 174 species of host plants for the nematode *M. enterolobii* were listed and grouped into 57 families. The majority of those belong to the Solanaceae, Lamiaceae, Myrtaceae and Euphorbiaceae families (Bellé et al. 2019; Rashidifard et al. 2019; Santos et al. 2019; Khan et al. 2022; Rusinque et al. 2023; Sikandar et al. 2023b). The graphical representation of these data is presented in Fig. 3.

It is important, however, to keep in mind that *M. enterolobii* continues to conquer new environments and hosts. The first report of this nematode on several crops around the world, in the last 5 years, has been recorded (Table 1). This clearly demonstrates the importance of publishing such data, especially through open access

3.1.3 Plant defense mechanisms against disease

Plants trigger robust defense mechanisms following infection by RKN, such as *M. enterolobii*. These defenses include physical barriers (cell wall and cuticle) and chemical defenses (defense proteins and secondary metabolites). Phenolic and carotenoid accumulations, reinforcement of cell walls with lignin and suberin, and the production of metabolites inhibiting egg hatching and nematode development are key components (Sato et al. 2019).

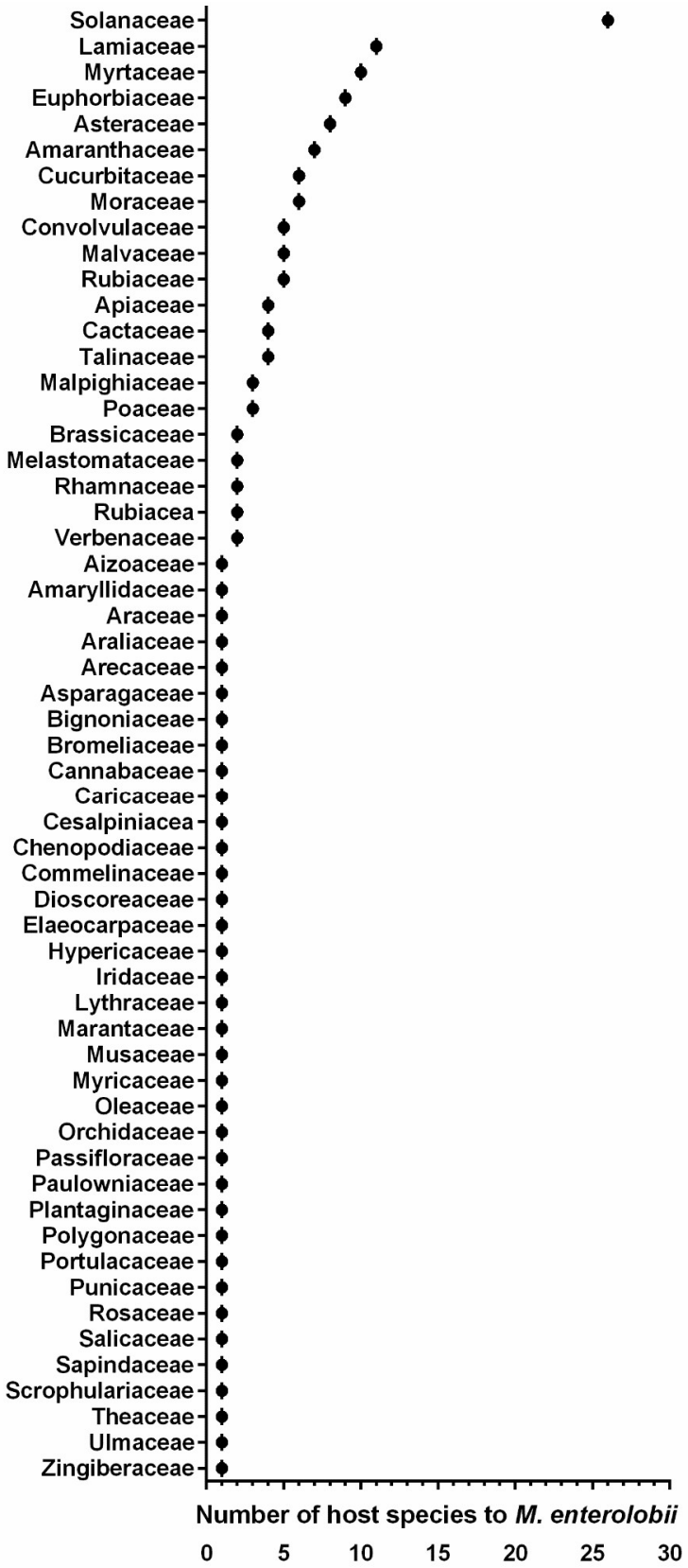

Figure 3 - Graphical representation of 174 host plant species for *M. enterolobii*, grouped into 57 families.

Table 1 - First report of M. enterolobii attack in diferent crops since 2018

Location	Family	Botanical name	Reference
Africa*	Euphorbiaceae	*Manihot esculenta*	(Oyetunde *et al.*, 2021)
	Poaceae	*Zea mays*	(Pretorius 2018)
	Fabacea	*Arachis hypogaea*	(Rashidifard et al. 2018)
Brazil	Convolvulaceae	*Ipomoea batatas*	(Silva *et al.*, 2021)
	Malvaceae	*Gossypium hirsutum*	(Galbieri *et al.*, 2020)
	Musaceae	*Musa* spp.	(Luquini *et al.*, 2019)
	Moraceae	*Morus celtidifolia*	(Soares, Lopes e Dias-Arieira, 2018)
China	Plantaginaceae	*Antirrhinum majus*	(Lu *et al.*, 2023)
	Rubiaceae	*Ixora chinensis*	(Fan *et al.*, 2022)
	Lamiaceae	*Mesona chinensis*	(Wu, C. *et al.*, 2022)
	Fabaceae	*Ormosia hosiei*	(Wu, C. R. *et al.*, 2022)
	Euphorbiaceae	*Acalypha australis*	(Jia *et al.*, 2022)
	Convolvulaceae	*Ipomoea batatas*	(Jia *et al.*, 2021)
	Theaceae	*Camellia oleifera*	(Zhu, Liu e Zhou, 2020)
	Cannabaceae	*Cannabis sativa*	(Ren *et al.*, 2020)
	Rubiaceae	*Gardenia jasminoides*	(Sun, Long e Lu, 2019)
	Moraceae	*Morus* spp.	(Sun, Long e Lu, 2019)
	Zingiberaceae	*Zingiber officinale*	(Zhuo *et al.*, 2018)
	Solanaceae	*Solanum negro*	(Chen *et al.*, 2023)
	Euphorbiaceae	*Euphorbia pulcherrima*	(Liang e Chen, 2021)
	Amaranthaceae	*Celosia argentea*	(Ho, Liang e Chen, 2022)
Egypt	Myrtaceae	*Psidium guajava*	(Ibrahim *et al.*, 2023)
India	Myrtaceae	*Psidium guajava*	(Bhati e Parashar, 2020)
Mexico	Rubiaceae	*Coffea arabica*	(Torres-López *et al.*, 2022)
	Amaranthaceae	*Beta vulgaris*	(Salinas-Castro *et al.*, 2022)
	Apiaceae	*Daucus carota*	(Salinas-Castro *et al.*, 2022)
	Solanaceae	*Solanum melongena*	(Salazar-Mesta *et al.*, 2022)
	Cucurbitaceae	*Cucumis sativus*	(Gómez-González *et al.*, 2020)
Nigeria	Musaceae	*Musa* spp.	(Olajide *et al.*, 2022)
United States	Ulmaceae	*Ulmus parvifolia*	(Moore *et al.*, 2020)
	Convolvulaceae	*Ipomoea batatas*	(Gu, M *et al.*, 2021; Hajihassani, Nugraha e Tyson, 2023),
	Lamiaceae	*Ocimum basilicum*	(Gu, M. *et al.*, 2021)

*There is no specific location information.

Although chemotaxis is considered the most critical feature for RKN to locate hosts, the mechanisms that attract them to root exudates are not fully understood. It has been reported that chemotactic responses are specifc to species within the genus *Meloidogyne*. A work by Silva et al (2020) showed that J2 of *M. enterolobii* migrate faster than *M. incognita* and are able of penetrating tomato roots as early as 3 days after infection. Both species penetrated marigold roots just at 9 DAI, indicating a delay in J2 migration of *M. incognita*. In this sense, further studies must be performed to elucidate how nematodes, through their sensory organs, are able to distinguish attractive and repellent substances of root exudates from the same host (Dutta et al. 2021).

Innate immunity or basal resistance is the frst system activated by the interaction between pathogen-associated molecular patterns (PAMPs) and damage-associated molecular patterns (DAMPs), leading to a pattern-triggered immunity (PTI). Efector-triggered susceptibility (ETS) occurs when PTI is neutralized, but plants can still exhibit disease resistance through efector-triggered immunity (ETI) activated by resistance genes (Avr-R). In non-host (resistant) plants, ETI is accelerated, and PTI is enhanced (Shao et al. 2021). The Hypersensitive Response (HR) is a critical innate mechanism against pathogens, characterized by rapid and specifc tissue collapse surrounding the infection. This response involves the release of toxic compounds afecting the pathogen, inducing programmed cell death, and triggering the production of Pathogenesis-Related (PR) proteins. HR results in necrotic lesions crucial for the Systemic Acquired Resistance (SAR), limiting the movement of plantparasitic nematodes (PPN) and disrupting their life cycle (Przybylska and Stęplowska 2020).

Plants have developed defense mechanisms against invasion by RKN, and if these are violated, more complex defense systems kick in. PPNs also serve as vectors for microorganisms, both benefcial and pathogenic, as they associate with the nematode cuticle and are transported to plant roots during feeding on root tissues (Li et al. 2023a). Example of such benefcial interaction was reported by Li et al (2023b) who showed signifcant enrichments of bacteria belonging to Rhizobiales, Betaproteobacteriales, and Rhodobacterales in the endophytic microbiota of *Meloidogyne*-parasitized tomato root samples. At the other end of the spectrum, co-infection of *M. enterolobii* with *Fusarium* spp. leads to a complex gall disease, impacting crop yields. In this synergistic interaction, the fungus colonizes inner root tissues after penetrating through lesions previously performed by the nematode.

Symptoms include curling of apical leaves, stunted growth, leaf discoloration, and fruit changes, posing challenges to control (Shi et al. 2019; Dutta et al. 2021).

Plant pathogen nematodes (PPN), including *M. enterolobii*, rely on pheromones for development and communication (Manohar et al. 2020). These molecules infuence their behavior and responses, such as the release of efector proteins that alter plant structure and functions, facilitating parasitism. Nematode secreted compounds possessing immunosuppressive properties play a pivotal role in parasitism, particularly in the modifcation and degradation of the plant cell wall (Khan et al. 2023a). They are collectively referred to as "secretomes" or "para sitomes" and have been associated with a diverse set of molecular functions, such as polysaccharide binding and cellulosic activity, all linked to plant cell wall modifcation and degradation. Pheromones from PPN serve as a "signature", initiating immune responses in the host plant and allowing nematodes to manipulate plant cellular machinery (Koutsovoulos et al. 2020; Manohar et al. 2020). Figure 4 shows the plant defense mechanisms triggered in response to nematodes, which follow diferent paths in host and non-host plants.

Ascarosides are one example of such pheromone molecules linked to the weakening of host immune responses. The Ascr #18 specifcally serves as a pathogen-associated molecular pattern (PAMP) known to activate early immune responses. It is recognized by the plant as a nematode-associated molecular pattern (NAMP), leading to the activation of pathways involving MAPKs, defense signaling, gene expression, and the generation of reactive oxygen species (ROS) (Klessig et al. 2019).

A recent study identifed the efector MeMSP1 as a key player in plant responses to both abiotic and biotic stresses, specifcally targeting glutathione-S-transferase class Phi family proteins (GSTFs). Arabidopsis mutant lines lacking AtGSTF9 exhibited increased susceptibility to RKN infection. Subsequent analyses revealed that MeMSP1 signifcantly infuenced A. thaliana metabolic pathways, leading to the accumulation of amino acids, nucleic acids, and organic acids, and disrupting favonoid production (Chen et al. 2023b).

In plants, two groups of essential compounds are distinguished: primary metabolites, crucial for growth and involved in major metabolic pathways; and secondary metabolites (specialized metabolites), related to plant interactions with the environment. The Fig. 1S (supplementary materials) illustrates the interconnectedness of primary and secondary metabolism pathways.

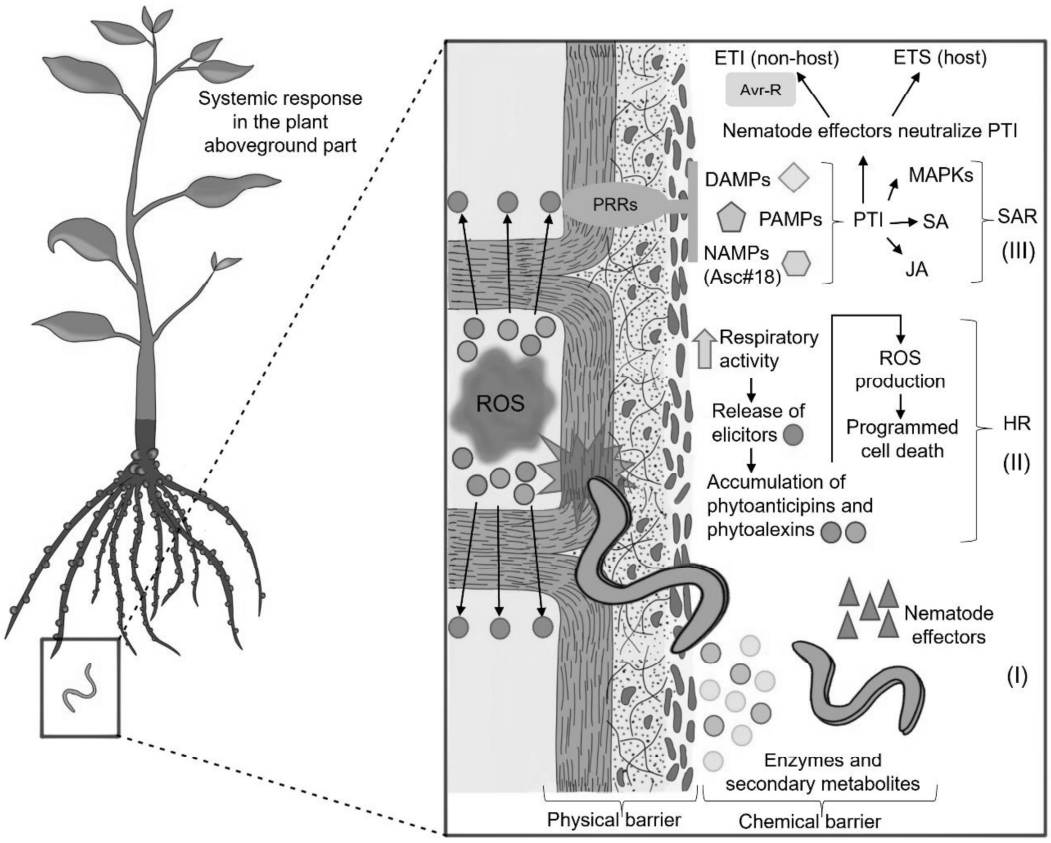

Figure 4 - Schematic representation of an infected plant and its defense mechanisms against *Meloidogyne* spp., including: (I) Physical and chemical barriers; (II) Hypersensitive Response (HR) - Programmed cell death; and (III) Systemic Acquired Resistance (SAR).

Plant metabolites stored in or exuded from roots to the rhizosphere signifcantly impact nematode behavior, development, and reproduction. About 5 to 20% of photosynthesis products are released into the rhizosphere via root exudates, emphasizing the potential for enhancing microbial control of plant-parasitic nematodes through a comprehensive understanding of chemical interactions among plants, rhizosphere microbiomes, and nematodes (Sikder and Vestergård 2020).

Anti-nematode phytochemicals (ANPs) fall into three categories: root-released metabolites with nematode-repelling action; with nematicidal activity regardless of nematode presence; and anti-nematode compounds produced in response to nematode penetration (Desmedt et al. 2020). Chemical signaling and transduction play vital roles in plantmicroorganism interactions, initiating metabolic responses involving key secondary metabolites such as alkaloids, peroxidase, polyphenol oxidase, phenylalanine ammonia-lyase, phenolic compounds, and terpenes in defense against biotic stresses (Jha and Mohamed 2022).

3.1.4 Integrated Nematode Management (INM) of *M. enterolobii* in plant species of interest to global agribusiness

Climate changes, including global warming, higher CO2 levels, and extreme environmental conditions, profoundly afect nematodes. They can boost or undermine their reproduction, extend or shorten transmission periods, alter gender ratios, and shift their abundance and diversity in hot and humid climates, akin to other parasites and pathogens (Dutta and Phani 2023). Pioneering work on the efect of these climate changes on the geographic distribution of *M. enterolobii* predicted that, by 2090, the nematode could reach higher latitudes, which, in the case of the country of origin of the authors, would make northern China a more suitable habitat for these pests, and globally highly suitable regions for the nematode would be concentrated in Africa, South America, Asia, and North America between latitudes 30°S to 30°N (Pan et al. 2023). Zhou et al. (2022) recommended that research be conducted spanning multiple trophic levels, including plants, soil microorganisms, and the nematodes themselves, in order to efectively understand the impact of global changes on soil nematodes. The complexity of the nematode distribution is related to global temperature, but organic carbon availability shall also be considered (van den Hoogen et al. 2019).

In addition, soil management practices also impact nematodes. Soil compaction can limit root growth in surface layers, where plant-parasitic nematodes thrive. This underscores the vital connection between soil physical properties (texture) and chemical attributes (pH, organic matter, nutrients), and phytonematode populations (Leiva et al. 2020). The addition of nitrogen, along with tillage reduction, had a synergistically negative impact, reducing soil nematode abundance and diversity (Wang et al. 2021). It has also been demonstrated that in highly inorganic soil, plant phosphorus acquisition depends heavily on phytate-mineralizing bacteria (Ranoarisoa et al. 2020). Soil properties and biology impact nematode survival and predation, revealing a strong interconnectedness of ecosystems.

The INM aims to control diseases in a sustainable and environmentally friendly manner, reducing the negative impacts of nematodes on agricultural crops, preventing disease outbreaks, and increasing agricultural production. Managing *M. enterolobii* poses challenges due to its multiple hosts and rapid reproductive cycles, but its suppression can be achieved through two or more control techniques, such as physical control, cultural practices, biological control, and genetic resistance (Philbrick et al.

2020; Timper and Davis 2022; Sikandar et al. 2023b).

Cultural control

Cultural control, a cost-efective nematode management method, is vital for *Meloidogyne* species, notably *M. enterolobii*. It involves tactics like crop rotation and cover crops. Rigorous studies on cultural measures and equipment sterilization are crucial for successful management, emphasizing preventive actions to curb nematode spread (Khan et al. 2023b). In a study focusing on mitigating nematode infestations in tomato plantations, researchers tested irrigation water treatment with ozone to render the eggs of *M. enterolobii* inviable. It was found that a low residual concentration of ozone for a short period reduces egg viability. Exposure to 0.2 mgO3 L−1 for 15 min resulted in almost 90% egg inactivation, while 0.55 mgO3 L−1 for 10 min inactivated over 95% of the nematode population (Fernández et al. 2019).

Crop rotation, a valuable technique for annual crops, ofers multiple approaches, including the use of non-host plants, diferent hosts, reservoir plants (weeds), and antagonist plants. These methods contribute to suppressing *M. enterolobii* populations through various mechanisms. A study on the impact of crop rotation on *M. enterolobii* found that combinations of sorghum/corn and alfalfa/corn signifcantly reduced the quantities of nematode eggs and juveniles compared to a monoculture of corn. Sorghum/corn rotations reduced the population density of *M. enterolobii* by 81% in the frst experiment and 60% in subsequent experiments, followed by alfalfa/corn rotations, with reductions of 54% and 43%, respectively (Rashidifard et al. 2021).

Antagonistic plants play a crucial role in nematode management by producing anti-helminthic compounds during growth. Key species like *Tagetes* spp., *Azadirachta indica, Brassica* spp., and *Crotalaria* spp. release nematotoxic compounds, acting as traps or triggering unfavorable responses for PPNs. For instance, *Crotalaria juncea* boosts nematode antagonistic microorganisms and releases the nematotoxic substance monocrotaline, while neem (*A. indica*) produces nematotoxic compounds like azadirachtins (Chetia et al. 2019; Abd-Elgawad 2021).

Cover crops have the ability to incorporate organic matter, which is fundamental for soil fertility. Efective selection of cover crops requires attributes such as easy establishment, rapid growth, efective soil coverage, resistance to pests and diseases, suitability for intercropping, and a robust root system capable of producing ample dry matter for no-till farming techniques (Djian-Caporalino et al. 2019; Zhang et al. 2022).

In a conducted study, it was observed that sunn hemp (*C. juncea*) and sudangrass (Sorghum sudanensis) were considered poor hosts or non-hosts for *M. enterolobii*. Therefore, these crops can be recommended as cover crops in most cases, except when root lesion nematodes are present in the feld. On the other hand, cowpea (*Vigna unguiculata*) and sunfower (*Helianthus annuus*) were identifed as good hosts for this RKN, consequently, they are not suitable options for cultivation in felds where RKN are present (Bui and Desaeger 2021).

In a U.S. evaluation of summer cover crops against *M. enterolobii*, sunfower (*Helianthus annuus* L.) and cowpea (*V. unguiculata* L.) elicited high nematode reproduction, while buckwheat (*Fagopyrum esculentum* M.) and sunn hemp (*C. juncea* L.) led to lower nematode reproduction. Sesame (*Sesamum indicum* L.) caused low reproduction. Millet and sorghum varieties, including pearl millet and sorghum-sudangrass, did not host nematodes and had greater biomass compared to tomatoes (Khanal and Harshman 2022).

Despite the efectiveness of cultural control techniques, their adoption by producers may be hindered due to the requirement for fallow periods or frequent crop rotation, especially when dealing with perennial crops of economic importance.

Chemical control

The utilization of chemical nematicides for the control of *Meloidogyne* species entails notable risks. Nematicides can be broadly classifed into two categories: fumigants, characterized as volatile gases or easily evaporated liquids, and nonfumigants, typically formulated as liquids or granules mixed with water or directly applied to the soil. Both types present substantial hazards as they can be absorbed by plants and accumulated in the environment, and they have already been detected at various levels in the food chain. Additionally, these nematicides disrupt soil ecosystems, adversely afecting benefcial microorganisms and potentially causing severe environmental consequences (Sikandar et al. 2023b, a).

However, there is a growing movement towards the gradual phase-out of methyl bromide and other toxic fumigants from the soil and nematicides due to their toxicity to humans and other non-target organisms (Oka 2020). The practice of soil fumigation faces increasing social and regulatory pressure, but it remains the primary management tool for nematodes in the production of many high-value crops. In the long term, improving soil health and developing more resilient soils may be one of the

greatest benefts of phasing out soil fumigants and adopting more selective and safer nematicides (Sikora et al. 2023). According to what was proposed by Desaeger et al (2020) the ideal characteristics of a nematicide vary between the perspectives of the producer and the regulator. For the producer, it's important that it controls a wide range of nematodes, has good mobility and residual activity in the soil, in addition to being low in toxicity to plants and requiring low dosages. For the regulator, selectivity is essential, protecting non-target organisms, avoiding leaching and residues in crops, without impacting the quality of the fnal product and with low human toxicity. Next-generation nematicides include fuazaindolizin, fuensulfone, fuopyram, spirotetramat, and cyclaniliprole. However, iprodione has been banned in Europe due to concerns about cancer and risks to aquatic life. The release of thiozafenone for seed treatment has been postponed due to reports of skin irritation. There is an urgency for more selective nematicides (Burns et al. 2023).

Common soil fumigants employed for controlling *Meloidogyne* spp. include 1,3-dichloropropene (e.g., Telone II), metam sodium (e.g., Vapam, Sectagon-42), and metam potassium (e.g., K-Pam). In the United States, non-fumigant nematicides such as fuensulfone (e.g., Nimitz), fuopyram (e.g., Velum Prime and Velum Total), oxamyl (e.g., Vydate), etoprope (e.g., Mocap), and terbufos (e.g., Counter) fnd application. In certain regions, like the European Union, metam sodium and dazomet (e.g., Basamid) have been shown effective against *M. enterolobii* (Philbrick et al. 2020). However, metam-sodium has been withdrawn by industry from the approval process under Regulation (EU) No 528/2012. The efect of that withdrawal is that metam-sodium is banned from all use in the subcategory ‘other pesticide including biocides’, by the Commission Delegated Regulation (EU) 2023/1656 of 16 June 2023 (EUR-Lex 2023).

The Phytosanitary Pesticides System of Brazil (Ministério da Agricultura Pecuária e Abastecimento do Brazil 2023) lists 34 formulated products with synthetic nematicidal activity for national agriculture. Among these, 24 are applicable to crops afected by the following species from the *Meloidogyne* genus: *M. javanica*, *M. incognita*, *M. exigua*, *M. hapla*, *M. paranaensis*, and *M. enterolobii*. In the toxicological and environmental classifcation of these pesticides, a lower index indicates greater danger, while a higher index indicates lesser danger. Figure 5 presents a comparison of the toxicological (between 1 and 5, below 5 are unclassifed) and environmental (between I and IV) classifcations of 24 synthetic (S) (Tab. 2S – supplementary materials) and 56 biological (B) (Tab. 3S – supplementary materials) nematicides

registered and commercially released in Brazil for control of *Meloidogyne* spp.

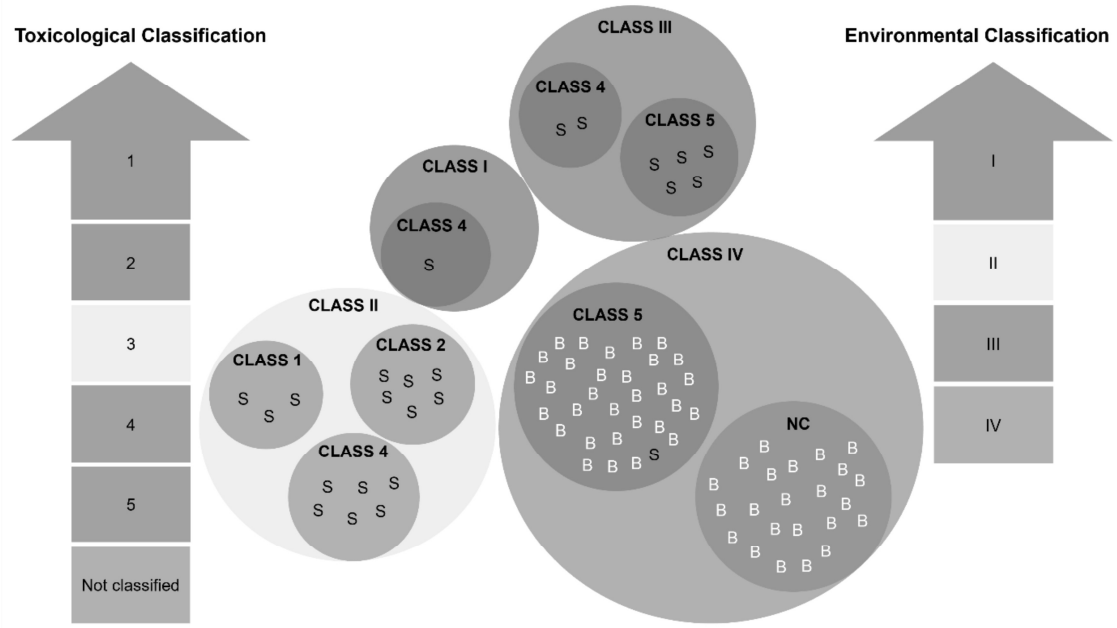

Figure 5 - Schematic representation of the comparison among toxicological (between 1 and 5, below 5 are those not classifed) and environmental (between I and IV) classifcations of synthetic (S) and biological (B) nematicides registered and commercially released in Brazil for control of *Meloidogyne* spp.

Specifcally designated for *M. enterolobii* control, there are only two chemical nematicides among the 24 previously mentioned as applicable to the genus Meloidogyne: Nimitz EC® (fuensulfone) for guava crops and Verango Prime® (benzamid) for various crops. Both are categorized as Class III, posing environmental hazards. These chemicals, while versatile and efective against diferent *Meloidogyne* species, are recognized for their environmental risks (Ministério da Agricultura Pecuária e Abastecimento do Brazil 2023). A comparative study on nematicide efcacy (fuopyram, fuensulfone, fuazaindolizine, and oxamyl) demonstrated similar reductions in root infectivity for both *M. enterolobii* and *M. incognita*. Fluopyram efectively inhibited hatching in both species, while fuensulfone strongly inhibited root penetration. Nematicide application at label-recommended doses reduced gall formation on roots and decreased egg production in both species (Watson 2022). Alam et al (2023) analysed the efects of non-fumigant nematicides on *M. enterolobii* and showed that fluensulfone caused decreases of 71% in eggs and 86% in J2 juveniles, fuopyram did not signifcantly afected nematode reproduction and oxamyl suppressed J2 by 80%, but had a lesser impact on eggs (50%). Fluensulfone showed the greatest reduction in

disease severity (64%), followed by oxamyl (54%) and fuopyram (48%). Except for fuensulfone, none of the nonfumigant nematicides signifcantly afected root or shoot biomass. Thus, the application of nematicides remains a more common short-term management strategy against RKN and although substitute chemical products have been developed, they have not been entirely successful in achieving hjgh levels of efciency, especially towards *M. enterolobii* (Forghani and Hajihassani 2020).

These studies underscore the complex interactions between phytonematicides, plant growth, and *M. enterolobii* control. Non-fumigant nematicide development, driven by concerns about fumigant properties, has progressed, but environmental and human health risks must be considered in their use.

Biological control

By 2030, UN's Sustainable Development Goal 2 aims to promote sustainable agriculture, boost productivity, enhance climate resilience, and ensure food security for the expanding global population (ONU 2015).

Biocontrol, or biological control, involves using organisms to reduce specifc pest populations, thereby diminishing their harmful impact. In the management of nematodes, biocontrol ofers a sustainable approach, reducing reliance on synthetic chemicals and minimizing risks to human health and the ecosystem (Francisco et al. 2021). Such interest in harnessing microorganisms has grown due to their crucial role in INM, but the efectiveness of this strategy depends on factors like adaptability, nematode density, microorganism selection, rhizosphere performance, cooperation with microbiota, nutrient competition, and host plant protection from pathogens (Tariq et al. 2020). Integrating agriculture and livestock farming enhances soil properties, such as organic matter, cation exchange capacity, microbial activity, and structural integrity (Dias-Arieira et al. 2021). Organic soil amendments enhance soil quality by bolstering water retention, microbial diversity and biomass, aiding pest management. However, careful application is crucial to prevent excessive salt and phosphorus levels, detrimental to plant growth and water quality. Organic waste composting further benefts soil and plant vitality (Kanagaraj and Sundaravadivelu 2021; Tefu et al. 2022).

In biological control for managing plant pathogens, antagonism (antibiosis) and the induction of resistance are recognized strategies. In nematode biocontrol, fungi and bacteria, particularly *Bacillus* spp. and *Trichoderma* spp., play key roles as antagonistic agents. The Brazilian Phytosanitary Pesticides System database lists 64

biological products formulated for nematicidal activity, with 41 using Bacillus spp. as active ingredients (Ministério da Agricultura Pecuária e Abastecimento do Brazil 2023). This bacteria exhibits nematicidal potential through the synthesis of proteases, chitinases, antibiotics, crystalline proteins, and secondary metabolites, enhancing systemic plant resistance (Tapia-Vázquez et al. 2022).

The combined efects of phytonematicides Biocult and Nemafric-BL on cowpea growth and *M. enterolobii* population reduction was evaluated. Biocult enhanced plant growth and decreased nematode populations, while the combination showed no signifcant efects on nematode population densities. These fndings suggest separate use for these phytonematicides in cowpea production (Pofu and Mashela 2022a). In 'Congo' watermelon plants, natural phytonematicides (Nemarioc-AL and Nemafric-BL) and Velum (fuopyram) enhanced plant growth, yield, and fruit quality. All three products signifcantly reduced nematode eggs and juveniles in both roots and surrounding soil, indicating their efectiveness (Pofu and Mashela 2022b).

Fungal biological agents can reduce RKN populations, leading to decreased damage compared to untreated conditions (Peiris et al. 2020). *Trichoderma* spp. employ mycoparasitism, antibiosis, and resource competition to target *Meloidogyne* spp. eggs and juveniles. Some strains produce enzymes that degrade cell walls and release secondary metabolites inhibiting egg hatching and killing juveniles (Mukhopadhyay and Kumar 2020; Gouveia et al. 2022). Additionally, *Trichoderma* species act as plant growthpromoting microorganisms, enhancing photosynthetic efciency, nutrient solubilization, and producing compounds benefcial to plant growth (Pofu and Mashela 2022b). For these arbuscular mycorrhizal fungi (AMF), which act as obligate symbionts of plant roots, the plant provides photosynthetic carbon, while they help roots absorb higher nutrients and promote root growth and structure. Additionally, they typically compete for nutrition and space with PPNs and induce systemic resistance in plants (Abd-Elgawad 2021).

Although a systematic analysis, carried out with 23 genera comprising 40 fungal species, indicated only *Trichoderma* as efective against M. *enterolobii* (Peiris et al. 2020), *Pochonia chlamydosporia* (var. catenulata and chlamydosporia) and Purpureocillium *lilacinum* strains negatively afected *M. enterolobii* populations in tomato and banana plants, but the intensity of the efects was dependent on the level of infestation (Silva et al. 2017). Also, when *Purpureocillium lilacinum* strain PL251 was combined with *Bacillus amyloliquefaciens* strains D747 (Ba) and these were

simultaneously inoculated on cucumber roots there was an 84% reduction in the number of *M. enterolobii* eggs (Paula et al. 2024). So, rather than isolated fungi species, for some cases the association among fungi species and strains may be the proper way to apply this biological control. Another study demonstrated that two formulations (specifc suspension and wettable powder) of *Metarhizium carneum*, a nematophagous fungus, decreased *M. enterolobii* population density by 78% and 66%, respectively, compared to the control. Additionally, the liquid formulation of *M. carneum* and *P. lilacinum* treatments inhibited nematode population density by 72% and 43%, respectively (López-Lima et al. 2023).

While the strategy is signifcant for crop protection and ecological equilibrium, introducing potent microorganisms requires caution to prevent disruptions in the delicate soil ecosystem.

Plant growth-promoting rhizobacteria enhance plant growth directly or indirectly by inhibiting pathogens, including nematodes. Predominant Gram-negative and Gram-positive bacteria contribute to plant well-being (Xiang et al. 2018). Also, research on the endophytic fungus *P. chlamydosporia* reveals positive efects on tomato growth beyond nematode control, infuencing phytohormones, root phenolic compounds, and favonoids (Gouveia et al. 2022). *Aspergillus tubingensis* GX3 fermentation produces nematicidal enzymes or substances harming *M. enterolobii* nematode eggs and juveniles (Sikandar et al. 2023a).

Certain plants produce natural compounds effective against nematodes, including volatile organic compounds (VOCs) like terpenoids, phenylpropanoids, benzenoids, fatty acid derivatives, and amino acid derivatives. Biofumigation with *Xanthosoma sagittifolium* controls *M. enterolobii* by reducing eggs and galls and this can be due the secondary compounds present in its composition, such as aliphatic ketones shown by GC–MS, but tests are yet necessary to prove this (Gomes et al. 2020).

Genetic resistance

A crucial strategy for enhancing the development of new disease-resistant cultivars involves selecting parent plants with high resistance to gall disease. Verssiani et al. (2023) found that *M. enterolobii* derived from cotton exhibited greater aggressiveness toward soybean cultivars compared to guava-derived races. Only the soybean 'BRS 7180 IPRO', genetically developed for resistance against *M. incognita*

and *M. javanica*, demonstrated moderate resistance among all 16 tested cultivars, stressing the complexity of the challenge in breeding genotypes resistant to *M. enterolobii*.

Ninety-one sweet potato (*Ipomoea batatas*) genotypes were evaluated for potential resistance to *M. enterolobii*. Only 19 displayed resistance (Schwarz et al. 2021). While nematodes could invade and thrive in resistant sweet potato cultivars, their egg production capacity was reduced compared to susceptible ones. 'CIP BRS Nuti' and 'Canadense' displayed resistance to *M. enterolobii* in greenhouse conditions, with reproduction factors of 0.14 and 0.04, respectively, after 90 days of nematode inoculation (Mello et al. 2022).

In 2010, Embrapa Semiárido in Brazil achieved a genetic improvement milestone by developing the BRS Guaraçá hybrid (Fig. 6) through crossbreeding of guava (*Psidium guajava*, Gua 116 PE) with araçá (*P. guineense*, ARA 138RR) (Souza et al. 2018). This cultivar, registered (#35,849) and protected (#20,180,185) by the Ministry of Agriculture, Livestock in Brazil (Flori and Deon 2022), demonstrates resistance to *M. enterolobii* and compatibility with guava trees (Simões et al. 2023). Seedling production is infuenced by factors such as branch health, growth regulators, substrate selection, misting regimen, and cutting method. Tailoring the seedling production process is crucial for optimizing yield, especially in cultivars resulting from interspecifc crosses like BRS Guaraçá (Castro and Ribeiro 2020; Santos 2020). Assessments of compatibility, productivity, and morphological variation revealed signs of incompatibility, but guava accessions grafted onto BRS Guaraçá produced healthy plants in the second harvest cycle (Lourenço et al. 2022).

The path to plant breeding is not always smooth and often involves extensive crosses and feld trials before selecting resistant genotypes, a process that can span decades before making resistant seedlings available for production. Also, limited molecular-level resistance information may render the whole operation vulnerable to various factors.

Figure 6 - Photographic records of *Psidium guajava* (Paluma) and BRS Guaraçá in the city of Petrolina, Pernambuco - Brazil: a) whole individual of Paluma attacked by *M. enterolobii*; b) emphasis on leaf chlorosis; c and d) presence of galls on the roots; e) the original BRS Guaraçá with 10 years of planting after crossing between *P. guajava* (susceptible to the nematode, mother) and *P. guineense* (resistant to the nematode, father), in the Embrapa Semiárido Bebedouro Field; f) aboveground part of an araçá tree using BRS-Guaraçá seedlings as rootstock; g) highlight of gall-free roots from a rootstock.

3.1.5 Innovative approaches for enhancing plant resistance against *M. enterolobii*

Enhancing plant identifcation based on desired traits is pivotal for farmers. Utilizing advanced selection methods and data analysis helps experts to pinpoint promising plants, expediting the development of high-quality varieties. While our understanding of molecular plant resistance to *M. enterolobii* remains incomplete, it guides improvement strategies. In this direction, some metabolites can either promote or reduce infection by PPN. Deepening our understanding of chemical interactions between plant roots and PPN lays the groundwork for pesticide-free strategies in crop cultivation (Sikder and Vestergård 2020). Metabolic analysis of healthy, infected, diseased, and resistant plants, can unveil disruptions in signaling or output pathways crucial in plant microorganism interactions. Gathering and associating data on the felds of metabolomics, proteomics, transcriptomics and genomics is essential for a more

solid knowledge on plant diseases, pathogen nutrient acquisition, as well as plant immunity activation and adaptation to disease pressure (Castro-Moretti et al. 2020).

The diverse functions of these substances can illuminate patterns of plant defense development, considering them as components of metabolic networks shaped by the environment (Marciniak et al. 2019). In a recent study, both polar (tannins and hydrolyzable lignans) and nonpolar (terpenes) substances were regulated in *Psidium* spp. after an *M. enterolobii* infection. Terpenes, acting as inhibitors, enhance guava resistance by repelling or reducing oxidative stress during infection (Costa et al. 2023). Alkaloids, basic nitrogenous organic compounds, originating from amino acids like phenylalanine, lysine, and tryptophan, are of growing interest in the Solanaceae family. Steroid glycoalkaloids (GAs) found in various plants, including potatoes, black nightshade, and tomatoes, are some examples (Marciniak et al. 2019). Such identifcation of anti-nematode phytochemicals (ANPs) ofers targets for crop improvement through genetic engineering. The ANPs can also serve as biomarkers for nematode resistance, aiding high-throughput metabolomics screening of breeding lines. Recent advancements in gene cloning for resistance, especially with genetically modifed plants containing cloned resistance genes, correlate with ANPs (Desmedt et al. 2020).

The importance of identifying and integrating disease resistance (R) genes is also crucial for controlling nematode infections. Despite the variable genetics of nematode resistance, recent advancements in gene cloning have emerged (Jiang et al. 2023). Resistance mediated by NtRk1 (Neurotrophic Receptor Tyrosine Kinase 1 gene) in tobacco plants against M. incognita involves early-stage expression changes. Overexpressing NtRk1 elevates resistance, while RNAi of NtRk1 in a resistant variety makes it susceptible. The Mi-1 gene provides nematode resistance in tomatoes, but Mi-9, isolated from wild tomatoes, ofers consistent resistance even at high temperatures, opposed to Mi−1. More relevant, the Ma and RMja genes from *Prunus cerasifera* were seen able to control both “the peach RKN,” *M. foridensis* (Handoo et al. 2004), and *M. enterolobii* (Claverie et al. 2011; Duval et al. 2019).

CRISPR/Cas9 technology has proven efective in precisely altering crop genomes, perfecting breeding programs (AbdElgawad 2022). Genome editing using CRISPR/Cas9 alters specifc DNA sequences, allowing large-scale efcient gene editing. Targeted changes in rice metallothionein-like protein 04 via CRISPR/Cas9

conferred resistance to rice RKN. Marker-Assisted Selection (MAS) has transformed plant breeding, employing markers to pinpoint desirable traits and streamline the breeding process. SNP (Single Nucleotide Polymorphisms) genotyping and genomic sequence analysis have led to the development of markers linked to nematode resistance loci in potatoes (Bali et al. 2022). Nematode resistance in cotton cultivars is inherited from specifc varieties, with QTLs (Quantitative Trait Locus) on chromosomes 11 and 14 playing key roles. Efector genes from nematode esophageal glands are also promising targets for nematode control through Host-Induced RNAi (HD-RNAi), as also the essential collagen gene Me-col-1, which is vital for egg formation in root-knot nematodes (Pei et al. 2022).

3.1.6 Conclusions

In summary, the root-knot nematode *Meloidogyne enterolobii* represents a serious threat to crops on a global scale. Understanding the molecular interactions between this nematode and plants is essential for developing molecular control strategies and effective management. Omics approaches, which focus on the genes and proteins involved in *M. enterolobii* activities and plant resistance responses, play a crucial role in this advancement. Continued progresses in computational biology and bioinformatics analysis support these techniques, allowing for precise identifcation of elements related to M. enterolobii parasitism and plant responses.

Genome editing technologies ofer a powerful tool for genetically improving plants by mapping relationships between genes and phenotypic traits. However, it is crucial to apply these methods with care to avoid unintended consequences, such as increased nematode virulence and impacts on crop productivity. Challenges arise, including the transfer of resistance to various diseases and the specifcity of virulent nematodes to established techniques. Ultimately, *M. enterolobii* control should be addressed through integrated pest and crop management, ensuring food security and crop health. This becomes crucial in a challenging scenario with increasing agricultural demands.

From a biotechnological perspective, the development of biological inputs for *M. enterolobii* control is promising. Compared to conventional non-biological products, bioinputs ofer advantages that extend beyond their direct efects. In the long term, this transition tends to favor the agriculture of the future, promoting sustainability and environmental preservation by reducing environmental impacts.

References

Abade A, Porto LF, Ferreira PA, de Barros VF (2022) NemaNet: A convolutional neural network model for identifcation of soybean nematodes. Biosyst Eng 213:39–62.

Abd-Elgawad MMM (2021) Optimizing safe approaches to manage plant-parasitic nematodes. Plants 10:1–16.

Abd-Elgawad MMM (2022) Understanding molecular plant–nematode interactions to develop alternative approaches for nematode control. Plants 11:1–16.

Alam MS, Khanal C, Roberts J, Rutter W (2023) Impact of non-fumigant nematicides on reproduction and pathogenicity of *Meloidogyne enterolobii* and disease severity in tobacco. J Nematol 55:1–6.

Bali S, Brown C, Majtahedi H et al (2022) Genomic markers linked to *Meloidogyne chitwoodi* resistance introgressed from *Solanum bulbocastanum* to cultivated potato and their utility in markerassisted selection. Mol Breed 42:1–10.

Bellé C, Ramos RF, Balardin RR et al (2019) Reproduction of *Meloidogyne enterolobii* on weeds found in Brazil. Trop Plant Pathol 44:380–384.

Bhati SS, Parashar A (2020) First report and morphological description of *Meloidogyne enterolobii* infecting Guava (*Psidium guajava* L.) in transitional plain of Luni Basin of Rajasthan. Int J Curr Microbiol Appl Sci 1–3.

de Brida AL, Rosa JMO, de Oliveira CMG et al (2018) Entomopathogenic nematodes in agricultural areas in Brazil. Nature 8:1–7.

Bui HX, Desaeger JA (2021) Host suitability of summer cover crops to *Meloidogyne arenaria*, *M. enterolobii*, *M. incognita* and *M. javanica*. Nematology 0:1–9.

Burns AR, Baker RJ, Kitner M et al (2023) Selective control of parasitic nematodes using bioactivated nematicides. Nature 618:102–108.

Castagnone-Sereno P (2006) Genetic variability and adaptive evolution in parthenogenetic root-knot nematodes. Heredity (Edinb) 96:282–289.

Castro-Moretti FR, Gentzel IN, Mackey D, Alonso AP (2020) Metabolomics as an

emerging tool for the study of plant–pathogen interactions. Metabolites 10:1–23.

Castro JM da C e, Ribeiro JM (2020) Pesquisa e desenvolvimento para a cultura da goiabeira contribuição da Embrapa Semiárido. Embrapa Semiárido 297:1–61.

Chen JW, Gao FY, Ma JK et al (2023a) First report of *Meloidogyne enterolobii* infecting *Solanum nigrum* in China. Plant Dis 106:2270.

Chen Y, Liu Q, Xuqian S, et al (2023b) *Meloidogyne enterolobii* MeMSP1 efector targets the glutathione-S-transferase phi GSTF family in *Arabidopsis* to manipulate host metabolism and promote nematode parasitism. New Phytol 1–10.

Chetia A, Gogoi P, Roy P, Goswami M (2019) Antagonistic plants as a tool of nematode management. J Med Plants Stud 7:113–116.

Claverie M, Dirlewanger E, Bosselut N et al (2011) The Ma gene for complete-spectrum resistance to *Meloidogyne* species in Prunus is a TNL with a huge repeated C-terminal post-LRR region. Plant Physiology 156:779–792.

Collett RL, Marais M, Africa S, et al (2021) Review article *Meloidogyne enterolobii*, a threat to crop production with particular reference to sub-Saharan Africa: an extensive, critical and updated review. Nematology 0:1–39.

Collett RL, Rashidifard M, Marais M et al (2023) Insights into the life - cycle development of *Meloidogyne enterolobii*, *M. incognita* and *M. javanica* on tomato, soybean and maize. Eur J Plant Pathol 168:137–146.

Costa SN de O, Silva MVT e., Ribeiro JM, et al (2023) Secondary metabolites related to the resistance of *Psidium* spp. against the nematode *Meloidogyne enterolobii*. Heliyon 9:1–10.

Desaeger J, Wram C, Zasada I (2020) New reduced-risk agricultural nematicides - rationale and review. J Nematol 52:1–16.

Desmedt W, Mangelinckx S, Kyndt T, Vanholme B (2020) A phytochemical perspective on plant defense against nematodes. Front Plant Sci 11:1–20.

Dias-Arieira CR, Ceccato FJ, Marinelli EZ et al (2021) Correlations between nematode

numbers, chemical and physical soil properties, and soybean yield under diferent cropping systems. Rhizosphere 19:1–6.

Diyapoglu A, Oner M, Meng M (2022) Application potential of bacterial volatile organic compounds in the control of root-knot nematodes. Molecules 27:1–12.

Djian-Caporalino C, Mateille T, Bailly-Bechet M et al (2019) Evaluating sorghums as green manure against root-knot nematodes. Crop Prot 122:142–150.

Dutta A, Mandal A, Kundu A et al (2021) Deciphering the behavioral response of *Meloidogyne incognita* and *Fusarium oxysporum* toward mustard essential oil. Front Plant Sci 12:1–16.

Dutta TK, Phani V (2023) The pervasive impact of global climate change on plant-nematode interaction continuum. Front Plant Sci 14:1–14.

Duval H, Van GC, Portier U et al (2019) New data completing the spectrum of the Ma, RMia, and RMja genes for resistance to root-knot nematodes (*Meloidogyne* spp.) in Prunus. Phytopathology 109:615–622.

EPPO (2024) EPPO datasheets on pests recommended for regulation. In: *Meloidogyne enterolobii*. EPPO (2016) PM 7/103 (2) *Meloidogyne enterolobii*. Eur Mediterr Plant Prot Organ Bull 46:190–201.

EUR-Lex (2023) Commission Delegated Regulation (EU) 2023/1656 of 16 June 2023 amending Regulation (EU) No 649/2012 of the European Parliament and of the Council as regards the listing of pesticides and industrial chemicals (Text with EEA relevance). In: Of J Eur Union.

Fan W, Zhou Y, Zhao W et al (2022) First report of *Meloidogyne enterolobii* infecting Ixora chinensis in China. Plant Dis 106:1–2.

Fernández IAL, Monje-Ramirez I, de Velásquez MTOL (2019) Tomato crop improvement using ozone disinfection of irrigation water. Ozone Sci Eng 41:398–403.

Flori JE, Deon MD (2022) BRS Guaraçá: novo porta-enxerto para o enfrentamento do nematoide-das-galhas da goiabeira. Embrapa Semiárido 190:1–7.

Forghani F, Hajihassani A (2020) Recent advances in the development of environmentally benign treatments to control root-knot nematodes. Front Plant Sci 11:1–13.

Francisco BGF, Ponce IM, Espinosa MÁP et al (2021) Advances in the biological control of phytoparasitic nematodes via the use of nematophagous fungi. World J Microbiol Biotechnol 37:1–14.

Galbieri R, Davis RF, Scoz LB et al (2020) First report of *Meloidogyne enterolobii* on cotton in Brazil. Plant Dis 60:1–3.

Gomes VA, de Jesus Silva F, Baquião EM, et al (2020) *Xanthosoma sagittifolium* is resistant to Meloidogyne spp. and controls *Meloidogyne enterolobii* by soil biofumigation. J Nematol 52:1–12.

Gómez-González G, Márquez-Zequera I, Cruz-Lachica I et al (2020) First report of *Meloidogyne enterolobii* parasitizing cucumber in Sinaloa, Mexico. Plant Dis 58:1–2.

Gouveia A de S, Monteiro TSA, Luiz PHD, et al (2022) The nematophagous root endophyte *Pochonia chlamydosporia* alters tomato metabolome. Rhizosphere 22:1–9.

Gu M, Bui HX, Desaeger JA, Ye W (2021a) First report of *Meloidogyne enterolobii* on thai basil in Florida, United States. Plant Dis 105:1–2.

Gu M, Bui HX, Ye W, Desaeger JA (2021b) First report of *Meloidogyne enterolobii* on sweet potato in Florida, USA. Nematropica 51:36–40.

Hajihassani A, Nugraha GT, Tyson C (2023) First report of the rootknot nematode *Meloidogyne enterolobii* on sweet potato in Georgia, United States. Plant Dis 65:1–3.

Handoo ZA, Nyczepir AP, Esmenjaud D et al (2004) Morphological, molecular, and diferential-host characterization of *Meloidogyne foridensis* n. sp. (Nematoda: Meloidogynidae), a root-knot nematode parasitizing peach in Florida. J Nematol 36:20–35.

Ho JT, Liang CC, Chen PJ (2022) First report of root-knot nematode *Meloidogyne enterolobii* on cockscomb (Celosia argentea var. cristata) in Taiwan. Plant Dis 68:1–8.

Hodson A, Celayir T, Quiroz Alonso A (2023) A real time PCR assay to detect and quantify root-knot nematodes from soil extracts. Plant Dis 107:2169–2176.

van den Hoogen J, Geisen S, Routh D et al (2019) Soil nematode abundance and functional group composition at a global scale. Nature 572:194–198.

Ibrahim DSS, Zawam HS, El-Deriny MM et al (2023) First report of *Meloidogyne enterolobii* (guava root-knot nematode) infecting guava (*Psidium guajava*) in Egypt. Plant Dis 75:1–2.

Ibrahima HMM, Ahmada EM, Martínez-Medinab A, Aly MAM (2019) Efective approaches to study the plant-root knot nematode interaction. Plant Physiol Biochem 141:332–342.

Jha Y, Mohamed HI (2022) Plant secondary metabolites as a tool to investigate biotic stress tolerance in plants: A review. Gesunde Pfanz 74:771–790.

Jia L, Wang Y, Gao F et al (2022) First report of the root-Knot nematode *Meloidogyne enterolobii infecting* Acalypha australis in China. Plant Dis 107:1–2.

Jia L, Wu H, Wang Y, Li H (2021) First report of the root-knot nematode *Meloidogyne enterolobii* on sweet potato in Guangxi province, China. Plant Dis 106:1–2.

Jiang L, Ling J, Zhao J et al (2023) Chromosome-scale genome assembly-assisted identifcation of Mi-9 gene in Solanum arcanum accession LA2157, conferring heat-stable resistance to *Meloidogyne incognita*. Plant Biotechnol J 21:1496–1509.

Jones JT, Haegeman A, Danchin EGJ et al (2013) Top 10 plant-parasitic nematodes in molecular plant pathology. Mol Plant Pathol 14:946–961.

Kanagaraj S, Sundaravadivelu S (2021) Microbial focculants as an alternate to chemical focculants for wastewater treatment. Weser Books, Republic of Kazakhstan

Khan A, Chen S, Fatima S et al (2023a) Biotechnological tools to elucidate the mechanism of plant and nematode interactions. Ecology 12:2–17.

Khan A, Khan A, Ali A, et al (2023b) Root-Knot nematodes (*Meloidogyne* spp.): biology, plant-nematode interactions and their environmentally benign management

strategies. Gesunde Pfanz 1–8.

Khan MR, Poornima K, Somvanshi VS, Walia RK (2022) *Meloidogyne enterolobii*: a threat to guava (*Psidium guajava*) cultivation. Arch Phytopathol Plant Prot 55:1961–1997.

Khanal C, Harshman D (2022) Evaluation of summer cover crops for host suitability of *Meloidogyne enterolobii*. Crop Prot 151:105821.

Klessig DF, Manohar M, Baby S et al (2019) Nematode ascaroside enhances resistance in a broad spectrum of plant–pathogen systems. J Phytopathol 167:265–272.

Koutsovoulos GD, Poullet M, Elashry A et al (2020) Genome assembly and annotation of *Meloidogyne enterolobii*, an emerging parthenogenetic root-knot nematode. Sci Data 7:1–13.

Leiva NPF, de Melo S-G, Zabini AV et al (2020) Soil chemical properties and their relationship with phytonematode populations inside and outside patches of soybean felds. Rhizosphere 15:1–7.

Li G, Liu T, Whalen JK, Wei Z (2023a) Nematodes: an overlooked tiny engineer of plant health. Trends Plant Sci 1–12.

Li Y, Lei S, Cheng Z et al (2023b) Microbiota and functional analyses of nitrogen-fxing bacteria in root-knot nematode parasitism of plants. Microbiome 11:1–23.

Liang C-C, Chen PJ (2021) First report of root-knot nematode Meloidogyne enterolobii on Poinsettia “Luv U Pink” in Taiwan. Plant Dis 106:1–2.

Liang Y, Ariyawansa HA, Becker JO, Yang J (2020) The evaluation of egg-parasitic fungi Paraboeremia taiwanensis and Samsoniella sp. for the biological control of Meloidogyne enterolobii on Chinese Cabbage. Microorganisms 8:.

López-Lima D, Alarcón-Utrera D, Ordáz-Meléndez JÁ et al (2023) Metarhizium carneum formulations: A promising new biological control to be incorporated in the integrated management of *Meloidogyne enterolobii* on tomato plants. Plants 12:1–10.

Lourenço AMS, Santos CAF, da Silva DOM (2022) Compatibility and phenotypic variability of guava accessions grafted on BRS Guaraçá rootstock: vegetative and fruit production traits. Pesqui Agropecu Trop 52:1–10.

Lu XH, Solangi GS, Huang JL et al (2023) First report of root-knot nematode *Meloidogyne enterolobii* on Antirrhinum majus in China. Plant Dis 106:1–2.

Luquini L, Barbosa D, Ferreira C et al (2019) First report of the rootknot nematode *Meloidogyne enterolobii* on Bananas in Brazil. Plant Dis 106:1–3.

Manohar M, Tenjo-Castano F, Chen S et al (2020) Plant metabolism of nematode pheromones mediates plant-nematode interactions. Nature 11:1–9.

Marciniak P, Kolińska A, Spochacz M et al (2019) Diferentiated efects of secondary metabolites from Solanaceae and Brassicaceae plant families on the heartbeat of Tenebrio molitor pupae. Toxins (Basel) 11:1–12.

Mello AFS, Silva G, De Sousa RL et al (2022) Sweetpotato genotypes “CIP BRS Nuti” and “Canadense” are resistant to *Meloidogyne incognita*, *M. javanica* and *M. enterolobii*. Plant Dis 106:1238–1243.

Ministério da Agricultura Pecuária e Abastecimento do Brazil (2023) Phytosanitary pesticide system. In: Ministério da Agric. Pecuária e Abast.

Moore MR, Brito JA, Qiu S, et al (2020) First report of root-knot nematodes (*Meloidogyne* species) infecting Chinese Elm (*Ulmus parvifolia*) in Florida, USA. J Nematol 52:1–4.

Mukhopadhyay R, Kumar D (2020) Trichoderma: a benefcial antifungal agent and insights into its mechanism of biocontrol potential. Egypt J Biol Pest Control 30:1–12.

Nisa RU, Tantray AY, Shah AA (2022) Shift from morphological to recent advanced molecular approaches for the identifcation of nematodes. Genomics 114:110295.

Oka Y (2020) From old-generation to next-generation nematicides. Agronomy 10:1–16.

Olajide E, Kolombia YA, Amah D et al (2022) First report of the rootknot nematode

Meloidogyne enterolobii parasitizing Pplantain (Musa spp. AAB) in Nigeria. Plant Dis 106:1–2.

ONU (2015) Transforming Our World: The 2030 Agenda for Sustainable Development. a/Res/70/1 1–49.

Oyetunde AK, Kolombia YA, Adewuyi O et al (2021) First report of *Meloidogyne enterolobii* infecting cassava (Manihot esculenta) resulting in root galling damage in Africa. Plant Dis 106:1–2.

De PLL, Campos VP, Terra WC et al (2024) The combination of *Bacillus amyloliquefaciens* and *Purpureocillium lilacinum* in the control of *Meloidogyne enterolobii*. Biol Control 189:105438.

Pei J, Feng T, Long H et al (2022) Molecular characterization and virus-induced gene silencing of a collagen gene, Me-col-1, in root-knot nematode *Meloidogyne enterolobii*. Life 12:1–12.

Peiris PUS, Li Y, Brown P, Xu C (2020) Fungal biocontrol against *Meloidogyne* spp. in agricultural crops: A systematic review and meta-analysis. Biol Control 144:1–10.

Philbrick AN, Adhikari TB, Louws FJ, Gorny AM (2020) *Meloidogyne enterolobii*, a major threat to tomato production: current status and future prospects for its management. Front Plant Sci 11:1–13.

Pofu KM, Mashela PW (2022a) Comparative efcacy of cucurbitacin phytonematicides and Velum on growth and fruit quality of watermelon cultivar ‘Congo’ and suppression of *Meloidogyne enterolobii* under feld conditions. Acta Agriculturae Scandinavica Section B Soil Plant Sci 72:105–110.

Pofu KM, Mashela PW (2022b) Interactive ffects of flamentous fungi and cucurbitacin phytonematicide on growth of cowpea and suppression of *Meloidogyne enterolobii*. Front Microbiol 13:1–6.

Poveda J, Abril-Urias P, Escobar C (2020) Biological control of plantparasitic nematodes by flamentous fungi inducers of resistance: Trichoderma, mycorrhizal and endophytic fungi. Front Microbiol 11:1–14.

Pretorius M. (2018) The abundance, identity and population dynamics of *Meloidogyne* spp. associated with maize in South Africa. MSc. thesis, North-West University, Potchefstroom, South Africa.

Przybylska A, Stęplowska AO (2020) Plant defense responses in monocotyledonous and dicotyledonous host plants during root-knot nematode. Plant Soil 451:239–260.

Rammah A, Hirschmann H (1988) *Meloidogyne mayaguensis* n. sp. (Meloidogynidae), a root-knot nematode from Puerto Rico. J Nematol 20:58–69.

Ranoarisoa MP, Trap J, Pablo AL et al (2020) Micro-food web interactions involving bacteria, nematodes, and mycorrhiza enhance tree P nutrition in a high P-sorbing soil amended with phytate. Soil Biol Biochem 143:1–9.

Rashidifard M, Fourie H, Veronneau P-Y, et al (2018) Genetic diversity and phylogeny of South African *Meloidogyne* populatios using genotyping by sequencing. Sci Rep 8:13816.

Rashidifard M, Ashraf S, Claassens S et al (2021) A pilot approach investigating the potential of crop rotation with sainfoin to reduce *Meloidogyne enterolobii* infection of maize under greenhouse conditions. Front Plant Sci 12:1–7.

Rashidifard M, Marais M, Daneel MS et al (2019) Molecular characterisation of *Meloidogyne enterolobii* and other *Meloidogyne* spp. from South Africa. Trop Plant Pathol 44:213–224.

Ren Z, Chen X, Luan M, et al (2020) First Report of *Meloidogyne enterolobii* on Industrial Hemp (*Cannabis sativa*) in China. Plant Dis 1–2.

Rusinque L, Camacho MJ, Serra C et al (2023) Root-knot nematode assessment: species identifcation, distribution, and new host records in Portugal. Front Plant Sci 14:1–11.

Salazar-Mesta RJ, Carrillo-Fasio JA, Retes-Manjarrez JE et al (2023) Characterization, pathogenicity, and reproduction of *Meloidogyne enterolobii* populations parasitizing vegetables in Sinaloa, Mexico. Trop Plant Pathol 48:394–407.

Salazar-Mesta RJ, Carrillo-Fasio JA, Tovar-Pedraza JM et al (2022) First report of the

root-knot nematode *Meloidogyne enterolobii* parasitizing eggplant in Mexico. Plant Dis 106:1–2.

Salinas-Castro A, Navarro de la Fuente L, Tapia-Vázquez I, López Lima D (2022) First report of *Meloidogyne enterolobii* on chard (*Beta vulgaris* subsp. vulgaris) and carrot (*Daucus carota*) in México. J Plant Diseas Protect 129:1263–1268.

Santos CAF (2020) Produção de mudas do BRS Guaraçá: porta-enxerto de goiabeira resistente ao nematoide-das-galhas. Embrapa Semiárido 174:1–5.

Santos D, Martins da Silva P, Abrantes I, Maleita C, (2020) Tomato Mi-1.2 gene confers resistance to *Meloidogyne luci* and *M. ethiopica*. Eur J P Pathol 156(2):571–580. https://doi.org/10. 1007/s10658-019-01907-8.

Santos D, Abrantes I, Maleita C (2019) The quarantine root-knot nematode *Meloidogyne enterolobii* – a potential threat to Portugal and Europe. Plant Pathol 68:1607–1615.

Sato K, Kadota Y, Shirasu K (2019) Plant immune responses to parasitic nematodes. Front Plant Sci 10:1–14.

Schwarz T, Li C, Ye W, Davis E (2020) Distribution of *Meloidogyne enterolobii* in Eastern North Carolina and comparison of four isolates. Plant Heal Prog 21:91–96.

Schwarz TR, Li C, Craig Yencho G et al (2021) Screening sweetpotato genotypes for resistance to a north carolina isolate of *Meloidogyne enterolobii*. Plant Dis 105:1101–1107.

Shao H, Fu Y, Zhang P et al (2021) Transcriptome analysis of resistant and susceptible mulberry responses to *Meloidogyne enterolobii* infection. BMC Plant Biol 21:1–16.

Shao H, Zhang P, Peng D, et al (2023) Current advances in the identifcation of plant nematode diseases: From lab assays to infeld diagnostics. Front Plant Sci 1–12.

Shi X, Qiao K, Li B, Zhang S (2019) Integrated management of *Meloidogyne incognita* and *Fusarium oxysporum* in cucumber by combined application of abamectin and fudioxonil. Crop Prot 126:104922.

Sikandar A, Gao F, Mo Y et al (2023a) Eficacy of *Aspergillus tubingensis* GX3 fermentation against *Meloidogyne enterolobii* in tomato (*Solanum lycopersicum* L.). Plants 12:1–18.

Sikandar A, Jia L, Wu H, Yang S (2023b) *Meloidogyne enterolobii* risk to agriculture, its present status and future prospective for management. Front Plant Sci 13:1–16.

Sikder MM, Vestergård M (2020) Impacts of root metabolites on soil nematodes. Front Plant Sci 10:1–18.

Sikora RA, Helder J, Molendijk LPG et al (2023) Integrated nematode management in a world in transition: constraints, policy, processes, and technologies for the future. Ann Rev Phytopathol 61:209–230.

Silva AK dos SO, Pedrosa EMR, Dickson DW, et al (2020) Migration and penetration of *Meloidogyne enterolobii* and *M. incognita* in soil columns with tomato and marigold. Eur J Plant Pathol 158:591–598.

Silva EM, Pollo AS, Nascimento DD et al (2021) First report of rootknot nematode *Meloidogyne enterolobii* infecting sweetpotato in the state of Rio Grande do Norte, Brazil. Plant Dis 106:1–2.

Silva SD, ReMDG C, FAria M, et al (2017) Evaluation of *Pochonia chlamydosporia* and Purpureocillium lilacinum for suppression of *Meloidogyne enterolobii* on tomato and banana. J Nematol 49:77–85.

Simões WL, De AVPM, Silva JS et al (2023) Fruit production and quality of 'Paluma' guava with nematode-tolerant rootstock irrigated in the semi-arid region. Rev Bras Eng Agrícola e Ambient 27:400–406.

Soares MRC, Lopes APM, Dias-Arieira CR (2018) First report on *Meloidogyne enterolobii* in *Morus celtidifolia* in Paraná state, Brazil. Plant Dis 106:1–3.

Song PAN, De-liang P, Ying-mei LI et al (2023) Potential global distribution of the guava root-knot nematode *Meloidogyne enterolobii* under diferent climate change scenarios using MaxEnt ecological niche modeling. J Integr Agric 22:2138–2150.

Souza RRC, Santos CAF, Costa SR (2018) Field resistance to *Meloidogyne enterolobii*

in a *Psidium guajava* x *P. guineense* hybrid and its compatibility as guava rootstock. Fruits 73:118–124.

Sun YF, Long HB, Lu FP (2019) First report of the root-knot nematode *Meloidogyne enterolobii* infecting mulberry in China. Plant Dis 105:1–3.

Tapia-Vázquez I, Montoya-Martínez AC, Santos-Villalobos SD los, et al (2022) Root-knot nematodes (*Meloidogyne* spp.) a threat to agriculture in Mexico: biology, current control strategies, and perspectives. World J Microbiol Biotechnol 38:1–18.

Tariq M, Khan A, Asif M et al (2020) Biological control: a sustainable and practical approach for plant disease management. Acta Agriculturae Scandinavica Section B Soil Plant Sci 25:507–524.

Tefu GM, De Waele D, Fourie H, Daneel MS (2022) Efect of pitcomposting on root-knot nematode (*Meloidogyne incognita* and *M. javanica*) population densities and yield of tomato under feld conditions. Int J Pest Manag 68:135–147.

Timper P, Davis RF (2022) Evaluation of host-plant resistance and high residue rye for management of *Meloidogyne incognita* in cotton. Crop Prot 161:1–8.

Torres-López J, López-Buenfl JA, Carrillo-Fasio JA, Tovar-Pedraza JM (2022) First report of the root-knot nematode *Meloidogyne enterolobii* on cofee in Mexico. Indian Phytopathol 75:915–917.

Velloso JA, Maquilan MAD, Campos VP et al (2022) Temperature effects on development of *Meloidogyne enterolobii* and M. *foridensis*. J Nematol 54:1–11.

Verssiani JBS, Souza CFB, Santos PS, et al (2023) Reaction of soybean cultivars to two races of *Meloidogyne enterolobii* and their aggressiveness under plastic house conditions. Nematology 0:1–12.

Wang H, Liu G, Huang B et al (2021) Long-term nitrogen addition and precipitation reduction decrease soil nematode community diversity in a temperate forest. Appl Soil Ecol 162:1–8.

Watson TT (2022) Sensitivity of *Meloidogyne enterolobii* and *M. incognita* to fuorinated nematicides. Pest Manage Sci 78:1398–1406.

Wu C, Chen Q, Wei C et al (2022a) First report of *Meloidogyne enterolobii* infecting Mesona chinensis in China. Plant Dis 107:1–2.

Wu CR, Zhou HL, Jia LM et al (2022b) First report of *Meloidogyne enterolobii* on Ormosia hosiei in China. Plant Dis 107:1–3.

Xiang N, Lawrence KS, Donald PA (2018) Biological control potential of plant growth - promoting rhizobacteria suppression of *Meloidogyne incognita* on cotton and *Heterodera glycines* on soybean: A review. J Phytopathol 166:449–458.

Yang and Eisenback (1988) First Report on the Root-Knot Nematode *Meloidogyne enterolobii* (Yang and Eisenback, 1988) Infecting Guava (*Psidium guajava*). Int J Curr Microbiol Appl Sci 7(4):1–5.

Ye W, Koenning SR, Zeng Y et al (2021) Molecular characterization of an emerging root-knot nematode *Meloidogyne enterolobii* in North Carolina, USA. Plant Dis 105:819–831.

Zhang C, Xue W, Xue J et al (2022) Leveraging functional traits of cover crops to coordinate crop productivity and soil health. J Appl Ecol 59:2627–2641.

Zhou J, Wu J, Huang J et al (2022) A synthesis of soil nematode responses to global change factors. Soil Biol Biochem 165:1–9.

Zhu JC, Liu JA, Zhou GY (2020) First report of *Meloidogyne enterolobii* on Camellia oleifera in China. Plant Dis 105:1–2.

Zhuo K, Hu MX, Liao JL, Rui K (2018) First report of *Meloidogyne enterolobii* on ginger (*Zingiber oficinale*) in China. Plant Dis 94:1–3.

D., Santos P., Martins da Silva I., Abrantes C., Maleita (2020) Tomato Mi-1.2 gene confers resistance to *Meloidogyne luci* and *M. ethiopica* European Journal of Plant Pathology 156(2) 571- 580. https://doi.org/10.1007/s10658-019-01907-8.

Supplementary materials

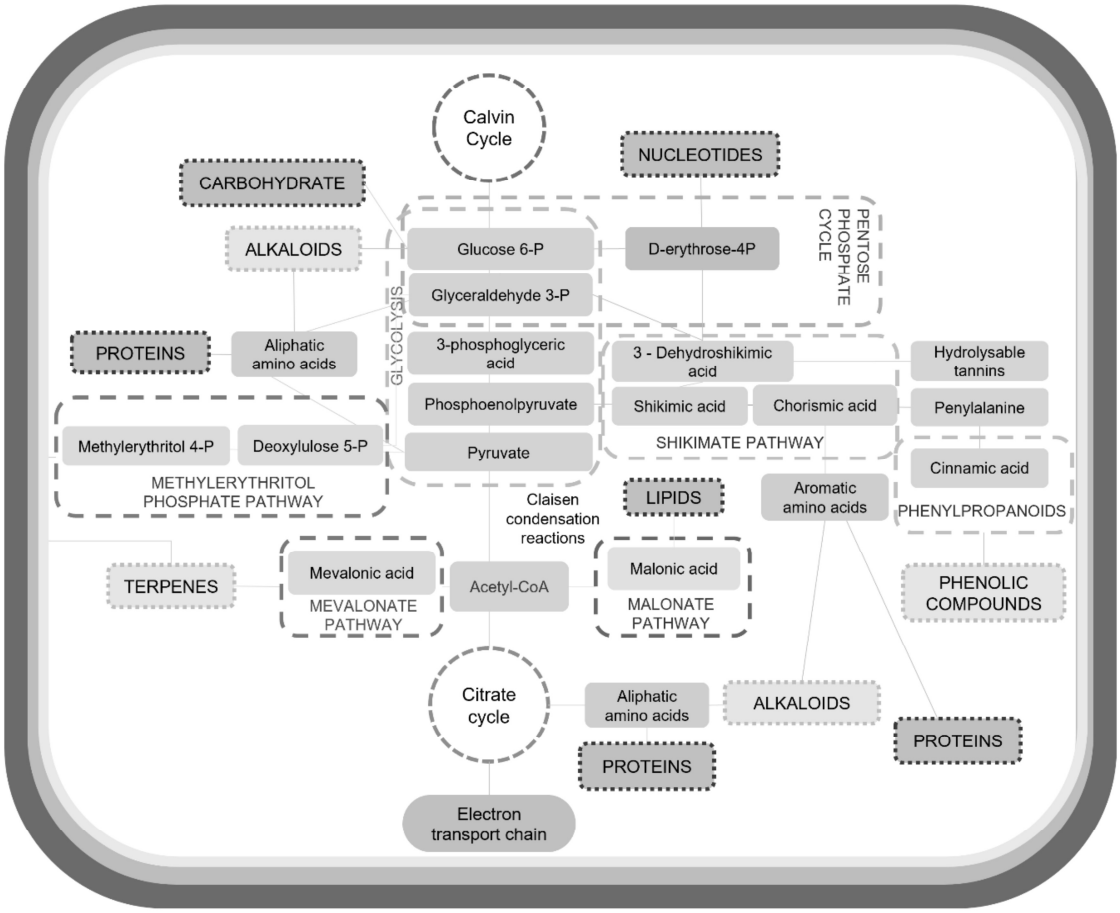

Figure 1S - General scheme of the interaction between primary (highlighted in rectangles outlined in red dashed lines) and secondary (in rectangles with orange dashed lines) plant metabolic pathways (Scheme built based on data available Kyoto Encyclopedia of Genes and Genomes, MAP01060 – KEGG).

Table 1S - Species of host plants for the nematode *Meloidogyne enterolobii*

Family	Botanical name	Family	Botanical name
Aizoaceae	*Lampranthus* spp.	Malpighiaceae	*Malpighia emarginata*
Amaranthaceae	*Amaranthus deflexus*	Malpighiaceae	*Malpighia glabra*
Amaranthaceae	*Amaranthus hybridus*	Malvaceae	*Sida rhombifolia*
Amaranthaceae	*Amaranthus spinosus*	Malvaceae	*Gossypium* spp.
Amaranthaceae	*Amaranthus viridis*	Malvaceae	*Abelmoschus esculentus*
Amaranthaceae	*Alternanthera pungens*	Malvaceae	*Gossypium hirsutum*
Amaranthaceae	*Spinacia oleracea*	Malvaceae	*Hibiscus grandiflorus*
Amaranthaceae	*Amaranthus tricolor*	Marantaceae	*Maranta arundinacea*
Amaryllidaceae	*Allium porrum*	Melastomataceae	*Tibouchina* spp.
Apiaceae	*Apium graveolens*	Melastomataceae	*Tibouchina elegans*
Apiaceae	*Daucus carota*	Moraceae	*Artocarpus heterophyllus*
Apiaceae	*Petroselynum crispum*	Moraceae	*Morus celtidifolia*
Apiaceae	*Coriandrum sativum*	Moraceae	*Morus nigra*
Araceae	*Syngonium* spp.	Moraceae	*Morus alba*
Araliaceae	*Hydrocotyle bonariensis*	Moraceae	*Fatoua villosa*
Arecaceae	*Washingtonia* spp.	Moraceae	*Ficus carica*
Asparagaceae	*Cordyline australis*	Musaceae	*Musa* spp.
Asteraceae	*Acanthospermum australe*	Myricaceae	*Myrica cerifera*
Asteraceae	*Bidens pilosa*	Myrtaceae	*Callistemon* spp.
Asteraceae	*Bidens subalternans*	Myrtaceae	*Psidium guajava*
Asteraceae	*Galinsoga parviflora*	Myrtaceae	*Callistemon citrinus*
Asteraceae	*Lactuca sativa*	Myrtaceae	*Callistemon rigidus*
Asteraceae	*Emilia sonchifolia*	Myrtaceae	*Callistemon viminalis*
Asteraceae	*Erechtites hieraciifolius*	Myrtaceae	*Melaleuca linearis*
Asteraceae	*Helianthus* spp.	Myrtaceae	*Melaleuca viminalis*
Bignoniaceae	*Tecoma capensis*	Myrtaceae	*Psidium guineense*
Brassicaceae	*Brassica oleracea*	Myrtaceae	*Psidium myrtoides*
Brassicaceae	*Raphanus sativus*	Myrtaceae	*Syzygium aromaticum*
Bromeliaceae	*Ananas comosus*	Oleaceae	*Ligustrum* spp.
Cactaceae	*Cereus hildmannianus*	Orchidaceae	*Oeceoclades maculata*
Cactaceae	*Stenocereus queretaroensis*	Passifloraceae	*Passiflora mucronata*
Cactaceae	*Cactus* spp.	Paulowniaceae	*Paulownia elongata*
Cactaceae	*Cereus fernambucensis*	Plantaginaceae	*Angelonia angustifolia*
Cannabaceae	*Cannabis sativa*	Poaceae	*Rhynchelytrum repens*
Caricaceae	*Carica papaya*	Poaceae	*Panicum* spp.
Cesalpiniacea	*Cassia occidentalis*	Poaceae	*Saccharum* spp.
Chenopodiaceae	*Beta vulgaris*	Polygonaceae	*Polygonum hydropiperoides*
Commelinaceae	*Commelina benghalensis*	Portulacaceae	*Portulaca oleracea*
Convolvulaceae	*Ipomoea grandifolia*	Punicaceae	*Punica granatum*
Convolvulaceae	*Ipomoea nil*	Rhamnaceae	*Ziziphus jujuba*
Convolvulaceae	*Ipomoea purpurea*	Rhamnaceae	*Zizyphus jujuba*
Convolvulaceae	*Ipomoea batatas*	Rosaceae	*Rosa* spp.
Convolvulaceae	*Merremia aegyptia*	Rubiacea	*Coffea arabica*

Cucurbitaceae	*Citrullus lanatus*	Rubiacea	*Gardenia jasminoides*
Cucurbitaceae	*Cucumis sativus*	Rubiaceae	*Coffea arabica*
Cucurbitaceae	*Cucurbita pepo*	Rubiaceae	*Gardênia jasminoides*
Cucurbitaceae	*Cucurbita moschata*	Rubiaceae	*Ixora chinensis*
Cucurbitaceae	*Cucumis melo*	Rubiaceae	*Morinda citrifolia*
Cucurbitaceae	*Luffa cylindrica*	Rubiaceae	*Pentas lanceolata*
Dioscoreaceae	*Dioscorea rotundata*	Salicaceae	*Salix* spp.
Elaeocarpaceae	*Elaeocarpus decipiens*	Sapindaceae	*Cardiospermum halicacabum*
Euphorbiaceae	*Euphorbia heterophylla*	Scrophulariaceae	*Buddleja davidii*
Euphorbiaceae	*Euphorbia punica*	Solanaceae	*Nicandra physaloides*
Euphorbiaceae	*Euphorbia tirucalli*	Solanaceae	*Solanum americanum*
Euphorbiaceae	*Acalypha australis*	Solanaceae	*Solanum sisymbriifolium*
Euphorbiaceae	*Chamaesyce hypericifolia*	Solanaceae	*Solanum pseudocapsicum*
Euphorbiaceae	*Eclipta prostrata*	Solanaceae	*Lycopersicum esculentum*
Euphorbiaceae	*Euphorbia punicea*	Solanaceae	*Capsicum annuum*
Euphorbiaceae	*Jatropha urens*	Solanaceae	*Nicotiana tabacum*
Euphorbiaceae	*Manihot esculenta*	Solanaceae	*Physalis peruana*
Fabaceae	*Canavalia ensiformis*	Solanaceae	*Solanum lycopersicum*
Fabaceae	*Enterolobium contortisiliquum*	Solanaceae	*Solanum melongena*
Fabaceae	*Glycine max*	Solanaceae	*Solanum* spp.
Fabaceae	*Phaseolus vulgaris*	Solanaceae	*Solanum tuberosum*
Fabaceae	*Phaseolus vulgaris*	Solanaceae	*Physalis viscosa*
Fabaceae	*Arachis hypogaea*	Solanaceae	*Capsicum frutescens*
Fabaceae	*Inga edulis*	Solanaceae	*Brugmansia suaveolens*
Fabaceae	*Ormosia hosiei*	Solanaceae	*Capsicum baccatum*
Fabaceae	*Senna alata*	Solanaceae	*Capsicum chinense*
Fabaceae	*Senna occidentalis*	Solanaceae	*Lycopersicon peruvianum*
Fabaceae	*Vigna unguiculata*	Solanaceae	*Lycopersicon hirsutum*
Hypericaceae	*Hypericum* spp.	Solanaceae	*Physalis angulata*
Iridaceae	*Crocus sativus*	Solanaceae	*Physalis peruviana*
Lamiaceae	*Leonurus sibiricus*	Solanaceae	*Solandra maxima*
Lamiaceae	*Ajuga reptans*	Solanaceae	*Solanum gilo*
Lamiaceae	*Ajuga carpet*	Solanaceae	*Solanum quitoense*
Lamiaceae	*Clerodendrum ugandense*	Solanaceae	*Solanum scabrum*
Lamiaceae	*Ocimum* spp.	Solanaceae	*Solanum paniculatum*
Lamiaceae	*Caryopteris clandonensis*	Talinaceae	*Talinum paniculatum*
Lamiaceae	*Leonotis nepetifolia*	Talinaceae	*Talinum patens*
Lamiaceae	*Mesona chinensis*	Talinaceae	*Talinum fruticosum*
Lamiaceae	*Ocimum basilicum*	Talinaceae	*Talinum triangulare*
Lamiaceae	*Rotheca myricoides*	Theaceae	*Camellia oleifera*
Lamiaceae	*Salvia leucanta*	Ulmaceae	*Ulmus parvifolia*
Lythraceae	*Lagerstroemia indica*	Verbenaceae	*Lantana camara*
Malpighiaceae	*Byrsonima cydoniifolia*	Verbenaceae	*Lantana montevidensis*
		Zingiberaceae	*Zingiber officinale*

Source: Based on data from (Bellé *et al.*, 2019; Khan *et al.*, 2022; Rashidifard *et al.*, 2019; Rusinque *et al.*, 2023; Santos, Abrantes e Maleita, 2019; Sikandar *et al.*, 2023).

Table 2S - The 24 synthetic nematicides registered in Brazil to control *Meloidogyne* spp.

Trade mark	TC*	EC**	Active ingredient	Chemical group	Type of formulation
Aba 400 WG Nortox	2	II	Abamectin	Avermectin	Granules in water
Abamectin Nortox 400 WG	2	II	Abamectin	Avermectin	Granules in water
Acarigen	4	III	Abamectin	Avermectin	Emulsifiable concentrate
Apache 100 GR	4	II	Cadusaphos	Organophosphate	Granulated
Augory	1	II	Abamectin	Avermectin	Concentrated Suspension for Seed Treatment
Avicta 500 FS	1	II	Abamectin	Avermectin	Concentrated Suspension for Seed Treatment
Avicta 500 FS Pro	1	II	Abamectin	Avermectin	Concentrated Suspension for Seed Treatment
Azir	5	III	Fluensulfone	Fluoroalkenyle (-thiother)	Encapsulated Suspension for Seed Treatment
Basamid	4	III	Dazomete	Methyl isothiocyanate	Micro Granules
Bunema 330 SL	4	I	Metam sodium	Methyl isothiocyanate	Soluble Concentrate
Cierto 100 GR	4	II	Fostiazate	Organophosphate	Granulated
Counter 150 G	2	II	Terbuphos	Organophosphate	Granulated
Epimec	4	II	Abamectin	Avermectin	Emulsifiable concentrate
Ilevo	4	II	Fluopyram	Benzamide	Concentrated Suspension for Seed Treatment
Legado	5	III	Luensulfone	Fluoroalkenyle (-thiother)	Emulsifiable concentrate
Mantis 400 WG	2	II	Abamectin	Avermectin	Granules in water
Marshal Star	2	II	Carbosulfan	Benzofuranyl methylcarbamate	Emulsifiable concentrate
Nimitz EC	5	III	Fluensulfone	Fluoroalkenyle (-thiother)	Emulsifiable concentrate

Nimitz TS	5	III	Fluensulfone	Fluoroalkenyle (-thiother)	Encapsulated Suspension for Seed Treatment
Pottente Max	2	II	Benfuracarb	Benzofuranyl methylcarbamate	Emulsifiable concentrate
Rugby 100 GR	4	II	Cadusaphos	Organophosphate	Granulated
Rugby 200 CS	4	II	Cadusaphos	Organophosphate	Suspension of Encapsulated
Verango Prime	5	III	Fluopyram	Benzamide	Concentrated Suspension
Vigga	5	IV	*Allium sativum*	Plant extract	Concentrated Suspension

* Toxicological classification – TC; Ratings range from 1 to 5, with the index being indirectly proportional to the toxic.
** Environmental classification – EC; Ratings range from I to IV, with the index being indirectly proportional to the danger.

Source: (Ministério da Agricultura Pecuária e Abastecimento do Brazil, 2023)

Table 3S - The 56 microbiological nematicides registered in Brazil to control *Meloidogyne* spp.

Trade mark	TC*	EC**	Active ingredient	Type of formulation
AgDommon/Nemaoff/Bionexus	5	IV	*Bacillus subtilis*	Wettable Powder
AmyloTrop	5	IV	*Bacillus amyloliquefaciens*	Concentrated Suspension
Andril Prime	NC	IV	*Bacillus firmus*	Concentrated Suspension for Seed Treatment
Arvatico	5	IV	*Bacillus velezensis*	Concentrated Suspension
Atialy/Lilatrix;	NC	IV	*Paecilomyces lilacinus*	Soluble Concentrate
Auba (Artefato,Teros e Nerut)	5	IV	**Uninformed**	Concentrated Suspension
Aveo EZ	NC	IV	*Bacillus amyloliquefaciens*	Concentrated Suspension for Seed Treatment
Bamytis; Royalprezor; Basuty	5	IV	*Bacillus amyloliquefaciens, Bacillus subtilis e Bacillus thuringiensis*	Concentrated Suspension
Bio Tramo	5	IV	*Bacillus subtilis, Bacillus licheniformis, Paecilomyces lilacinus*	Wettable Powder
Biobaci/Baci-Attack/Baci-Guard/ Vitalforce Bio Phako/Cropwinner Eco Vastax	NC	IV	*Bacillus subtilis*	Concentrated Suspension
Bioessence Drive	5	IV	*Bacillus subtilis*	Concentrated Suspension
Biomagno/Bioharmer	5	IV	*Bacillus velezensis, Bacillus amyloliquefaciens, Bacillus thuringiensis*	Concentrated Suspension
Biostat WP/Gratto Nema	5	IV	*Purpureocillium lilacinum*	Wettable Powder
Biotrinsic N11 FP/Biotrinsic Habitans/Biotrinsic Nematrix/ Indigo 407	5	IV	*Pseudomonas oryzihabitans*	Powder for Dry Seed Treatment
BN40.001/19	5	IV	*Paecilomyces lilacinus*	Wettable Powder

Boneville	5	IV	*Bacillus amyloliquefaciens*	Wettable Powder
BTP 007-19	5	IV	*Bacillus velezensis*	Concentrated Suspension
BV0518	5	IV	*Purpureocillium lilacinum*	Oil Dispersion or Concentrated Suspension in Oil
Certano	5	IV	*Bacillus velezensis*	Concentrated Suspension
Chevelle	5	IV	*Bacillus amyloliquefaciens*	Wettable Powder
Furatro/Nematrop/Biotrinsic Nemafree/Submax;	NC	IV	*Bacillus subtilis*	Concentrated Suspension
Hope	5	IV	*Paecilomyces lilacinus*	Wettable Powder
Inlayon Eco	NC	IV	*Bacillus amyloliquefaciens*	Concentrated Suspension
KBR PDG07	5	IV	*Trichoderma harzianum*	Oil Dispersion or Concentrated Suspension in Oil
KBR PDG08	5	IV	*Trichoderma harzianum*	Wettable Powder
Lalnix Over SC	NC	IV	*Bacillus methylotrophicus*	Concentrated Suspension
Loyalty Bio/Trunemco/Vinemco/	NC	IV	*Bacillus amyloliquefaciens*	Concentrated Suspension for Seed Treatment
Lumialza	NC	IV	*Bacillus amyloliquefaciens*	Concentrated Suspension for Seed Treatment
Messenger	5	IV	*Bacillus subtilis, Bacillus licheniformis e Paecilomyces lilacinus*	Wettable Powder
Nemacontrol	5	IV	*Bacillus amyloliquefaciens*	Concentrated Suspension
Nemacontrol Super	NC	IV	*Bacillus amyloliquefaciens*	Concentrated Suspension
Nemakill	NC	IV	*Paecilomyces lilacinus*	Soluble Concentrate
Nemaster	NC	IV	*Bacillus subtilis*	Concentrated Suspension
Nemat; Nemaouro	5	IV	*Paecilomyces lilacinus*	Wettable Powder
NemaZak	5	IV	*Bacillus amyloliquefaciens, Bacillus subtilis, Bacillus thuringiensis*	Concentrated Suspension

Nembac 42/Amyprotec 42	5	IV	*Bacillus velezensis*	Concentrated Suspension
Nimaxxa	NC	IV	*Bacillus subtillis, Bacillus paralicheniformis, Bacillus paralicheniformis,*	Concentrated Suspension
No-Nema/Nema-Attack/Nema-Guard/Bio Baciens/Cropwinner Eco Nemaxy/Vitalforce Bio Amilofaciens	5	IV	*Bacillus amyloliquefaciens*	Concentrated Suspension
Onix OG	NC	IV	*Bacillus methylotrophicus*	Concentrated Suspension
Paladyo	NC	IV	*Bacillus subtilis*	Concentrated Suspension
Presence Flex/Kalivar/Presence Full	NC	IV	*Bacillus subtilis, Bacillus licheniformis,*	Powder for Paste Preparation in Water
Presence/Fortmax	NC	IV	*Bacillus subtilis, Bacillus licheniformis*	Powder for Paste Preparation in Water
Profix/Volga Goplan	5	IV	*Bacillus subtilis, Bacillus licheniformis e Paecilomyces lilacinus,*	Wettable Powder
Protege	5	IV	*Bacillus amyloliquefaciens, Bacillus thuringiensis, Bacillus velezensis,*	Concentrated Suspension
Purpureonyd FR 25	5	IV	*Paecilomyces lilacinus*	Emulsifiable Gel
Quartzo/Surface	NC	IV	*Bacillus subtilis, Bacillus licheniformis*	Powder for Paste Preparation in Water
Rizos	NC	IV	*Bacillus subtilis*	Concentrated Suspension
Rizos OG	NC	IV	*Bacillus subtilis*	Concentrated Suspension
Rizotec/Rizotec Crops	5	IV	*Pochonia chlamydosporia*	Wettable Powder
RIZO-TURBO/PC-Attack/PC-Guard	NC	IV	*Pochonia chlamydosporia*	Concentrated Suspension
SoluBio Raiz Performance	5	IV	*Bacillus subtilis,*	Concentrated Suspension
Unnat	NC	IV	*Bacillus paralicheniformis, Bacillus paralicheniformis, Bacillus subtillis*	Concentrated Suspension
Veraneio	5	IV	*Bacillus amyloliquefaciens*	Wettable Powder
Votivo Prime	NC	IV	*Bacillus firmus*	Concentrated Suspension for Seed Treatment

* Toxicological classification – TC; Ratings range from 1 to 5, with the index being indirectly proportional to the toxic. NC - Not classified, below 5.
** Environmental classification – EC; Ratings range from I to IV, with the index being indirectly proportional to the danger.

Source: (Ministério da Agricultura Pecuária e Abastecimento do Brazil, 2023).

3.2 *Psidium* defenses against *Meloidogyne enterolobii*: proteomic and microscopic analysis of this plant-predator association

Sara Nállia de Oliveira Costa [1], Roberta Pena da Paschoa [2], Camilla Ribeiro Alexandrino [3], Pamela Maciel Cremonez [3], Juliana Martins Ribeiro [4], José Mauro da Cunha e Castro [5], Maura Da Cunha [3], Vanildo Silveira [2], Antônia Elenir Amâncio Oliveira [1] and Kátia Valevski Sales Fernandes [1]

[1] Laboratório de Química e Função de Proteínas e Peptídeos, Universidade Estadual do Norte Fluminense Darcy Ribeiro, Campos dos Goytacazes - Rio de Janeiro, Brasil
[2] Laboratório de Biotecnologia, Universidade Estadual do Norte Fluminense Darcy Ribeiro, Campos dos Goytacazes - Rio de Janeiro, Brasil
[3] Laboratório de Biologia Celular e Tecidual, Universidade Estadual do Norte Fluminense Darcy Ribeiro, Campos dos Goytacazes - Rio de Janeiro, Brasil
[4] Empresa Brasileira de Pesquisa Agropecuária Semiárido, Petrolina - Pernambuco, Brasil
[5] Empresa Brasileira de Pesquisa Agropecuária Soja, Londrina - Paraná, Brasil

Published in Proteomics (2025) - doi.org/10.1002/pmic.70015

Abstract

Guava (*Psidium guajava*), referred to as the "tropical apple," is esteemed for its sweet flavor, nutritional density, and medicinal attributes, being rich in ascorbic acid, phenolics, carotenoids, fibers, and minerals. Despite its agricultural significance, guava cultivation faces considerable challenges from plant-parasitic nematodes, particularly root-knot nematodes from the Meloidogyne spp. In South America, *Meloidogyne enterolobii* causes severe root damage and economic losses to this crop. Plants fight nematodes through complex immune mechanisms involving pattern recognition receptors and signaling pathways, such as pattern-triggered immunity. The present research employed comparative shotgun proteomic analysis complemented by microscopic imaging and histochemical assays of roots from susceptible *Psidium guajava* and resistant *P. guineense*, inoculated or not with *M. enterolobii*. *Psidium-M. enterolobii* interactions revealed intricate plant cellular responses such as giant cells

formation, hypersensitivity reactions, and biochemical pathway adjustments in sucrose transport and antioxidant enzyme activities. Synthesis and accumulation of secondary metabolites like terpenes, alkaloids, and phenolics in inoculated and resistant plants were positively correlated to plant resilience. Heat shock proteins and protein disulfide isomerases also emerged as pivotal in plant response, being upregulated during nematode infection.

Keywords: Crop resistance, Guava (*Psidium guajava*), Immune mechanisms, Plant-parasitic nematodes, Root anatomy.

3.2.1 Introduction

The guava (*Psidium guajava)*, known as the "tropical apple," is a fruit belonging to the Myrtaceae family cultivated in various regions, including India, Pakistan, and South America. In 2024, global production reached approximately 63.1 million tons [1] and guava market size is estimated to reach US$ 1,250 million by 2027 [2]. A sweet, tasty fruit, it also bears nutritive and therapeutic properties. Various parts of the guava tree, such as roots, leaves, bark, stem, and fruits, are utilized in treatments of respiratory and gastrointestinal disorders [3]. Contemporary research has identified phenolic compounds and terpenes as bioactive constituents of guava leaf extract, abundant in antioxidants, and employed as a food preservative and medication [4].

However, there is a problematic challenge in guava cultivation which is the frequent infestation of its roots by nematodes. It is estimated that plant-parasitic nematodes (PPNs) cause over 100 billion dollars in crop losses annually, with approximately US$ 500 million spent on PPNs management each year. Root-knot nematodes (RKNs), such as those from the *Meloidogyne* genus, are sedentary endoparasites and represent one of the economically important PPNs. The females deposit up to 1,000 eggs near the roots, forming a gelatinous mass. Second-stage juveniles invade the root tip, migrating through the vascular system. RKNs become sedentary at feeding sites, inducing the formation of giant cells for their development [5]. *M. enterolobii*, known as the guava RKN, poses a global threat to this fruit culture and is highly virulent even to plants resistant to other nematode species [6]. Inflicting significant damage to guava trees in South America, it can lead to losses exceeding

65%, often detected only post-harvest when a high number of galls is observed in the roots [6,7].

Plants exhibit complex immune systems against nematodes, producing anti-nematode molecules either constitutively or post-infection. Plant resistance encompasses the ability to restrict the growth and reproduction of pests or pathogens and can be qualitative, preventing reproduction entirely, or quantitative, reducing the severity of the disease [8]. Over the course of evolution, plants have evolved defense mechanisms to counteract the invasion of gall-forming nematodes [9]. The signaling process begins with the nematode chemotaxis towards the root, attracted by exudates. Signaling takes place through nematode-associated molecular patterns (NAMPs) recognized by plant pattern-triggered immunity (PTI) [10]. PTI results in gene expression, production of reactive oxygen species, and physical responses. However, pathogens can overcome this defense through effectors, suppressing PTI by inhibiting proteins or altering their active state [9].

Progress in genomics, proteomics, natural product chemistry and biotechnology represents a potential avenue for enhancing our comprehension of root-nematode interactions and translating this information into environmentally sound management strategies. The current study aimed to conduct a comparative shotgun proteomic analysis of the roots from *Psidium guajava* (susceptible to *M. enterolobii*) and *P. guineense* (resistant to this nematode), both inoculated and non-inoculated by this pathogen. To observe modifications in root anatomy resulting from infection, microscopic images were recorded, and histochemical assays were conducted to evaluate secondary metabolites, such as phenolic compounds, terpenes, and alkaloids.

3.2.2 Materials and methods

Biological material

Psidium guajava and *P. guineense* were germinated from seeds in a greenhouse at Embrapa Semiárido, in Petrolina, PE (Latitude: 9°09'S, longitude: 40°22'W, altitude: 365.5m), using appropriate cultural practices. Thirty days after planting, seedlings were inoculated with a suspension containing 10,000 eggs and second-stage juvenile nematodes. Inoculation was performed by applying the

suspension into two holes, each 2 cm deep in the soil, at 2 cm from the seedling stem. After inoculation, the holes were filled with soil, and a light irrigation was carried out.

Root samples were collected 20 days after inoculation (20 DAI), for microscopy analysis. At this time, the oviposition activity of the nematodes was at its peak under our environmental conditions. The samples were washed in running water to remove the substrate. Samples without inoculation were collected as a control for the study (20 days non-inoculated [DNI]).

For proteomic analyses, 30 roots were collected from each test condition, at 5 and 20 DAI as well as other 30 without inoculation (20 DNI). All samples were washed in running water and lyophilized, and three groups of ten roots for each species were prepared for each test condition. The material was crushed, pulverized in liquid nitrogen using a mortar and pestle, and stored at - 4 ºC in Falcon tubes.

Light, transmission electron, and scanning electron microscopy

The root samples were placed at room temperature in 2.5% glutaraldehyde, 4.0% formaldehyde, and 0.05 M sodium cacodylate buffer with pH 7.2 for 2 h, and then washed three times for 30 min each in the same buffer, before post-fixed for 1 h in a solution of 1% osmium tetroxide and 1 M sodium cacodylate buffer with pH 7.2. After three 30 min washes in the same buffer, the samples were subjected to a series of acetone dehydration steps: 30%, 50%, 70%, 90%, 100%, and two times 100% super dry. After the fixation and dehydration steps, epoxy resin (Epon 812)® was gradually infiltrated to replace acetone. The resin-impregnated samples were placed in molds and polymerized in an oven at 60 °C for 48 h. Semi-thin sections between 0.60 and 0.70 µm were obtained using an ultramicrotome (Reichert Ultracuts) and a diamond knife.

Light microscopy (LM)

The 0.60-0.70 µm sections were mounted on slides and stained with 1% toluidine blue for 1 min [11]. After sealing the slides with Entellan®, the samples were analyzed using a bright-field light microscope Axioplan (ZEISS, USA) coupled with a Canon PowerShot A640 camera. The images were used for qualitative description.

Transmission electron microscopy (TEM)

After infiltration and embedding steps, the 0.60-0.70 µm sections were collected on 300 mesh copper grids and contrasted with 5% uranyl acetate for 40 min and 1% lead citrate for 5 min, at room temperature [11]. The sections were then observed using a JEOL TEM 1400 PLUS microscope.

Scanning electron microscopy (SEM)

After the acetone dehydration steps, the root samples underwent critical point drying, using the Bal-tec Critical Point Dryer CPD 030 equipment. The fragments were mounted on appropriate supports using carbon adhesive tape and coated with a thin layer of 20 nm gold using the Bal-tec Sputter Coater SCD 050. The samples were observed under a EVO40-ZEISS microscope, at an acceleration of 25 kV.

Histochemical tests: phenolic compounds, terpenes, and alkaloids

The fixed and washed root samples were dehydrated in an alcohol series: 50%, 70%, 90%, and 100% and infiltrated, and embedded in Historesin (Leica Instruments®, Wetzlar, Germany). Using a disposable blade, thin sections of 4 µm thickness were obtained at a rotary microtome (Cut 4050 Slee Mainz).

The sections were exposed to specific reagents and mounted between a slide and coverslip with 50% glycerin. For phenolic compounds detection, sections were treated with a 10% ferric chloride solution in water for 30 min, and quickly rinsed with water. Total phenolic compounds stain from brown to black [12]. For terpenes, sections were incubated for 1 h in the dark in NADI solution (0.5 mL of 0.1% alpha-naphthol in 40% ethanol; 0.5 mL of 1% dimethyl-p-phenylenediamine hydrochloride in water; and 49 mL of 0.05 M sodium phosphate buffer pH 7.2). Then, they were washed for 2 min with 0.1 M sodium phosphate buffer pH 7.2. Terpenes stain from blue (essential oils) to red (acidic resins) and acquire a violet to purple coloration when there is a mixture of these substances [13]. For alkaloids, sections were incubated for 10 min in Wagner's reagent (0.01 M potassium iodide and 0.01 M iodine in 100 mL of water) and quickly rinsed with water. Alkaloids stain reddish-brown [14].

All microscopic preparations were examined and captured under a bright-field light microscope Axioplan (ZEISS, USA) coupled with a Canon PowerShot A640

camera. The images were used for qualitative description.

Comparative shotgun proteomic analysis

Total protein extraction and quantification

Pulverized roots (500 mg) were divided into two 2 mL microtubes. To each microtube, 1.5 mL of urea/thiourea extraction buffer (7 M urea, 2 M thiourea, 1 mM PMSF in ethanol, 65 mM DTT, and 2% Triton X-100) was added. The tubes were constantly shaken at 4°C for 30 min and incubated at -20°C for 30 min before centrifuged at 16,000 g at 4°C for 20 min. Protein concentration of the resulting supernatants was estimated using the 2-D Quant Kit (Cytiva, Marlborough, MA, USA).

Precipitation and protein digestion

Before the trypsin digestion step, aliquots of 100 µg of proteins were precipitated using the methanol/chloroform methodology to remove any contaminants from the samples [15]. Each biological replicate was then digested using a Microcon-30 kDa filter (Millipore) with the Filter-Aided Sample Preparation (FASP) methodology [16] with modifications [17], at a trypsin-to-protein ratio of 1:100 (V5111, Promega).

Obtained peptides were vacuum-dried, solubilized in 0.7 $\mu g.\mu L^{-1}$ in 95% water and 5% acetonitrile plus 0.1% formic acid and quantified at a NanoDrop 2000c spectrophotometer (Thermo Fisher Scientific, Waltham, USA) for mass spectrometry (MS).

Mass spectrometry analysis

Mass spectrometry was performed using a nanoACQUITY Ultra Performance Liquid Chromatography (UPLC) system coupled to a Q-TOF SYNAPT G2-Si instrument (Waters, Manchester, United Kingdom) [18] and details of procedures and conditions are compiled in Supplementary Materials (Suppl. S1).

Proteomic data analysis

The spectral processing and database search conditions were performed using ProteinLynx Global SERVER (PLGS) software (version 3.02, Waters). The parameters

for HDMSE analysis are in Suppl. S1. The proteome of the species *Eucalyptus grandis* (ID: UP000030711), deposited in UniProtKB (https://www.uniprot.org/), was used as the reference proteome, because it belongs to the same botanical family of Myrtaceae and is phylogenetically the closest relative to *Psidium* spp. with proteomic data available.

The label-free quantification analysis was performed using ISOQuant software v.1.8 [19,20], with parameters described in Suppl. S1. For comparative analysis, only proteins present or absent (for unique proteins) in the three biological replicates were accepted for differential abundance analysis. The following comparisons were performed: GUA_20DAI / GUA_20DNI; GUA_20DAI / GUA_5DAI; GUI_20DAI / GUI_20DNI; GUI_20DAI / GUI_5DAI (GUA stands for *P. guajava* and GUI stands for *P. guineense*). The data were analyzed by the two-tailed Student's t-test. Proteins with a p-value < 0.05 were considered increased if the Log2 fold change (FC) was > 0.6 and decreased if the Log2 FC was < -0.6.

From the list of proteins between the six conditions tested, a principal component analysis (PCA) was performed using the MetaboAnalyst 6.0 program (https://www.metaboanalyst.ca/). Volcano plots were generated with GraphPad Prism 6 for Windows program, GraphPad Software, Boston, Massachusetts, USA (www.graphpad.com) to identify proteins with increased and decreased accumulation over 20 days, with and without inoculation of *M. enterolobii*, for the two species studied.

Proteins identified as upregulated or downregulated over 20 days were grouped into sets using a Venn Diagram (https://bioinformatics.psb.ugent.be/webtools/Venn/). Interaction networks of the differentially abundant proteins (DAPs) were constructed considering the first interaction level retrieved from STRING version 12.0 (https://string-db.org). To generate a protein-protein interaction (PPI) network, *Eucalyptus grandis* was the reference plant species, using a minimum interaction score of 0.7 through Cytoscape, version 3.10.1 (https://cytoscape.org). After identifying the upregulated and downregulated groups for each species, heatmaps were generated for each cluster using Heatmapper (http://www.heatmapper.ca/).

3.2.3 Results and discussion

Microscopy images and qualitative analysis of secondary metabolites from the roots of Psidium spp. inoculated and not inoculated by M. enterolobii

To initially confirm the identification of the nematode structure present in the plant vascular cylinder, transmission electron microscopy images of the pathogen extracted from the inoculum used in this study were acquired (Fig. 1S).

Figure 1 presents images of transverse root sections acquired through bright-field light microscopy. In 20 days, samples of both *P. guajava* and *P. guineense* non-inoculated with *M. enterolobii* (GUA and GUI_20DNI, respectively), the structure of the root vascular cylinder exhibits general organization without alteration (Figures 1A-D). In inoculated *P. guajava* (GUA_20DAI) (Figures 1E-F), the presence of the nematode along with feeding sites containing multinucleated giant cells (GC) indicates successful infection in the host plant. In the case of *P. guineense* after 20 days of inoculation (GUI_20DAI) (Figures 1G-H), this organization of vascular tissues is no longer evident, and a reduction of the vascular cylinder is mainly noted. The presence of the nematode in the peripheral region of the cylinder is observed, accompanied by the appearance of grayish-colored cells, suggesting the formation of compounds associated with the presence of the phytopathogen. The tissue disorganization and a reduction in the vascular cylinder of the resistant phenotype, where no GC were seen, suggests that these structures are essential for infection and the formation of the pathosystem.

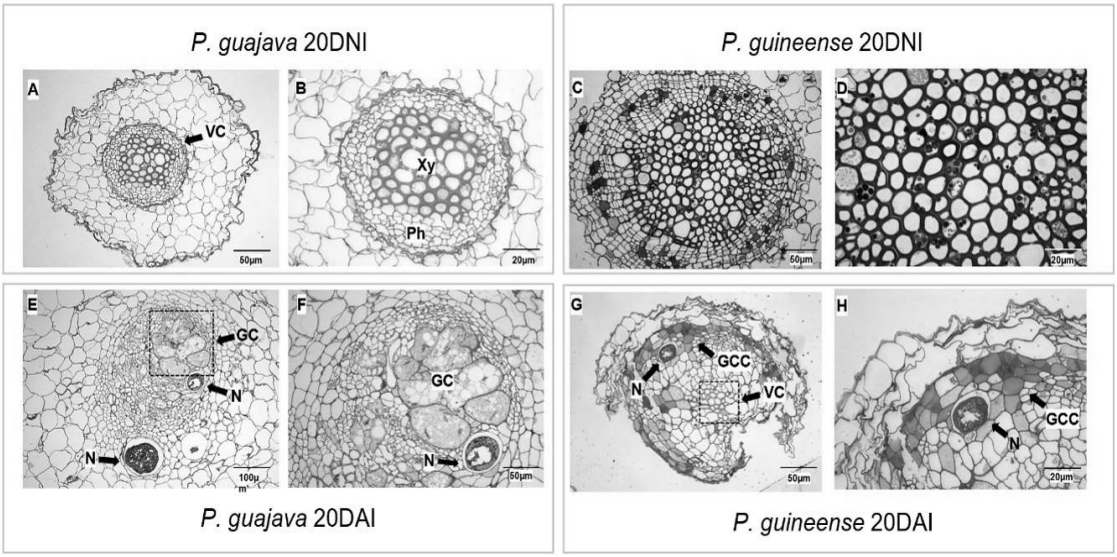

Figure 1 - Images of the roots obtained by bright field light microscopy: GUA_20DNI (A and B); GUI_20DNI (C and D); GUA_20DAI (E and F) e; GUI_20DAI (G and H). *P. guajava* – GUA; *P. guineense* – GUI; 20 days non-inoculated – 20DNI; 20 days after inoculation – 20DAI; Vascular cylinder – VC; Xylem–Xy; Phloem – Ph; Giant cells – GC; Nematode – N; Grayish-colored cells – GCC.

The formation of giant cells (GC) and the hypersensitivity response (HR) are plant defense mechanisms during pathogen invasion [21]. A histopathological study of okra (*Abelmoschus esculentus*) roots revealed that second-stage juveniles of *M. incognita* were able to feed and reproduce due to the formation of GC [22]. The accelerated metabolic activity at these feeding sites causes nutrient deficiency in plant tissues, leading to systemic responses throughout the organism [23]. GCs are crucial for the establishment of the nematode in the vascular cylinder, and such location is strategic. According to Xu et al. [24], sucrose transport through plasmodesmata leads to an efficient nutrient distribution through the plant vascular system, supplying energy to regulate plant metabolism. In this context, pectins are essential in the cell wall, promoting adhesion and porosity, with emphasis on homogalacturonans, whose methylesterification is associated with nematode-induced lesions and gall formation, disrupting nutrient transport and altering cell structure and function [25]. Infection can modify pectic polysaccharides, affecting cell expansion and nutrient absorption [26]. The endodermis, with walls reinforced by suberin and lignified Casparian strips (CS), protects the vascular cylinder against biotic and abiotic threats. Studies in *Arabidopsis* with defects in CS have shown an impact on the infectivity of *M. incognita* and on the size of the feeding site [27]. After infection by *Meloidogyne* spp., the expression of several cell wall-modifying enzymes, such as expansins, endoglucanases, extensins, hydrolases, and structural proteins, was altered [28].

To investigate cell morphology, images of root sections were examined by TEM (Fig. 2a). For *P. guajava*, at the GUA_20DNI condition, Figure 2aA displays the xylem, and Figure 2aB, the organized xylem and pericycle. At the GUA_20DAI condition, Figure 2aE reveals the central cylinder with substance accumulation, and Figure 2aF shows multinucleated cells indicating the development of feeding sites of *M. enterolobii*. In contrast, in *P. guineense*, there is no change in cell wall thickness when comparing the conditions with and without nematode inoculation. It is observed that, in *P. guineense*, high concentrations of substances are present in both conditions (Figures 2aC to 2aH), but the density of these substances increases in response to the pathogen (Figures 2aG-H).

From the SEM images (Fig. 2b), changes in the surface layer of the roots were observed after inoculation with *M. enterolobii* in both species. In *P. guajava*, at the non-

inoculated condition (GUA_20DNI) (Figure 2bA), root hairs, which play a crucial role in the absorption of water and nutrients by the plant, can be seen. After inoculation (GUA_20DAI) (Figure 2bC), reduction and morphological alterations of root hairs were seen. In *P. guineense* (GUI_20DAI) (Figure 2bD), there is also a reduction in root hairs, although they are still present, with slight peeling of the outermost layer of the root compared to the control (GUI_20DNI) (Figure 2bB).

a

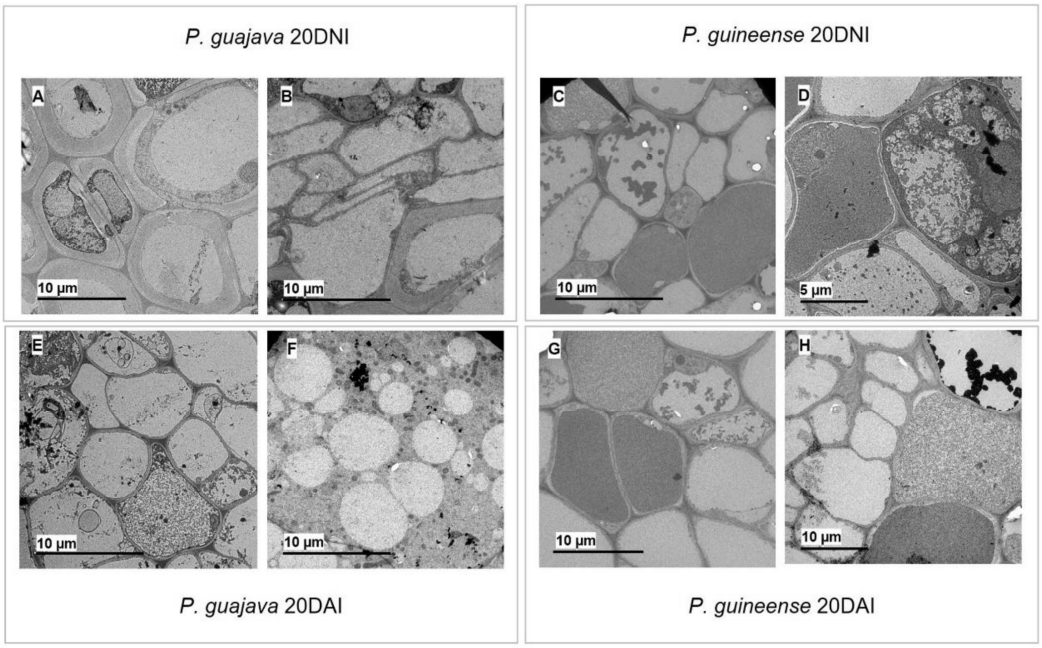

b

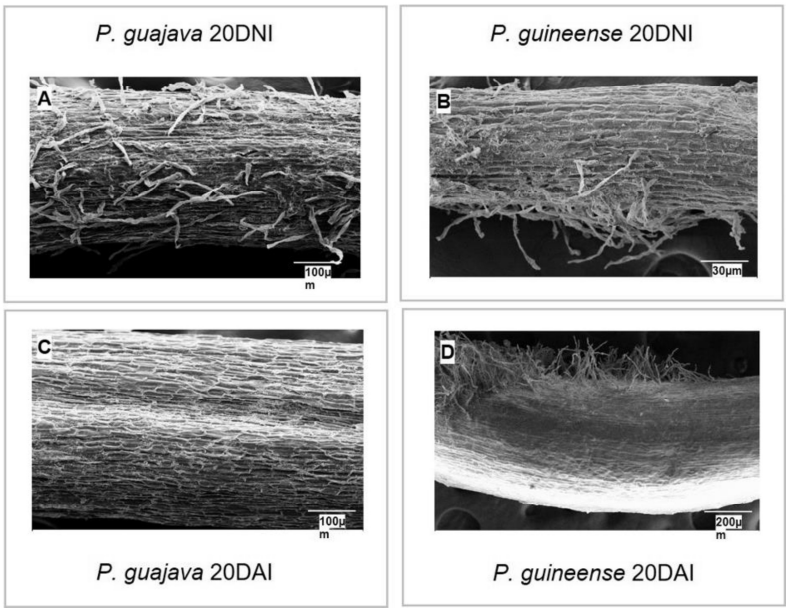

Figure 2 - Images of roots obtained by transmission electron microscopy (a) - GUA_20DNI (A and B); GUI_20DNI (C and D); GUA_20DAI (E and F); and GUI_20DAI (G and H). and scanning electron microscopy (b) - GUA_20DNI (A); GUI_20DNI (B); GUA_20DAI (C); and GUI_20DAI (D). *P. guajava* – GUA; *P. guineense* – GUI; 20 days non-inoculated – 20DNI; 20 days after inoculation – 20DAI.

Root-knot nematodes inhibit plant growth by reducing the root system and decreasing water and nutrient absorption, resulting in water stress and nutritional deficiency [29]. Phytohormones are crucial as signaling molecules in root hair growth and development. Auxin and ethylene, in particular, play vital roles in this regulation, interacting with jasmonic acid, abscisic acid, strigolactones, and brassinosteroids [30]. Our following data on changes in secondary metabolites also suggest that these may affect the production of phytohormones essential for maintaining root hairs.

A homogeneous distribution of phenolic compounds from the epidermis to the endodermis in both species (GUA and GUI_20DNI) was observed under non-inoculated condition (Figs. 3E and 3F). However, after inoculation (GUA and GUI_20DAI), besides an increased diameter of the root intersection, there was an increase in the production of these compounds (Figs. 3G and 3H). In *P. guajava*, this increase is more notable in the endodermis, while in *P. guineense*, this trend extends to the central areas of the cylinder. A significant presence of terpenes was observed throughout the structure of *P. guineense* inoculated roots compared to the control condition of both species (GUA and GUI_20DNI) (Figs. 3I and 3J). After inoculation (GUA and GUI_20DAI), there was an amplification of terpenes staining (Figs. 3K and 3L). Alkaloids were seen throughout the structure of control roots of *P. guajava* (Fig. 3M) compared to the control roots of *P. guineense* (Figs. 3M and 3N, respectively). After inoculation (GUA and GUI_20DAI), a pronounced increase is observed in both species (Figs. 3O and 3P).

Our histochemical analysis, in summary, showed increases in root diameter and in the production of phenolic compounds, terpenes, and alkaloids in both *P. guajava* and *P. guineense* after inoculation with *M. enterolobii*. In the roots of *P. guineense*, there was a greater accumulation of these compounds, suggesting an efficient activation of defense responses by the species. A hypersensitive reaction in the root cortex of *Oryza glumaepatula* was similarly recorded two days after inoculation with *M. graminicola*, when few nematode juveniles were established in the central cylinder,

with rare collapsed giant cells surrounded by degenerated female bodies displaying accumulation of phenolic compounds [31].

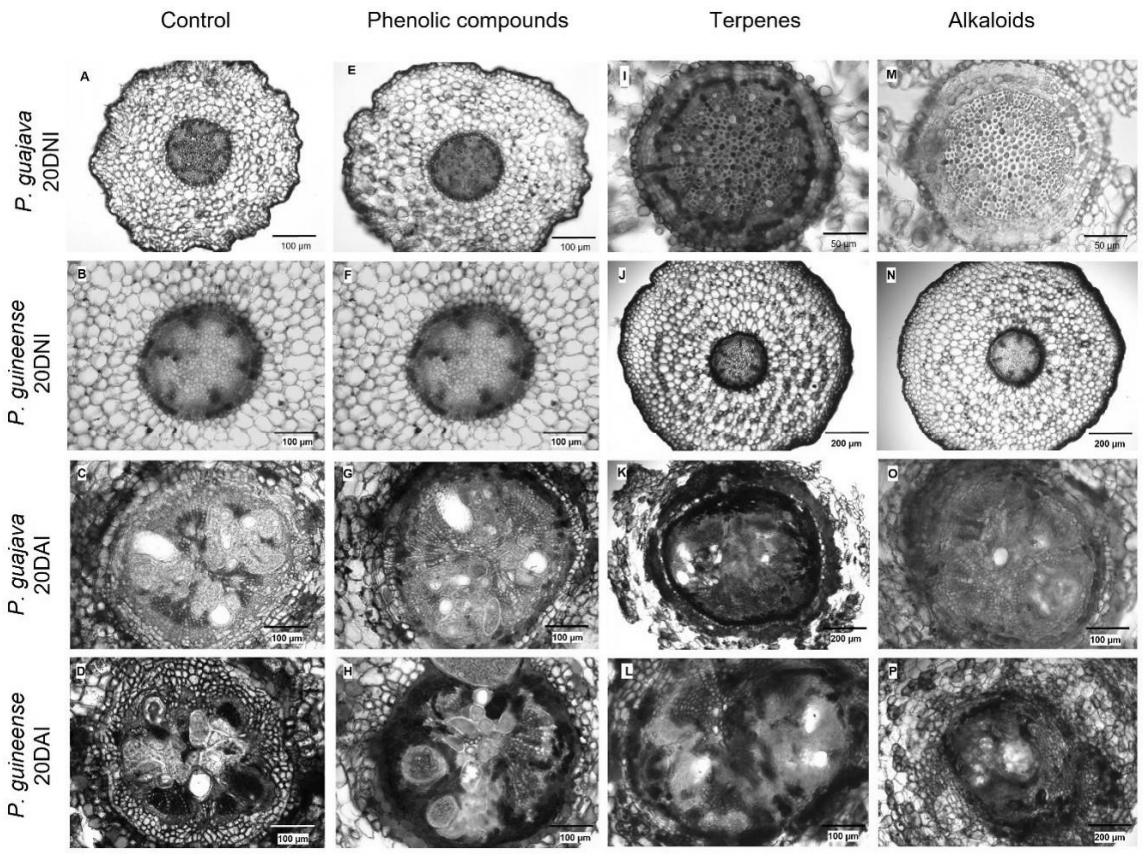

Figure 3 - Images obtained by light field optical microscopy after staining for histochemical testing of *Psidium* roots: control roots of *P. guajava* (non-inoculated with *M. enterolobii*) – GUA_20DNI (row 1), control roots of *P. guineense* (non-inoculated) – GUI_20DNI (row 2), *P. guajava* roots 20 days after inoculation – GUA_20DAI (row 3) and *P. guineense* roots 20 days after inoculation – GUI_20DAI (row 4): control (column 1); phenolic compounds stained with ferric chloride (column 2); terpenes stained with NADI solution (column 3); and alkaloids stained with Wagner's Reagent (column 4).

Secondary metabolites, such as phenolic compounds, terpenes, and alkaloids, possess various properties, including antifungal, antibacterial, antioxidant, and insecticidal activities [32]. Phenolic compounds, synthesized through shikimic acid and phenypropanoid pathways, are essential for various plant functions, including cell wall thickening, hormonal synthesis, pigmentation, and defense against pathogens [33,34]. The role of the shikimic acid pathway in nematode infection, as observed in *P.*

guineense and *P. cattleianum* infected by *M. enterolobii*, highlights the importance of tannins and hydrolysable lignans in the protection of infected tissues [35]. Increases in hydrogen peroxide, superoxide dismutase activity and catalase in pumpkins [36] and the stimulation of phenylpropanoid biosynthesis in watermelons [37], both infected by *M. incognita,* were reported. In guava, after infection by *M. enterolobii*, increases in phenols, proline, peroxidase, and polyphenol oxidase were observed [38]. These findings highlight the dynamic interaction between plants and nematodes, mobilizing antioxidant defenses against infectious stress. Terpenes are essential in plant interactions with soil organisms [39] contributing to the synthesis of hormone-induced defense molecules such as salicylic acid, jasmonic acid and ethylene [40]. Non-host Asteraceae plants show potential as nematode repellents through compounds like (E)-β-farnesene and 1,8-cineole, highlighting the role of terpenoids in nematode control [41]. Pyrrolizidine alkaloids (PAs) from *Crotalaria* spp. exhibited nematotoxicity, with field tests showing significant reductions in nematode populations [42]. Tryptophan acts as a precursor for indole alkaloids, phytoalexins and glucosinolates, which are essential in plant defense against microbial infections and herbivore attacks, including nematicidal activity [43,44].

Comparative proteomic analysis of the roots of Psidium spp. inoculated and non-inoculated

Based on statistical criteria, 416 proteins were identified and selected between the treatments. Figure 4a shows a multivariate principal component analysis (PCA), allowing observation of the behavior of the groups of individuals. According to the PCA for *P. guajava*, the GUA_20DNI set forms a distinct space, without overlapping with the samples from the condition after 5 and 20 days of inoculation. Notably, there is overlap between part of the GUA_20DAI set and the universe of GUA_5DAI. In the case of *P. guineense*, it stands out for the proximity of control individuals GUI_20DNI with those inoculated after 5 days and after 20 days. Additionally, it is relevant to observe that individuals GUA_20DAI occupy an opposite position in relation to individuals GUI_20DAI.

The Volcano plot (Fig. 4b) represents the changes at the levels of the 416 proteins from *P. guajava* and *P. guineense* samples, classified as up- and down-

regulated at the 20-day time point, in presence or absence of nematode. In *P. guajava*, inoculation led to an increase of 61 proteins (14.7%) and a decrease of 33 proteins (7.9%) in protein expression, with 69.4% of the proteins showing no changes in their accumulation (Fig. 4bA). In *P. guineense*, values were 7.2% (30 proteins) and 5% (21 proteins) for up- and down-regulated proteins, respectively, and 82% of unaltered proteins (Fig. 4bB).

From the 145 proteins with altered expression in both species, 135 proteins were increased or decreased exclusively in one or other species and condition, with the remaining 10 proteins being shared among them. This can be observed by the Venn Diagram (Fig. 4c), where clusters generated by the proteins are discriminated.

Among the analyzed proteins, the following were up-regulated in both species: A0A059DIT8 (Ribosomal protein S7 domain-containing protein) and A0A058ZUU6 (5-methyltetrahydropteroyltriglutamate--homocysteine S-methyltransferase). On the other hand, the proteins A0A059AZ85 (isopentenyl-diphosphate delta-isomerase) and A0A059D4J5 (L-ascorbate peroxidase), related to the biosynthetic process of dimethylallyl diphosphate, an intermediate metabolite of the mevalonate pathway, were down-regulated in both species. Some proteins showed different patterns between the two species. For example, A0A059AGF2 (related to NADP+-dependent isocitrate dehydrogenase (IDH) activity), A0A058ZSX3 (Bet v I/Major latex protein domain-containing protein), A0A059B9X7 (Coatomer subunit gamma), and A0A059A4C7 (UDP-arabinopyranose mutase) were up-regulated in *P. guajava* but down-regulated in *P. guineense*. Meanwhile, A0A059DGU6 (14-3-3 domain-containing protein) and A0A059CN57 (NAD_binding_2 domain-containing protein) showed the opposite pattern, being down-regulated in *P. guajava* and up-regulated in *P. guineense*. In *P. guajava*, it was observed that 55 DAPs increased, while 29 DAPs decreased when comparing the conditions of 20 days post non-inoculation and inoculation (Fig 4c). On the other hand, in *P. guineense*, 17 DAPs were up-regulated and 24 DAPs down-regulated, when comparing the same conditions (Fig. 4c). The enrichment of the groups of up- and down-regulated proteins in each species was analyzed.

a

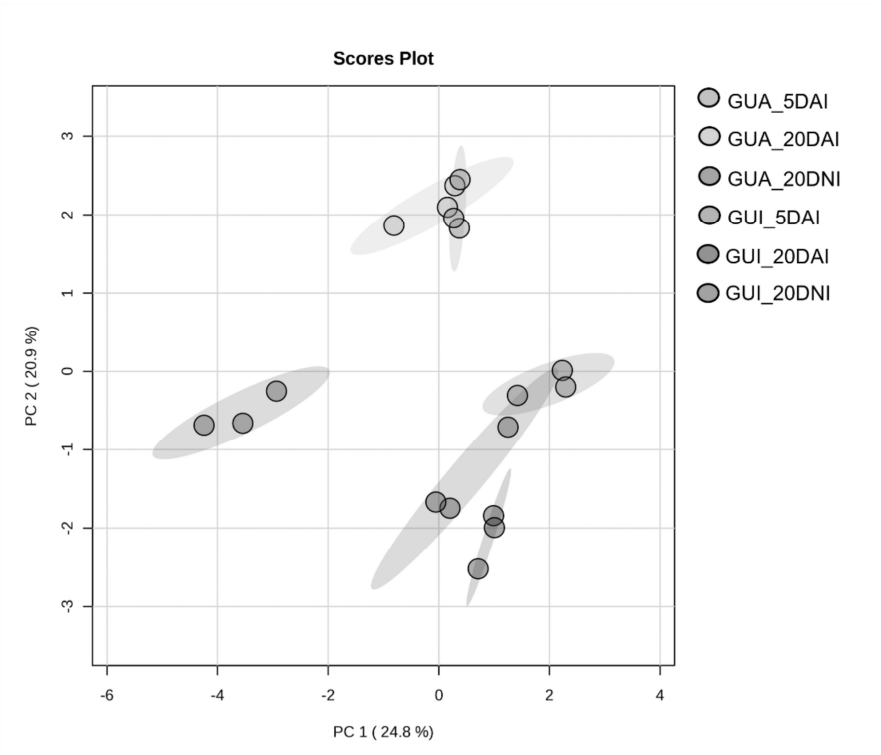
Scores Plot
GUA_5DAI
GUA_20DAI
GUA_20DNI
GUI_5DAI
GUI_20DAI
GUI_20DNI
PC 2 (20.9 %)
PC 1 (24.8 %)
-6
-4
-2
0
2
4
3
2
1
0
-1
-2
-3

b

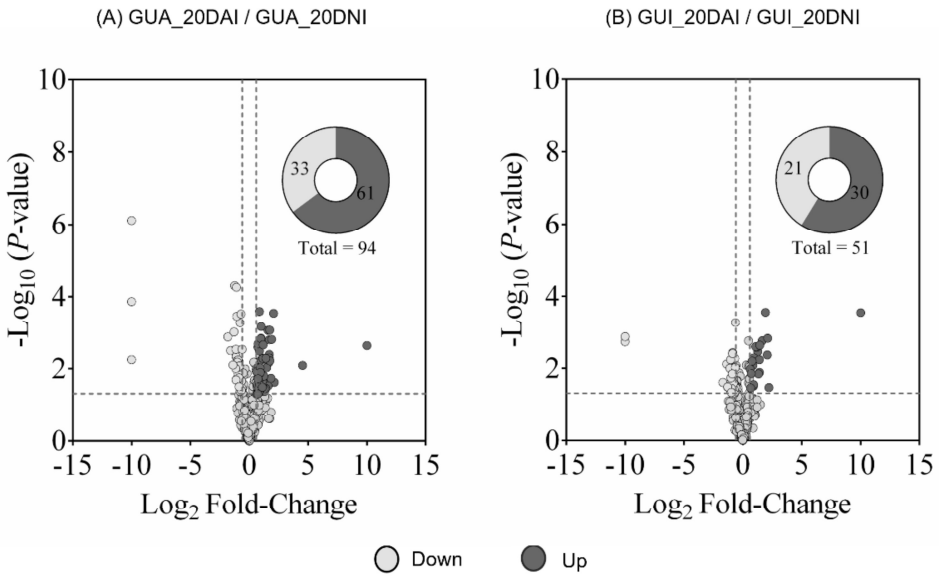
(A) GUA_20DAI / GUA_20DNI
(B) GUI_20DAI / GUI_20DNI
-Log10 (P-value)
Log2 Fold-Change
33
61
Total = 94
21
30
Total = 51
Down
Up

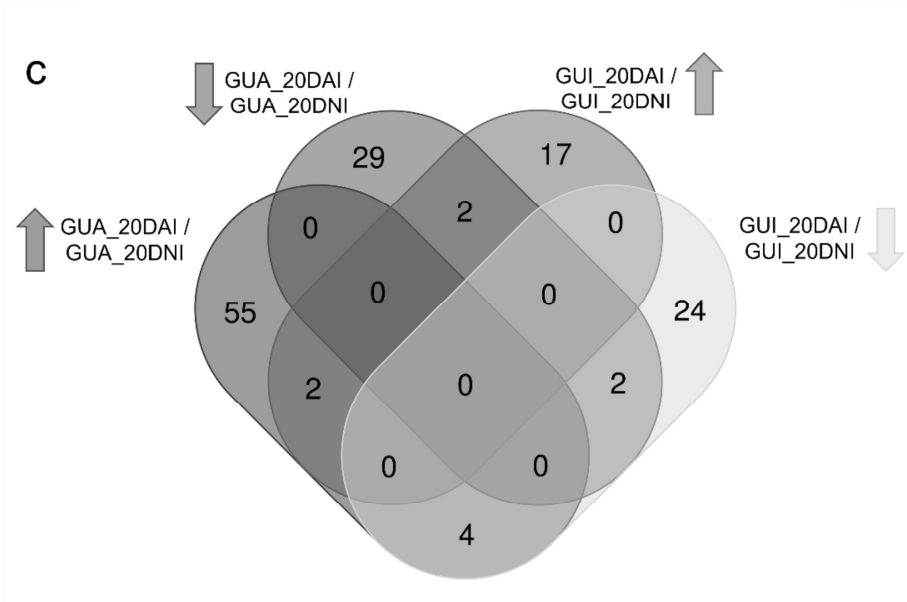

Figure 4 - Multivariate analysis of principal components for the set of 416 selected proteins from roots of *Psidium.* (a) [*P. guajava* 5 days after inoculation - GUA_5DAI; *P. guajava* 20 days after inoculation – GUA_20DAI; *P. guajava* after 20 days non-inoculation of *M. enterolobii* – GUA_20DNI; *P. guineense* 5 days after inoculation – GUI_5DAI; *P. guineense* 20 days after inoculation – GUI_20DAI; *P. guineense* after 20 days non-inoculation – GUI_20DNI], Volcano distribution plot of the up- and down-regulated proteins among the whole 416 protein set from *P. guajava* and *P. guineense* samples (b) [(A) GUA_20DAI / GUA_20DNI – comparison between *P. guajava* 20 days after inoculation and *P. guajava* 20 days after non-inoculation with *M. enterolobii*; B) GUI_20DAI / GUI_20DNI – comparison between *P. guineense* 20 days after inoculation and *P. guineense* after 20 days of non-inoculation with the nematode; grey circles – unchanged], and a Venn diagram of 135 differentially accumulated proteins (DAPs) after 20 days. (c) [GUA_20DAI / GUA_20DNI – comparison between *P. guajava* 20 days after inoculation and *P. guajava* 20 days after non-inoculation with *M. enterolobii*, up (blue) and down-regulated (pink); GUI_20DAI / GUI_20DNI – comparison between *P. guineense* 20 days after inoculation and *P. guineense* after 20 days after non-inoculation with *M. enterolobii*, up (green) and down-regulated (yellow).

In Figure 5a, based on minimum required interaction score criteria, interaction networks among the identified proteins were established for *P. guajava* (GUA_20DAI / GUA_20DNI, 14 up-regulated proteins, 12 down-regulated proteins - total of 26 proteins). In Figure 5b, the representation for the networks of *P. guineense* is shown (GUI_20DAI / GUI_20DNI, 6 up-regulated proteins and 5 down-regulated proteins - total of 11).

When investigating the behavior of proteins after five days of nematode inoculation and comparing with the data after 20 DAI, volcano plots were generated

for each species in the study (Figure 2S). In *P. guajava*, out of the 26 analyzed proteins, only one (A0A059AGF2, isocitrate dehydrogenase [NADP]) was accumulated from 5 to 20 DAI, while the others did not show significant changes according to statistical analysis (Figure 2SA). On the other hand, in *P. guineense*, all 11 proteins remained unchanged, suggesting that changes in plant metabolism mainly occur within the first 5 DAI and persist in the subsequent days (Figure 2SB).

Based on the protein networks, it was observed that *P. guajava* exhibits an increased accumulation of proteins associated with the activities of catalase (CAT), adenosylhomocysteinase, and hydrolase 20 DAI of *M. enterolobii*. This suggests that these pathways may be related to the infection process caused by the nematode. When stressed, plants activate signaling molecules, such as ROS. The invasion of pathogens disrupts this production, causing oxidative damage to lipids, proteins, and nucleic acids [45]. Catalase and ascorbate oxidase are essential in antioxidant defense, neutralizing ROS before they cause harm. During nematode infections, the activity of hydrogen peroxide and catalase increases rapidly [46]. In a study with *M. incognita*, the enzymes CAT, superoxide dismutase (SOD), guaiacol peroxidase (GuPOX), ascorbate peroxidase (APOX), polyphenol oxidase (PPO), glutathione S-transferase (GST), and non-enzymatic antioxidants increased in tomatoes under nematode stress [47]. CAT is inhibited in resistance responses but increases in successful infections [48].

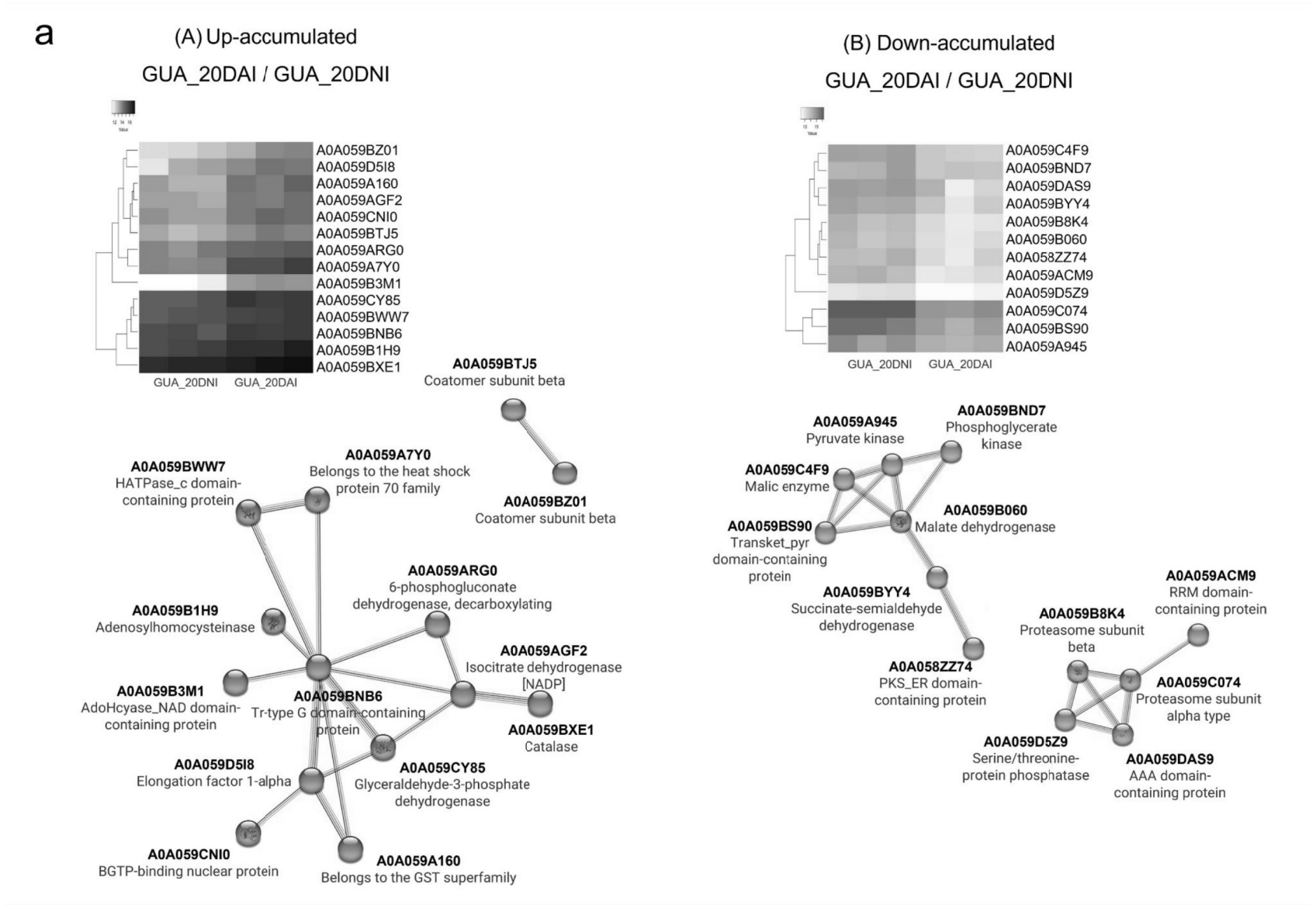
a
(A) Up-accumulated
GUA_20DAI / GUA_20DNI
A0A059BZ01
A0A059D5I8
A0A059A160
A0A059AGF2
A0A059CNI0
A0A059BTJ5
A0A059ARG0
A0A059A7Y0
A0A059B3M1
A0A059CY85
A0A059BWW7
A0A059BNB6
A0A059B1H9
A0A059BXE1
GUA_20DNI
GUA_20DAI
A0A059BTJ5
Coatomer subunit beta
A0A059BZ01
Coatomer subunit beta
A0A059BWW7
HATPase_c domain-containing protein
A0A059A7Y0
Belongs to the heat shock protein 70 family
A0A059ARG0
6-phosphogluconate dehydrogenase, decarboxylating
A0A059B1H9
Adenosylhomocysteinase
A0A059AGF2
Isocitrate dehydrogenase [NADP]
A0A059B3M1
AdoHcyase_NAD domain-containing protein
A0A059BNB6
Tr-type G domain-containing protein
A0A059BXE1
Catalase
A0A059D5I8
Elongation factor 1-alpha
A0A059CY85
Glyceraldehyde-3-phosphate dehydrogenase
A0A059CNI0
BGTP-binding nuclear protein
A0A059A160
Belongs to the GST superfamily
(B) Down-accumulated
GUA_20DAI / GUA_20DNI
A0A059C4F9
A0A059BND7
A0A059DAS9
A0A059BYY4
A0A059B8K4
A0A059B060
A0A058ZZ74
A0A059ACM9
A0A059D5Z9
A0A059C074
A0A059BS90
A0A059A945
GUA_20DNI
GUA_20DAI
A0A059A945
Pyruvate kinase
A0A059BND7
Phosphoglycerate kinase
A0A059C4F9
Malic enzyme
A0A059B060
Malate dehydrogenase
A0A059BS90
Transket_pyr domain-containing protein
A0A059BYY4
Succinate-semialdehyde dehydrogenase
A0A058ZZ74
PKS_ER domain-containing protein
A0A059ACM9
RRM domain-containing protein
A0A059B8K4
Proteasome subunit beta
A0A059C074
Proteasome subunit alpha type
A0A059D5Z9
Serine/threonine-protein phosphatase
A0A059DAS9
AAA domain-containing protein

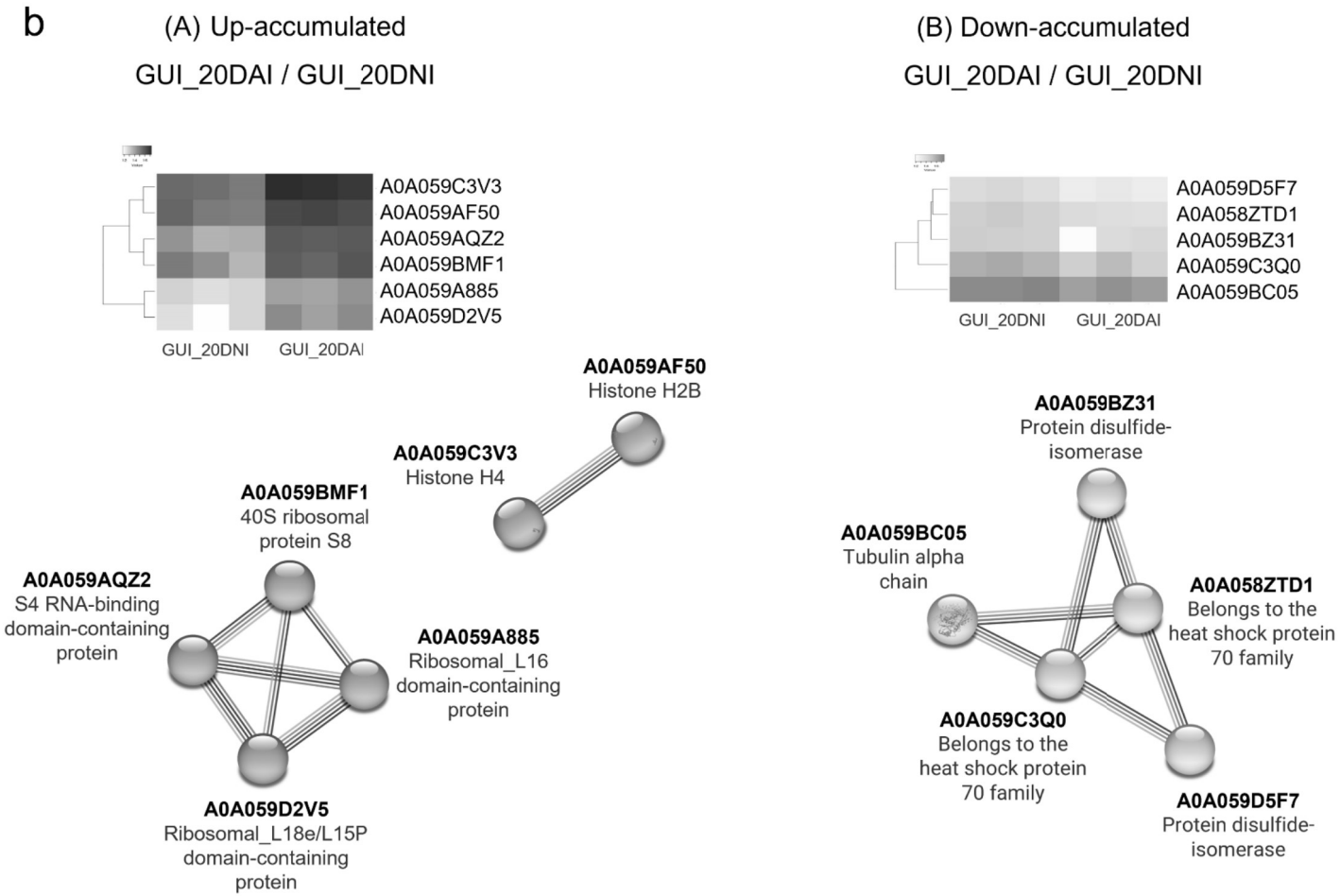

Figure 5 - Heatmaps together with interaction networks showing the up (A) and down (B) regulated proteins, comparing *P. guajava* 20 DAI and non-inoculated with *M. enterolobii* (GUA_20DAI / GUA_20DNI) (a) and *P. guineense* 20 DAI and non-inoculation with *M. enterolobii* (GUI_20DAI / GUI_20DNI) (b).

In the last decade, studies on epigenetic regulators revealed how these mechanisms influence plant-nematode interactions. While plants respond rapidly to infection, nematodes can manipulate epigenetic modifications to suppress plant defenses [49]. The balance between histone acetyltransferases and histone deacetylases controls histone acetylation, influencing gene expression and biological processes [50,51]. On the other hand, histone hypoacetylation promotes gene silencing [52,53]. In *P. guineense*, a significant increase in histone proteins H4 and H2B is observed 20 DAI with *M. enterolobii*, suggesting they are related to resistance against nematode infection. Studies indicate that histone-modifying enzymes are deregulated in nematode-induced galls in rice, suggesting a dynamic response of histone modifications during RKN infection [50]. The interaction between rice and *M. graminicola* revealed different expression profiles of components of the epigenetic machinery, reinforcing that DNA hypomethylation and changes in histone acetylation and methylation are part of the immune response against RKN [54].

Disulfide isomerase (PDI) was negatively regulated in *P. guineense* 20 DAI with *M. enterolobii*. Protein disulfide isomerases (PDI), found in the endoplasmic reticulum (ER), catalyze the formation, breaking, and rearrangement of disulfide bonds between cysteine residues in proteins [55]. In pathogens, they play essential roles in protecting them against ROS released by hosts during infection [56]. Recent studies have characterized nematode effectors, such as PDIs, that induce cell death in plants and contribute to parasitism. For example, MiPDI1 from *M. incognita* increases *Arabidopsis* susceptibility to the nematode [57].

Under inoculation with *M. enterolobii*, *P. guajava* showed an increase in the accumulation of a 70 kDa heat shock protein, while *P. guineense* experienced a decrease. The HSP70s regulate stress responses and activate the plant immune system against infections. Deficiency in HSP70s, compared to other HSPs, results in plant growth retardation, especially under stress conditions [58]. After stress relief, HSPs return to nearly normal levels through mechanisms that are not yet fully understood, involving a transient reprogramming of cellular activities and specific induction of molecular chaperones [59]. The GmHsp22.4 gene, strongly induced in soybean lines resistant to *M. javanica* but repressed in susceptible ones, reduced nematode reproduction by up to 82% in transgenic *Arabidopsis* [60]. The heat shock

proteins HSP-4, HSP90 and HSP20 were also seen to be accumulated in *Vigna unguiculata* infected by *M. incognita* [61].

Proteomic and transcriptomic analyses have shown that plants respond to nematode stress by accumulating various proteins, such as HSPs and PDIs, as well as other proteins related to defense and detoxification. These studies are essential for developing integrated management strategies and genetically improving plant resistance to these pathogens [62, 63].

3.2.4 Conclusions

Psidium responses to *M. enterolobii* involve a complex interplay of cellular processes, including giant cell formation, hypersensitivity responses, and alterations in biochemical pathways such as sucrose transport, pectin modification, and antioxidant enzyme activity. These responses are reinforced by the synthesis and accumulation of secondary metabolites like terpenes, alkaloids, and phenolic compounds, contributing to plant resilience. Moreover, epigenetic regulation through histone modifications and the role of molecular chaperones such as heat shock proteins and protein disulfide isomerases are also undertaken as adaptive strategies that inoculated plants employ to combat nematode infections.

References

[1] World Population Review. Guava Production by Country 2024. Available online: https://worldpopulationreview.com/country-rankings/guava-production-by-country (accessed on 13th.January.2025)

[2] Industry ARC 2025. Guava Market Size Report, 2022-2027. Available online: https://www.industryarc.com/Research/Global-Guava-Market-Research-513404 (accessed on 13th.January.2025)

[3] Kumar, M., Kapoor, S., Dhumal, S. Tkaczewska, J, Changan, S., Saurabh, V., … Bhuyan, D.J. (2022). Guava (*Psidium guajava* L.) seed: a low-volume, high-value byproduct for human health and the food industry. Food Chemistry 386, 132694. https://doi.org/10.1016/j.foodchem.2022.132694.

[4] Qin, J., Wang, J., Shao, X., Zhang, S., Chen, X., Lai, D., …, Kuang, S. (2023).

Evaluation of bioactive compounds, antioxidant capacity and mineral elements in the leaves of guava (*Psidium guajava* L.) genotypes from China. Scientia Horticulturae 322, 112436. https://doi.org/10.1016/j.scienta.2023.112436.

[5] Chen, Y., Long, H., Feng, T., Pei, Y., Sun, Y., Zhang, X. (2022). Development of a novel primer–TaqMan probe set for diagnosis and quantification of *Meloidogyne enterolobii* in soil using qPCR and droplet digital PCR assays. International Journal of Molecular Sciences, 23, 11185.

[6] Sikandar, A., Jia, L., Wu, H., Yang, S. (2023). *Meloidogyne enterolobii* risk to agriculture, its present status and future prospective for management. Frontiers in Plant Science, 13, 1093657. https://doi.org/10.3389/fpls.2022.1093657.

[7] Philbrick, A.N., Adhikari, T.B., Louws, F.J., Gorny, A.M. (2020). *Meloidogyne enterolobii*, a major threat to tomato production: current status and future prospects for its management. Frontiers in Plant Science, 11, 609365.s. https://doi.org/ 10.3389/fpls.2020.606395.

[8] Desmedt, W., Mangelinckx, S., Kyndt, T., Vanholme, B. 2020. A phytochemical perspective on plant defense against nematodes. Frontiers in Plant Science, 11, 602079. https://doi.org/10.3389/fpls.2020.602079.

[9] Shao, H., Fu, Y., Zhang, P., You, C., Li, C., Peng, H. (2021). Transcriptome analysis of resistant and susceptible mulberry responses to *Meloidogyne enterolobii* infection. BMC Plant Biology, 21, 338. https://doi.org/10.1186/s12870-021-03128-w.

[10] Khan, M., Khan, A.U. (2021). Plant parasitic nematodes effectors and their crosstalk with defense response of host plants: a battle underground. Rhizosphere, 17, 100288. https://doi.org/10.1016/j.rhisph.2020.100288.

[11] O'Brien, T. P., Feder, N., McCully, M.E. (1964). Polychromatic staining of plant cell walls by toluidine blue O. Protoplasma, 59, 368–373.

[12] Johansen, D.A. (1940). Plant Microtechnique. McGraw-Hill Book Company. 1st ed. New York.

[13] David, R., Carde, J.P. (1964). Coloration différentielle dês inclusions lipidique et terpeniques dês pseudophylles du pin maritime au moyen du reactif Nadi. Comptes Rendus de l'Académie des Sciences, 258, 1338–1340.

[14] Furr, M., Mahlberg, P.G. (1981). Histochemical analyses of lacticifers and glandular trichomes in *Cannabis sativa*. Journal of Natural Products, 44, 153–159. https://doi.org/10.1021/np50014a002.

[15] Nanjo, Y., Skultety, L., Uvackova, L., Klubicova, K., Hajduch, M., Komatsu, S. (2012). Mass spectrometry-based analysis of proteomic changes in the root tips of flooded soybean seedlings. Journal of Proteome Research, 11, 372–85. https://doi.org/10.1021/pr200701y.

[16] Wiśniewski, J.R., Zougman, A., Nagaraj, N., Mann, M. (2009). Universal sample preparation method for proteome analysis. Nature Methods, 6, 359–62. https://doi.org/10.1038/nmeth.1322.

[17] Burrieza, H.P., Rizzo, A.J., Vale, E.M., Silveira, V., Maldonado, S. (2019). Shotgun proteomic analysis of quinoa seeds reveals novel lysine-rich seed storage globulins. Food Chemistry, 293, 299–306. https://doi.org/10.1016/j.foodchem.2019.04.098.

[18] Reis, R.S., Vale, E.M., Sousa, K.R., Santa-Catarina, C., Silveira, V. (2021). Pretreatment free of 2,4-dichlorophenoxyacetic acid improves the differentiation of sugarcane somatic embryos by affecting the hormonal balance and the accumulation of reserves. Plant Cell, Tissue and Organ Culture, 145, 101–115. https://doi.org/10.1007/s11240-020-01995-z.

[19] Distler, U., Kuharev, J. , Navarro, P., Levin, Y., Schild, H., Tenzer, S. (2014). Drift time-specific collision energies enable independent acquisition proteomics. Nature Protocols, 11, 167-170. https://doi.org/10.1038/nmeth.2767.

[20] Distler, U., Kuharev, J., Navarro, P., Tenzer, S. (2016). Label-free quantification in ion mobility – enhanced data-independent acquisition proteomics. *Nature Protocols* 11, 795–812. https://doi.org/10.1038/nprot.2016.042.

[21] Vernet, H., Fullana, A.M., Sorribas, F.J., Gualda, E.J. (2022). Development of microscopic techniques for the visualization of plant – root-knot nematode interaction. Plants, 11, 1–15. https://doi.org/10.3390/plants11091165.

[22] Tagi, N., Mahanta, B., Borah, A., Kumar, P. (2023). Histopathological study of nanocomposite treated okra roots infected with *Meloidogyne incognita*. The Pharma Innovation, 12, 4451–55.

[23] Siddique, S., Grundler, F.M.W. (2015). Metabolism in nematode feeding sites. In: Plant nematode interactions – a view on compatible interrelationships.Eds.: Escobar, C., Fenoll, C., Elsevier Publ., chapter 5, pp. 119-138.

[24] Xu, L.H., Xiao, L.Y., Xiao, Y.N., Peng, D.L., Xiao, X.Q., Huang, W.K., …, Wang, G.F. (2021). Plasmodesmata play pivotal role in sucrose supply to *Meloidogyne graminicola*-caused giant cells in rice. Molecular Plant Pathology, 22, 539–550. https://doi.org/10.1111/mpp.13042.

[25] Vilela, R.M.I.F., Kuster, V.C., Magalhães, T.A., Martini, V.C., Oliveira, R.M., Oliveira, D.C. (2023). Galls induced by a root - knot nematode in *Petroselinum crispum* (Mill.): impacts on host development, histology, and cell wall dynamics. Protoplasma, 260, 1287–1302. https://doi.org/10.1007/s00709-023-01849-3.

[26] Meidani, C., Ntalli, N.G., Giannoutsou, E., Adamakis, I.S. (2019). Cell wall modifications in giant cells induced by the plant parasitic nematode *Meloidogyne incognita* in wild-type (Col-0) and the Fra2 *Arabidopsis thaliana* katanin mutant. International Journal of Molecular Sciences 20, 1–17. https://doi.org/10.3390/ijms20215465.

[27] Holbein, J., Franke, R.B., Marhavy, P., Fujita, S., Gorecka, M., Sobczak, M., …, Siddique, S. (2019). Root endodermal barrier system contributes to defence against plant-parasitic cyst and root-knot nematodes. The Plant Journal 100, 221–236. https://doi.org/10.1111/tpj.14459.

[28] Przybylska, A., Stęplowska, A.O. (2020). Plant defense responses in monocotyledonous and dicotyledonous host plants during root-knot nematode.

Plant Soil 451, 239–260. https://doi.org/10.1007/s11104-020-04533-0.

[29] Pereira, B.M., Arraes, F., Martins, A.C.Q., Alves, N.S.F., Melo, .P., Morgante, C.V., ..., Brasileiro, A.C.M. (2023). A novel soybean hairy root system for gene functional validation. Plos One, 18, e0285504. https://doi.org/10.1371/journal.pone.0285504

[30] Li, M., Zu, Y., Li, S., Zhang, W., Yin, C., Lin, Y. (2022). Regulation of phytohormones on the growth and development of plant. Frontiers in Plant Science, 13, 865302. http://dx.doi.org/10.3389/fpls.2022.865302.

[31] Mattos, V.S., Leite, R.R., Cares, J.E., Gomes, A.C.M.M., Moita, A.W., Lobo, V.L.S., Carneiro, R.M.D.G. (2019). *Oryza glumaepatula*, a new source of resistance to *Meloidogyne graminicola* and histological characterization of its defense mechanisms. Phytopathology 109, 1941–1948. https://doi.org/10.1094/PHYTO-02-19-0044-R

[32] Lengai, G.M.W., Muthomi, J.W., Mbega, E.R. (2020). Phytochemical activity and role of botanical pesticides in pest management for sustainable agricultural crop production. Scientific African, 7, e00239. https://doi.org/10.1016/j.sciaf.2019.e00239.

[33] Babenko, L.M., Smirnov, O.E., Romanenko, K.O., Trunova, O.K. (2019). Phenolic compounds in plants: biogenesis and functions. Ukrainian Biochemical Journal, 91, 5-18. https://doi.org/10.15407/ubj91.03.005.

[34] Wallis, C.M., Galarneau, E.R. (2020). Phenolic compound induction in plant-microbe and plant-insect interactions: a meta-analysis. Frontiers in Plant Science, 11, 580753. https://doi.org/10.3389/fpls.2020.580753.

[35] Costa, S.N.O., Silva, M.V.T., Ribeiro, J.M., Castro, J.M.C., Muzitano, M.F., Costa, R.G.,..., Fernandes, K.V.S. (2023). Secondary metabolites related to the resistance of *Psidium* spp. against the nematode *Meloidogyne enterolobii*. Heliyon 9, e17778. https://doi.org/10.1016/j.heliyon.2023.e17778.

[36] Tzean, Y., Wang, K.T., Chen, E.G., Wang, H.W., Wu, T.M., Liu, C.A. (2024).

Antioxidant responses and growth impairment in *Cucurbita moschata* infected by *Meloidogyne incognita.* Biology 13, 267. https://doi.org/10.3390/biology13040267

[37) Zhu, Y., Yuan, G., Zhao, R., An, G., Li, W., Si, W., ..., Sun, D. (2022). Comparative transcriptome analysis reveals differential gene expression in resistant and susceptible watermelon varieties in response to *Meloidogyne incognita*. Life, 12, 1003. https://doi.org/10.3390/life12071003

[38] Kavya, G.S., Muthuvel, I., Rajangam, J., Prabhu, S. (2019). Bio chemical profiling to identify resistant guava varieties against *Meloidogyne enterolobii*. Journal of Pharmacognosy and Phytochemistry 8, 3442–3449.

[39] Zhou, F., Pichersky, E. (2020). More is better: the diversity of terpene metabolism in plants. Current Opinion in Plant Biology, 55, 1–10. https://doi.org/10.1016/j.pbi.2020.01.005.

[40] Hammerbacher, A., Coutinho, T.A., Gershenzon, J. (2019). Roles of plant volatiles in defence against microbial pathogens and microbial exploitation of volatiles. Plant, Cell and Environment, 42, 2827–2843. https://doi.org/10.1111/pce.13602.

[41] Mwamba, S., Kihika-Opanda, R., Murungi, L.K., Losenge, T., Beck, J.J., Torto, B. (2021). Identification of repellents from four non-host Asteraceae plants for the root knot nematode, *Meloidogyne incognita*." *Journal of Agricultural an* 69: 15145–15156. https://doi.org/10.1021/acs.jafc.1c06500

[42] Scupinari, T., Mannochio-Russo, H., Marcheafave, G.G., Bolzani, V.S., Nunes, E.O., Dias, W.P., ..., Zeraik, M.L. (2024). Effects of *Crotalaria spectabilis* extract in *Meloidogyne javanica* and *Heterodera glycines* soybean nematodes. European Journal of Plant Pathology, 170, 985-996. https://doi.org/10.1007/s10658-024-02821-4.

[43] Divekar, P.A., Narayana, S., Divekar, B.A., Kumar, R., Gadrataji, B.G., Ray, A., …, Behera, T.K. (2022). Plant secondary metabolites as defense tools against

herbivores for sustainable crop protection. International Journal of Molecular Sciences, 23, 2690. https://doi.org/10.3390/ijms23052690.

[44] Kuang, M.S., Liu, T.T., Wu, H.B., Lan, H.P., Wen, Y.X., Wu, H.B., Li, X.M. (2020). Constituents leached by tomato seeds regulate the behavior of root-knot nematodes and their antifungal effects against seed-borne fungi. Journal of Agricultural and Food Chemistry, 68, 9061–9069. https://doi.org/10.1021/acs.jafc.0c01797.

[45] Ahmadi, M., Moghadam, E.M., Rouhani, R., Mehrvar, M., Ahmady, V. (2023). Effect of root-knot nematode *Meloidogyne incognita* on barley: morphological alterations and the role of enzymes in interactions. Russian Journal of Plant Physiology, 70, 150. https://doi.org/10.1134/S1021443723601635.

[46] Khan, A., Hussain, A., Ali, F., Hamayum, M., Iqbal, A., Elansary, H.O., Kim, H.Y. (2024). Biocontrol of root knot nematodes by endophytic fungus isolated from garlic. Scientia Horticulturae 332, 113223. https://doi.org/10.1016/j.scienta.2024.113223.

[47] Ali, M., Ohri, P. (2023). Deciphering the synergistic effect of jasmonic acid and spermine in mitigating root-knot nematode stress in tomato plants through enhancing growth and activity of antioxidant enzymes. South African Journal of Botany, 161, 21–35. https://doi.org/10.1016/j.sajb.2023.07.063.

[48] Leonetti, P., Molinari, S. (2020). Epigenetic and metabolic changes in root-knot nematode-plant interactions. International Journal of Molecular Sciences, 21, 7759. https://doi.org/10.3390/ijms21207759.

[49] Hewezi, T.(2020). Epigenetic mechanisms in nematode – plant interactions. Annual Review of Phytopathology, 58, 119–138. https://doi.org/10.1146/annurev-phyto-010820-012805.

[50] Atighi, M.R., Verstraeten, B., De Meyer, T., Kyndt, T. (2021). Genome-wide shifts in histone modifications at early stage of rice infection with *Meloidogyne graminicola*. Molecular Plant Pathology, 22, 440–455.

https://doi.org/10.1111/mpp.13037.

[51] Bennett, M., Piya, S., Baum, T.J., Hewezi, T. (2022). MiR778 mediates gene expression, histone modification, and DNA methylation during cyst nematode parasitism. Plant Physiology, 189, 2432–2453. https://doi.org/10.1093/plphys/kiac228.

[52] Despot-slade, E., Mravinac, B. (2021). The centromere histone is conserved and associated with tandem repeats sharing a conserved 19-Bp box in the holocentromere of *Meloidogyne* nematodes. Molecular Biology and Evolution, 38, 1943–1965. https://doi.org/10.1093/molbev/msaa336.

[53] Pratx, L., Rancurel, C., Da Rocha, M., Danchin, E.G.J., Castagnone-Sereno, P., Abad, P., Perfus-Barbeoch, L. (2018). Genome-wide expert annotation of the epigenetic machinery of the plant-parasitic nematodes *Meloidogyne* spp., with a focus on the asexually reproducing species. BMC Genomics, 19, 321. https://doi.org/10.1186/s12864-018-4686-x

[54] Verstraeten, B., Atighi, M.R., Ruiz-Ferrer, V., Escobar, C., De Meyer, T., Kyndt, T. (2021). Non-coding RNAs in the interaction between rice and *Meloidogyne graminicola*. BMC Genomics, 22, 560. https://doi.org/10.1186/s12864-021-07735-7.

[55] Chen, P.H., Tjong, W.Y., Yang, H.C., Liu, H.Y, Stern, A., Chiu, D.T.Y. (2022). Glucose-6-phosphate dehydrogenase, redox homeostasis and embryogenesis. International journal of Molecular Sciences, 23, 2017. https://doi.org/10.3390/ijms23042017.

[56] Gross, R, Zhang, S., Wei, L., Caplan, A., Kuhl, J., Dandurand, L., …, Xiao, F. (2020). The *Globodera pallida* effector GpPDI1 is a functional thioredoxin and triggers defense-related cell death independent of its enzymatic activity. Phytopathology, 110, 1838–1844. https://doi.org/10.1094/PHYTO-02-20-0038-R.

[57] Zhao, J., Mejias, J., Quentin, M., Chen, Y., Almeida-Engler, J., Mao, Z., …, Jian, H. (2020). The root-knot nematode effector MiPDI1 targets a stress-associated

protein (SAP) to establish disease in Solanaceae and Arabidopsis. New Phytologist, 228, 1417–1430. https://doi.org/10.1111/nph.16745

[58] Aghaie, P., Ali, S., Tafreshi, H. (2020). Central role of 70-KDa heat shock protein in adaptation of plants to drought stress. Cell Stress and Chaperones, 25, 1071–1081. https://doi.org/10.1007/s12192-020-01144-7

[59] Pagliuso, D.C., Bodas, D.M., Pasquinelli, A.E.. (2021). Recovery from heat shock requires the microRNA pathway in *Caenorhabditis elegans*. PLoS Genetics, 17, e1009734. http://dx.doi.org/10.1371/journal.pgen.1009734.

[60] Hishinuma-Silva, S.M., Lopes-Caitar, V.S., Nomura, R.B.G., Sercero, B.C., Silva, A.G., Carvalho, M.C.C.G., ..., Guimarães, F.C.M. (2020). The soybean gene GmHsp 22.4 is involved in the resistance response to *Meloidogyne javanica* in *Arabidopsis thaliana*. BMC Plant Biology, 20, 535. https://doi.org/10.1186/s12870-020-02736-2.

[61] Ribeiro, D.G., Mota, A.P.Z., Santos, I.R., Arraes, F.B.M., Grynberg, P., Fontes, W., ..., Mehta, A. (2022). NBS-LRR-WRKY genes and protease inhibitors (PIs) seem essential for cowpea resistance to root-knot nematode. Journal of Proteomics, 261, 104575. https://doi.org/10.1016/j.jprot.2022.104575.

[62] Tian, Z.L., Zhou, J.Y., Zheng, J.W., Han, S.J. (2023). Mgr-Mir-9 implicates *Meloidogyne graminicola* infection in rice by targeting the effector MgPDI. Journal of Integrative Agriculture, 22, 1445–1454. https://doi.org/10.1016/j.jia.2022.08.127.

[63] Costa, S.N.O., Ribeiro, J.M., Castro, J.M.C., Fernandes, K.V.S. (2025) Tackling the plant parasitic nematode *Meloidogyne enterolobii*: Challenges and strategies for control in relevant crops. Tropical Plant Pathology, 50:39, 1-17. https://doi.org/10.1007/s40858-025-00734-z.

Supplementary materials

S1 - Mass Spectrometry Procedures and Conditions

The runs consisted of three biological replicates of 2.0 µg of peptides. Samples were loaded onto a nanoAcquity UPLC M-Class Symmetry C18 trap column (5 µm, 100 Å, 180 µm × 20 mm, 2D) at a flow rate of 5 µL/min for 3 min, then onto a nanoAcquity M-Class HSS T3 analytical column (1.8 µm, 100 Å, 75 µm × 150 mm) at 400 nL/min and at 45°C.

Peptides were eluted by a varying binary gradient between a mobile phase A (water with 0.1% formic acid), and a phase B (acetonitrile with 0.1% formic acid) as follows: 5% B for 3 min, increasing from 5 to 41% B over 92 min, increasing from 41 to 97% B over 96 min, holding at 97% B for 100 min, and decreasing to 5% B at 102 min.

Mass spectrometry was performed in positive mode and resolution mode (V mode), with 35,000 full widths at half maximum (FWHM) resolutions and ion mobility, and in data-independent acquisition (DIA) mode. Ion mobility separation (IMS) utilized an IMS wave velocity of 800 m/s (HDMSE); transfer collision energy increased from 19 to 55 V in high-energy mode; cone and capillary voltages were 30 V and 3000 V, respectively; and the source temperature was 100°C. For time-of-flight (TOF) parameters, scan time was set to 0.5 s in continuous mode, and the mass range was from 50 to 2000 Da. Human fibrinopeptide B [Glu1] at 100 fmol μL^{-1} was used as an external calibrant, and lock mass acquisition was performed every 30 s. Mass spectrum was acquired using MassLynx software (version 4.1, Waters).

Proteomic data analysis

The HDMSE analysis are followed these parameters: 150 counts for low-energy threshold; 50 counts for elevated-energy threshold; 750 counts for intensity threshold; one missed cleavage; minimum fragment ions per peptide equal to three; minimum fragment ions per protein equal to seven; minimum peptides per protein equal to two; fixed carbamidomethyl (C) modifications and variable oxidation (M) and phosphorylation (STY) modifications; false discovery rate (FDR) set to 1%; automatic peptide and fragment tolerance.

Parameters for label-free quantification analysis were: peptide and protein FDR 1%; minimum peptide sequence length of at least six amino acid residues; and

minimum peptide score equal to six. The samples were treated by a multidimensional normalization process and the software performed relative protein quantification based on the TOP3 method. Based on the relative abundances of uniquely assigned peptides, the abundances of shared peptides were redistributed to their respective originating proteins, followed by TOP3-based quantification [20].

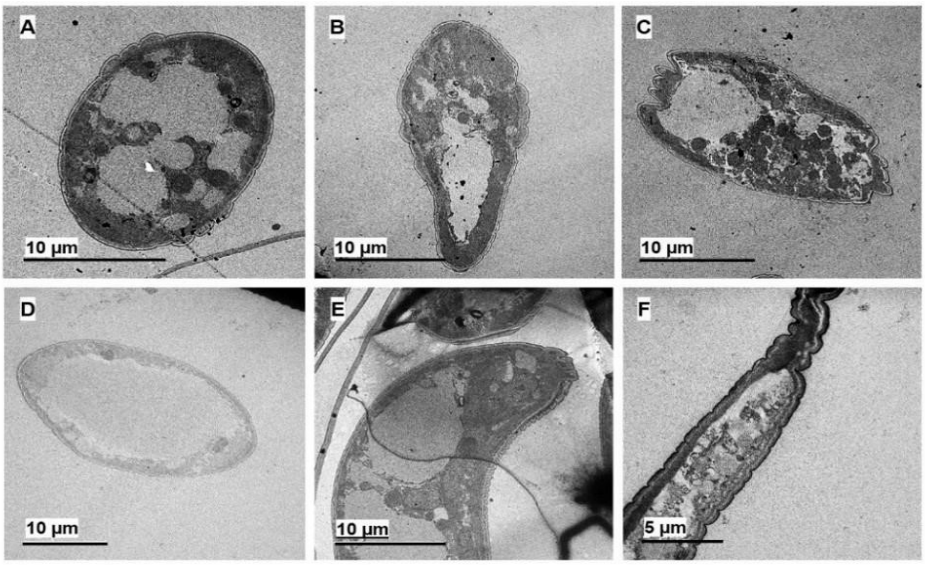

Figure 1S - Images obtained by transmission electron microscopy of the developmental phases of the nematode *Meloidogyne enterolobii* present in the inoculum used in the experiment of this study: eggs (A, B and C); eggshell (D); a juvenile individual emphasizing its anterior feeding region (E) and its posterior region (F).

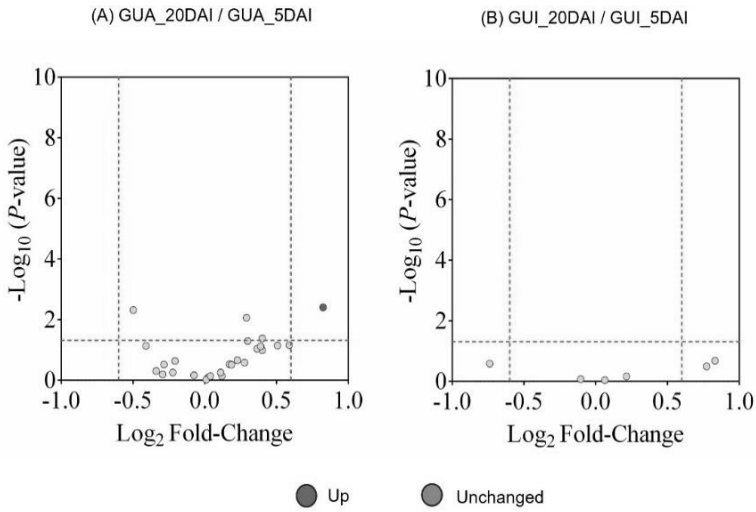

Figure 2S - Volcano plot displaying the distribution of 26 proteins in *P. guajava* and 11 in *P. guineense* between the time points of 5 and 20 DAI: (A) e (B).

3.3 Transcriptomic analysis reveals systemic leaf responses underlying resistance *of P. friedrichsthalianium* to *Meloidogyne enterolobii*

Lucas Felipe da Silva [1,2*]; Sara Nállia de Oliveira Costa [3,4*]; Raulzito Fernandes Moreira [1]; Emanuela de Oliveira Alves Araújo [2]; Paula Machado de Araújo [3,4]; Clicia Grativol Gaspar de Matos [4]; Kátia Valevski Sales Fernandes [3,4], José Mauro da Cunha e Castro [5]; João Paulo Matos Santos Lima [1,6]; Juliana Martins Ribeiro [5]; Katia Castanho Scortecci [1,2]

**Both authors contributed equally to the paper.*

[1] Programa de Pós-Graduação em Bioinformática, Instituto Metrópole Digital (IMD), Universidade Federal do Rio Grande do Norte, Brazil;
[2] Departamento de Biologia Celular e Genética, Centro de Biociências, Universidade Federal do Rio Grande do Norte, Brazil;
[3] Programa de Pós-Graduação em Biociências e Biotecnologia, Universidade Estadual do Norte Fluminense Darcy Ribeiro, Brazil;
[4] Laboratório de Química e Função de Proteínas e Peptídeos, Centro de Biociências Biotecnologia, Universidade Estadual do Norte Fluminense Darcy Ribeiro, Rio de Janeiro, Brazil;
[5] Empresa Brasileira de Pesquisa Agropecuária (Embrapa), Centro de Pesquisa Agropecuária do Trópico Semiárido, Petrolina, Pernambuco, Brazil;
[6] Departamento de Bioquímica, Centro de Biociências, Universidade Federal do Rio Grande do Norte, Brazil.

Abstract

The guava tree (*Psidium guajava*) is a key tropical fruit crop, yet its productivity is threatened by the root-knot nematode *Meloidogyne enterolobii*, which can reduce yields by up to 65%. To uncover resistance mechanisms, we compared a resistant species (*P. friedrichstalianium*) with a susceptible cultivar (*P. guajava* 'Paluma'), analyzing systemic transcriptomic responses in leaves post-infection. This study represents one of the first transcriptomic surveys of Psidium under nematode stress,

revealing strong systemic signaling from roots to shoots. In *P. friedrichstalianium*, infection triggered precise transcriptional reprogramming of 444 genes linked to photosynthesis, carbon metabolism, redox balance, and phenolic biosynthesis, supporting sustained energy production and antioxidant defense. In contrast, *P. guajava* exhibited 387 genes with broader, less coordinated responses, indicating weaker systemic adjustment. Interactome analyses confirmed integration of photosynthetic regulation, oxidative stress mitigation, and cytoskeletal organization in resistant leaves. These results emphasize the central role of systemic leaf responses in nematode resistance and provide a foundation for breeding resilient guava cultivars.

Keywords: Guava; Biotic stress; RNA-Seq data; Differential gene expression; Systemic responses; Plant breeding.

3.3.1 Introduction

The guava tree (*Psidium guajava*) is native to the northern regions of South America and is widely cultivated in tropical and subtropical areas (Altendorf, 2019). India is the world's leading producer of guava, while Brazil also occupies a prominent position in global production. In Brazil, guava cultivation is concentrated in the semi-arid Northeast, particularly in the states of Pernambuco, Bahia, and Ceará, and in the Southeast, mainly in São Paulo. Brazil ranks fourth in global production, after India, Pakistan, and Mexico (Ribeiro et al., 2018).

Guava fruits are consumed fresh and are widely processed into jams, juices, desserts, and gourmet products, gaining increasing attention from chefs. Nutritionally, they are rich in polyphenols, carotenoids, sugars, essential nutrients, and vitamins A, B, and C. In addition, guava leaves are recognized for their potential therapeutic properties (Todorov and Bogsan, 2016).

Among the major phytosanitary threats to guava cultivation is *Meloidogyne enterolobii*, a root-knot nematode that also affects several economically important crops, such as tomato and potato, and is distributed worldwide (Philbrick et al., 2020; Sikandar et al., 2023). In Brazil and other countries, infestations significantly reduce crop yields by impairing plant growth, fruit development, and ripening (Simões et al., 2023). Losses may reach up to 65% of production, often becoming evident only at

harvest (Castagnone-Sereno and Castillo, 2014; Sikandar et al., 2023). Diagnosis is challenging, as symptoms frequently overlap with those caused by other root-knot nematodes (Sikandar et al., 2023).

Current research efforts focus on identifying resistant genotypes and developing effective field management strategies (Castagnone-Sereno et al., 2013; Philbrick et al., 2020). *M. enterolobii* employs effector proteins to degrade plant cell walls, thereby facilitating penetration and inducing the formation of specialized feeding structures. Insights into nematode–plant interactions, particularly from studies on *M. incognita*, have demonstrated the capacity of nematodes to manipulate host gene expression (Philbrick et al., 2020).

Advances in omics technologies have expanded genomic knowledge, particularly in model plants such as *Arabidopsis thaliana* and rice (Thudi et al., 2021). However, omics data for *Psidium* species remain scarce, with the closest available genomic information derived from *Eucalyptus grandis*. Proteomic and metabolomic studies on *P. guajava* have primarily focused on fruit ripening (Monribot-Villanueva et al., 2021), while assessments of genetic diversity rely mostly on morphological and biochemical traits (Guagappa et al., 2022).

Biotechnological tools such as marker-assisted selection (MAS) have shown promise in accelerating the genetic improvement of perennial crops, including guava (Tiwari et al., 2022). MAS is independent of environmental influence and enables the early identification of commercially important traits, eliminating the need to wait for phenotypic expression (Jabran et al., 2023).

In this context, Souza et al. (2018) identified *P. guajava* genotypes with high levels of resistance to *M. enterolobii*, including the rootstock “BRS Guaraçá.” Nevertheless, little is known about the molecular responses of *Psidium* species to infection by this nematode. Notably, this study represents one of the first transcriptomic analyses of *Psidium* species infected by *Meloidogyne*, providing novel insights into the genes and pathways involved in nematode resistance. To address this knowledge gap, the present study investigates two contrasting species: a resistant genotype (*P. friedrichstalianium* – Araçá tree, Costa Rica) and a susceptible cultivar (*P. guajava* – ‘Paluma’). Both species were inoculated with *M. enterolobii* to identify genes potentially associated with resistance or susceptibility to infection.

3.3.2 Material and method

Plant material and growth conditions

Seedlings of *P. friedrichstalianium*, Araçá tree Costa Rica (nematode resistant species Costa Rica) and *P. guajava* 'Paluma' (nematode susceptible) were germinated and maintained in a greenhouse at Embrapa Semiarid (Petrolina, PE, Brazil). At 40 days old, seedlings were inoculated with 6,000 second-stage juvenile (J2) eggs of *Meloidogyne enterolobii*. A control group of seedlings remained uninoculated. At 26 days post inoculation (DPI), plants were harvested, and leaves were collected, frozen in liquid nitrogen, and stored at -80 °C for subsequent analyses.

RNA extraction and sequencing

For RNA extraction, 500 mg of leaves were collected from P. friedrichstalianium (resistant) and P. guajava (susceptible), both non-inoculated (control) and inoculated (test). The RNA extraction method followed Gasik et al. (2004), with modifications. Briefly, 500 mg of leaves were ground in liquid nitrogen, and 500 µL of extraction buffer (200 mM Tris-HCl pH 5; 100 mM LiCl; 5 mM EDTA; 1/10 volume SDS 10%) was added. The mixture was combined with 500 µL of phenol/chloroform (v/v) and centrifuged at 13,000 g for 5 min at 4°C. The upper phase was transferred to a new tube, mixed with 1 volume of 6 M LiCl, and incubated at 4°C overnight. After centrifugation (13,000 g, 10 min, 4°C), the pellet was resuspended in 1 mL of 3 M LiCl and centrifuged again. The new pellet was then resuspended in 250 µL of RNase-free water, combined with 0.1 volume of sodium acetate (pH 5.2) and 2 volumes of ethanol, and stored at -80°C for 15 min. After centrifugation (13,000 g, 15 min, 4°C), the final pellet was washed with 70% ethanol, air-dried, and resuspended in 50 µL of RNase-free water. A 3% agarose gel was done to analyse the quality of total RNA as well as the reading at Nano Drop (Thermo).

The total RNA samples were treated with DNase I (Ambion), and their quality was assessed by agarose gel electrophoresis and Bioanalyzer 2000 after this treatment. Samples from leaves with an RNA Integrity Number (RIN) of ≥7.0 were sent to a sequencing facility for further analysis using the Illumina Hi Seq 2000 platform.

De novo assembly and sequence processing

Quality control analysis of the RNA-seq data was performed using the built-in QuaCRS version 1.2 tool. FastQC software (version 0.10.1) was integrated into QuaCRS to analyze the raw sequence data. Only reads with Phred scores ≥ 30 were retained for further analysis. Sequence quality was assessed using RNA-SeQC (version 1.1.8) (KrolL et al., 2014). The reference genome used was Eucalyptus grandis due to the limited availability of omics data for Psidium spp. In the absence of genome or transcriptome data for *P. friedrichstalianium* and *P. guajava*, the RNA-seq reads from each species were processed separately. De novo transcriptome assembly was performed independently for each species using Trinity (v2.2.0), allowing for the construction of a robust RNA-seq transcriptome without a reference genome. This approach ensured that transcripts remained species-specific and avoided sequence dilution. Three Trinity modules (Inchworm, Chrysalis, and Butterfly - Grabherr, 2011) were employed during assembly. Duplicate contigs were removed using cd-hit, resulting in unique gene sequence files for each library. To minimize bias in downstream analysis, differential expression analysis was conducted separately for each species, preserving dataset specificity. The quality of the data was assessed using hierarchical cluster analysis (HCA) and multidimensional scaling (MDS).

All analyses and assembly steps were conducted on a supercomputer at the High-Performance Processing Centre (NPAD) at the Federal University of Rio Grande do Norte (UFRN). The data are available in the SRA/NCBI under BioProject PRJNA779437.

Differential gene expression analysis

The consensus assembly of the P. *friedrichstalianium* and *P. guajava* libraries was used as a reference to obtain abundances of read. The resulting read counts and gene expression data were processed for all libraries and analysed using the Bioconductor edgeR package (version 3.4.2). Differential expressions were assessed using Fisher exact test (Robinson et al., 2010). Expression intensities were transformed into log fold change (logFC), and the distance between libraries was calculated using Pearson Correlation Coefficient and Ward Minimum Variance method. Differential expression analysis was performed separately by comparing

control (non-inoculated) and *M. enterolobii*-inoculated libraries for both *P. friedrichstalianium* and *P. guajava*.

Functional annotation

Enrichment analyses of Gene Ontology (GO) terms and KEGG pathways were performed using the Bioconductor STRINGdb package (version 3.8) (Szklarczyk et al., 2015), from information available for the model organism *Arabidopsis thaliana*. Only terms or pathways with adjusted P-values ≤ 0.05 were considered for further analysis.

Genes with Phytozome annotation and expression levels > 50 TPM were included in a differential expression-based clustering analysis (Table S1). TPM values were log2 transformed to reduce discrepancies. Heatmapper (http://www.heatmapper.ca/) was used to generate the heatmap, resulting in the inclusion of 83 genes. The Eucgr.L01887 sequence was excluded due to extrapolated expression values, leaving 82 genes for the analysis. An interactome analysis was conducted using these 82 genes, built using STRING (https://string-db.org/) in program parameters.

3.3.3 Results

Transcriptome analysis

Leaf tissues were selected for transcriptome analysis since nematode infection in the roots can trigger systemic signaling to the aerial parts. A total of 350,803,184 raw reads were obtained from the libraries of *P. guajava* and *P. friedrichstalianium*, comprising both inoculated and non-inoculated samples. Approximately 80% of the reads were of high quality.

The libraries were designated as follows: 1_S68 (*P. friedrichstalianium*, control – non-inoculated), 2_S69 (*P. friedrichstalianium*, inoculated with *M. enterolobii*), 3_S70 (*P. guajava*, control – non-inoculated), and 4_S71 (*P. guajava*, inoculated). The number of raw reads generated per library was 67,965,134 (1_S68), 62,078,986 (2_S69), 57,680,600 (3_S70), and 51,240,140 (4_S71).

De novo assembly produced 60,836 contigs, with an N50 of 786, N10 of 1,915, mean length of 563.95 bp, and a median length of 363 bp. The overall G+C content was 48.95%. From the assembled data, 16,722 contigs were commonly expressed across all libraries. In *P. friedrichstalianium*, 43,321 contigs were identified in the

control library and 29,828 in the inoculated condition. In *P. guajava*, 31,333 contigs were expressed in the control library, while 43,739 were detected in the inoculated samples (Figure 1).

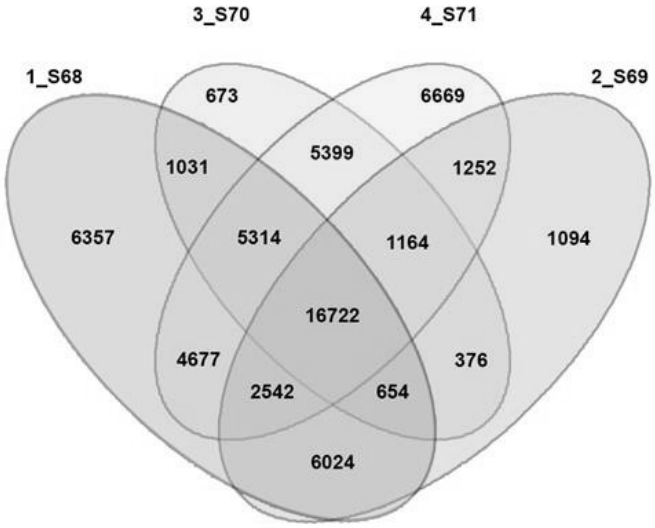

Figure 1 - Venn diagram showing the overlap between the libraries. The numbers above indicate the specific libraries analyzed. Library 1_S68 represents the *P. friedrichstalianium* control (non-inoculated, shown in blue); 2_S69 represents the *P. friedrichstalianium* inoculated library (test, shown in red); 3_S70 corresponds to the *P. guajava* control (non-inoculated, shown in green); and 4_S71 corresponds to the *P. guajava* inoculated library (test, shown in yellow). The Venn diagram depicts the total number of contigs aligned per library: 1_S68 – 43,260; 2_S69 – 29,827; 3_S70 – 31,332; 4_S71 – 43,738.

After filtering out low-count contigs, a total of 17,413 contigs remained, providing a robust dataset for subsequent analyses. The normalized data were subjected to hierarchical cluster analysis (HCA) and multidimensional scaling (MDS). Both approaches consistently grouped the contigs according to species (Figure 2).

HCA revealed a clear separation of the libraries into two main clusters (Figure 2A), while MDS, based on LogFC intensity, highlighted the distance between *P. friedrichstalianium* and *P. guajava* (Figure 2B). These results confirm the reliability of the transcriptome assembly and reinforce the evidence of differential gene expression between the two species.

Notably, *P. friedrichstalianium* (resistant) displayed a distinct transcriptional profile compared with *P. guajava* (susceptible), suggesting a specific molecular response against *M. enterolobii*. In contrast, *P. guajava* libraries, whether inoculated or not, clustered closely together, indicating a more limited or less differentiated

response to nematode infection.

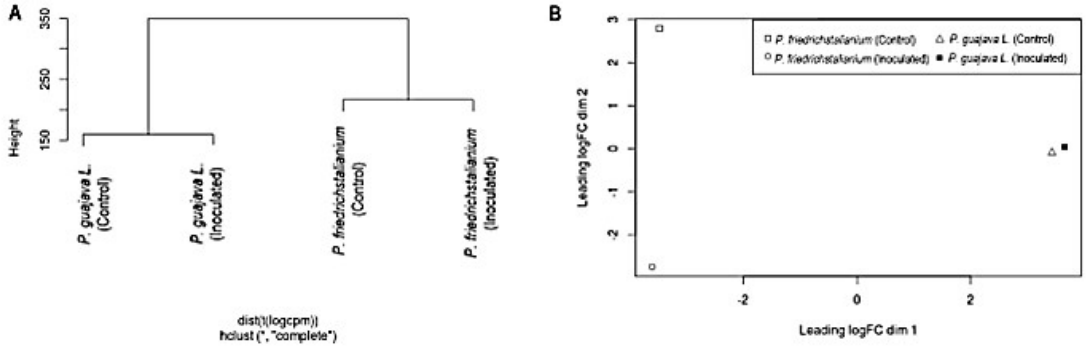

Figure 2 - Hierarchical cluster analysis (HCA) and multidimensional scaling (MDS) for the expression profiles of libraries in *Psidium* spp. (a): Hierarchical clustering analysis. (b): Multidimensional scaling. In the case of *P. friedrichstalianium,* the empty blue square represents the expression profile for the control samples, while the empty green circle represents the samples inoculated with the nematode. For the susceptible species *P. guajava* the empty red triangle represents the control samples (not inoculated), and the filled blue square represents the samples inoculated with the nematode.

The greater number of expressed contigs in *P. guajava* under inoculated conditions compared to *P. friedrichstalianium* suggests differences in their immune strategies. As a susceptible species, *P. guajava* appears to trigger a broader transcriptional response involving numerous stress- and defense-related genes, which may be less efficient in containing *M. enterolobii*. In contrast, the resistant *P. friedrichstalianium* likely activates more specific and effective defense mechanisms, requiring fewer transcriptomic changes. This indicates a more controlled and efficient response in *P. friedrichstalianium*, whereas *P. guajava* exhibits a wider but less effective transcriptional activation.

Global gene dispersion was also estimated across all libraries, including biased dispersion, in which gene variability was modeled relative to abundance (Figure 3). The estimated interlibrary dispersion parameter was 0.067, indicating a similar overall dispersion profile among the libraries. Despite this similarity, the transcriptional responses diverged between species: *P. guajava* displayed a broader activation under inoculated conditions, while *P. friedrichstalianium* maintained a more focused and controlled response, consistent with its resistant phenotype.

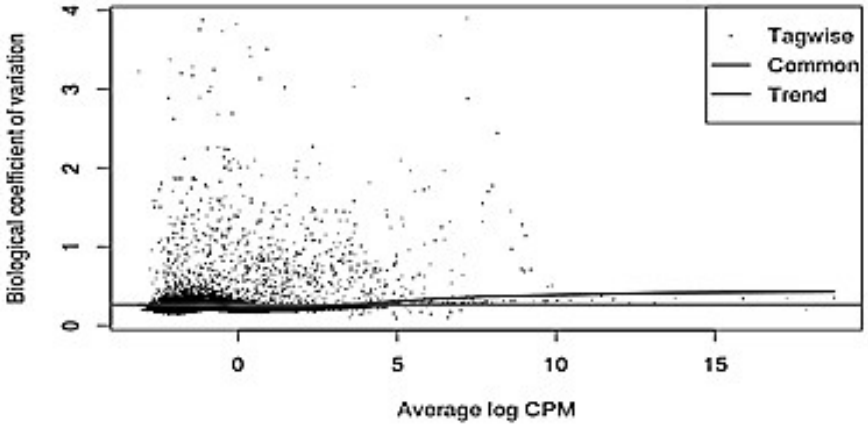

Figure 3 - Common dispersion among *Psidium* spp. The Y-axis represents the coefficient of biological variation (BCV), and the X-axis represents the average abundance of each gene. The points highlighted in black correspond to genes present in the libraries under study. The red line represents the estimate of common dispersion among the genes, while the blue line represents the dispersion trend.

Differential expressions from libraries

Following dispersion estimation, differential gene expressions were assessed in *P. friedrichstalianium* and *P. guajava*. Transcripts were identified using Fisher's exact test with a false discovery rate (FDR) ≤ 0.05 (Figure 4).

The relationship between log fold-change (logFC) and normalized read concentration (logCPM) is shown in Figures 4A and 4B. The distribution of values centered around zero on the ordinate axis indicates that library normalization was effective. Differentially expressed genes are highlighted in red, revealing 444 transcripts in *P. friedrichstalianium* and 387 in *P. guajava* (Table S2).

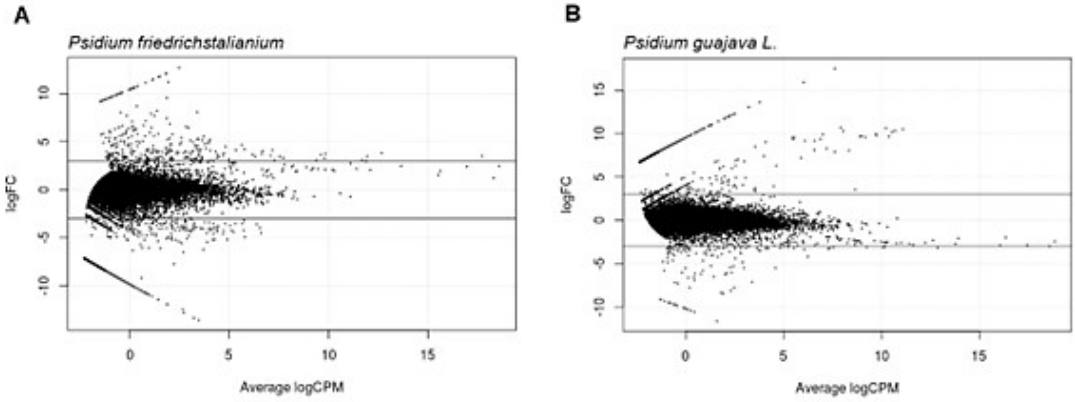

Figure 4 - MA-plot of differentially expressed transcripts in the libraries. (A): Differential expression in *P. friedrichstalianium*. (B) Differential expression in *P. guajava*. Differentially expressed genes with an FDR less than 10% are highlighted in red, and blue lines represent a four-fold change in expression. Black dots indicate genes that were not differentially expressed.

To evaluate relationships among samples and verify expression patterns, gene expression dispersion was calculated for control and inoculated libraries of *P. friedrichstalianium* and *P. guajava* (Figure 5). Scatterplots of control versus inoculated conditions (Figures 5A and 5D) showed similar overall distributions. In contrast, comparisons between species (Figures 5B and 5C) revealed greater dispersion, particularly along the *P. friedrichstalianium* axis. This broader variation suggests that *P. friedrichstalianium* activates a wider transcriptional response, which may be associated with its resistance to *M. enterolobii*.

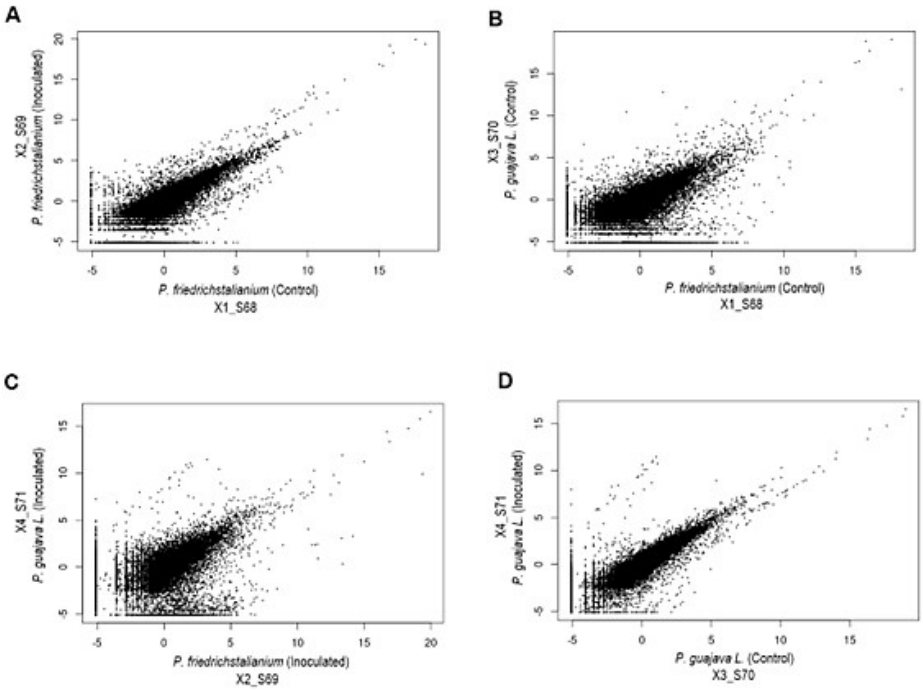

Figure 5 - Gene expression dispersion between different samples of *P. guajava* and *P. friedrichstalianium*. (A) *P. friedrichstalianium* control (not inoculated) (X1_S68) vs. inoculated *P. friedrichstalianium* (X2_S69). (B) *P. friedrichstalianium* control (not inoculated) (X1_S68) vs. *P. guajava* control (not inoculated) (X3_S70). (C) Inoculated *P. friedrichstalianium* (X2_S69) vs. inoculated *P. guajava* (X4_S71). (D) *P. guajava* control (not inoculated) (X3_S70) vs. inoculated *P. guajava* (X4_S71).

Gene Ontology and KEGG pathways after sequence enrichment

To investigate how *P. friedrichstalianium* and *P. guajava* respond to nematode infection, potential KEGG pathways were evaluated alongside Gene Ontology (GO) classifications. Three main GO categories were considered: molecular function (MF), cellular component (CC), and biological processes (BP). Within BP, the top 50 enriched terms were analyzed for each species (Figure S1).

Both species shared highly enriched terms, including *biological process*, *metabolic process*, *cellular process*, *cellular metabolic process*, *primary metabolic process*, *organic substance metabolic process*, and *cellular nitrogen compound metabolic process*. In *P. friedrichstalianium*, enrichment was particularly evident in *nucleobase-containing compound metabolic process* and *oxidation–reduction process* (Figure S1A), whereas in *P. guajava*, broader enrichment was observed in *gene expression* and *protein metabolic process* (Figure S1B).

KEGG enrichment analysis further highlighted similarities and differences between the species (Figure 6). Shared pathways included *Ribosome*, *Plant hormone signal transduction*, *Plant-pathogen interaction*, and *Carbon metabolism*. Distinct enrichments were also detected: in *P. guajava* (susceptible), *Protein processing in the endoplasmic reticulum*, *Protein export*, *Phagosome*, and *Biosynthesis of amino acids* were overrepresented. In contrast, *P. friedrichstalianium* (resistant) showed exclusive enrichment in *Valine, leucine and isoleucine degradation*, *Photosynthesis – antenna proteins*, *Carotenoid biosynthesis*, and *Amino sugar and nucleotide sugar metabolism*.

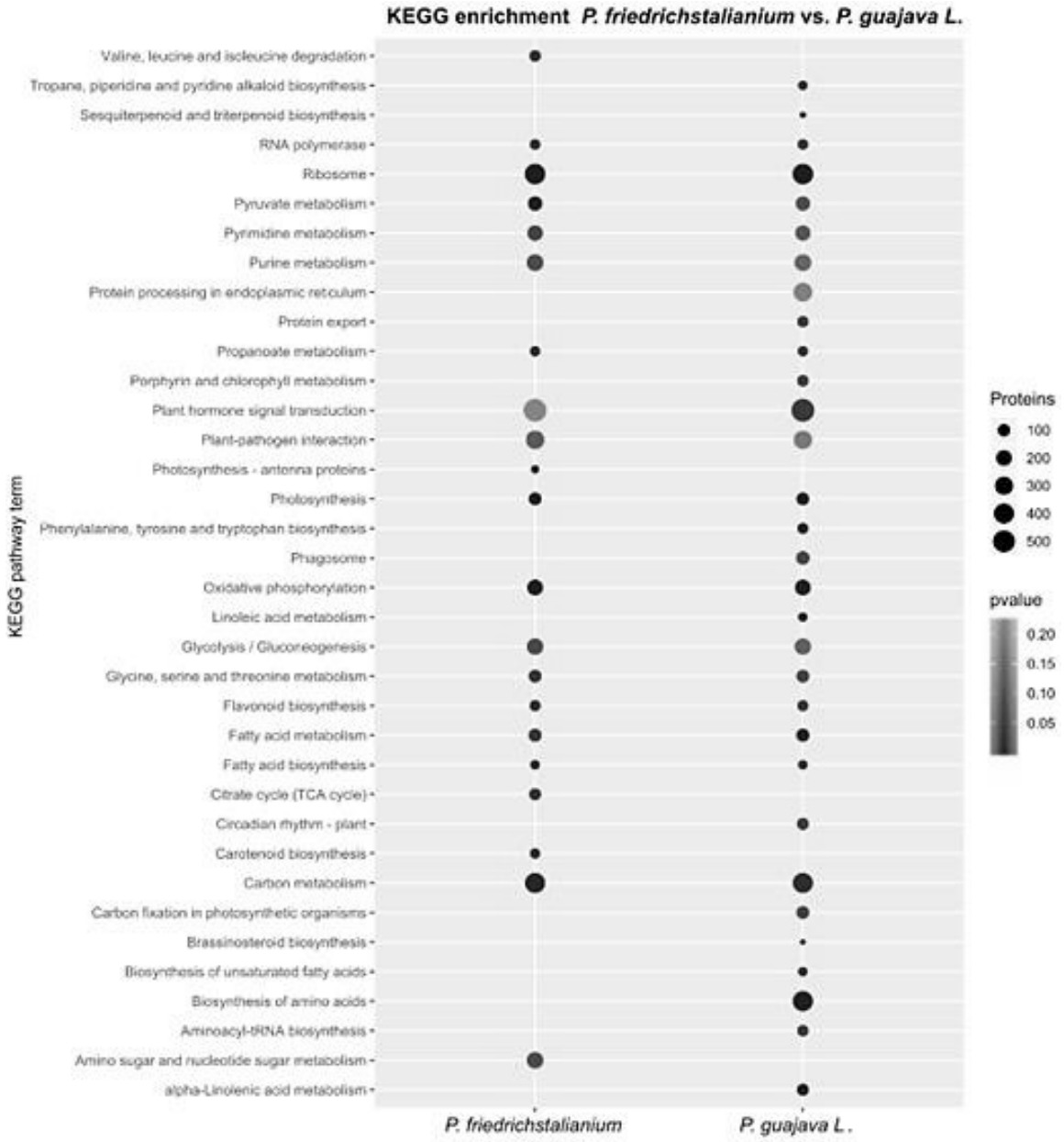

Figure 6 - KEGG enrichment. The size of the circles represents the quantity of protein associated with each term. The fill color gradient within the circles signifies terms with the highest P-value (highlighted in light blue) and those with the lowest P-value (highlighted in dark blue).

Heatmap and interactome

To investigate the transcriptional responses of *Psidium* species to *Meloidogyne enterolobii* infection, a heatmap of 82 genes was constructed, comparing *P. friedrichstalianium* (resistant) and *P. guajava* (susceptible) under inoculated and non-inoculated (control) conditions (Figure S2). Analyses revealed significant metabolic changes, particularly in photosynthesis. In inoculated *P. friedrichstalianium*, genes associated with Photosystem I and Photosystem II were prominently upregulated, suggesting a metabolic adjustment to maintain photosynthetic efficiency under biotic stress, which may represent an important component of its resistance response.

Additionally, genes involved in chlorophyll biosynthesis, electron transport (ferredoxin, NAD(P)H-dependent oxidoreductase), and Complexes I and II of the mitochondrial electron transport chain were upregulated in *P. friedrichstalianium*, whereas they were downregulated in inoculated *P. guajava*. This pattern indicates that maintaining electron transport chain integrity may support energy generation and mitigate oxidative damage in the resistant species.

Key enzymes of carbon metabolism, including phosphoribulokinase (PRK), glyceraldehyde-3-phosphate dehydrogenase (GAPDH), phosphoglycerate kinase (PGK), fructose-bisphosphate aldolase, glutamine synthetase, and the ATP synthase F1 complex, were also upregulated in inoculated *P. friedrichstalianium* but downregulated in inoculated *P. guajava*. Their induction suggests enhanced carbon utilization and energy balance in the resistant species, which may contribute to a more effective response to nematode infection.

Post-translational modification and stress-response pathways were likewise activated in *P. friedrichstalianium*, including serine hydroxymethyltransferase, thiamine biosynthesis protein THI4, and ADP-ribosylation-related proteins. These factors are associated with cofactor regeneration and modulation of cellular stress responses, suggesting an enhanced capacity to cope with pathogen attack.

Interactome analysis revealed three major functional hubs: (1) photosynthesis-related proteins (Photosystems I and II, oxygen-evolving complexes); (2) oxidative stress and phenolic metabolism proteins (catalase, peroxidase); and (3) cytoskeleton and DNA regulation proteins (elongation factor 1-alpha, tubulin, actin, ubiquitin, ADP-ribosylation). Collectively, these findings suggest that *P. friedrichstalianium*

coordinates photosynthesis, energy metabolism, and stress-response pathways in a more efficient and integrated manner, which may underline its resistance to *M. enterolobii* (Figure 7).

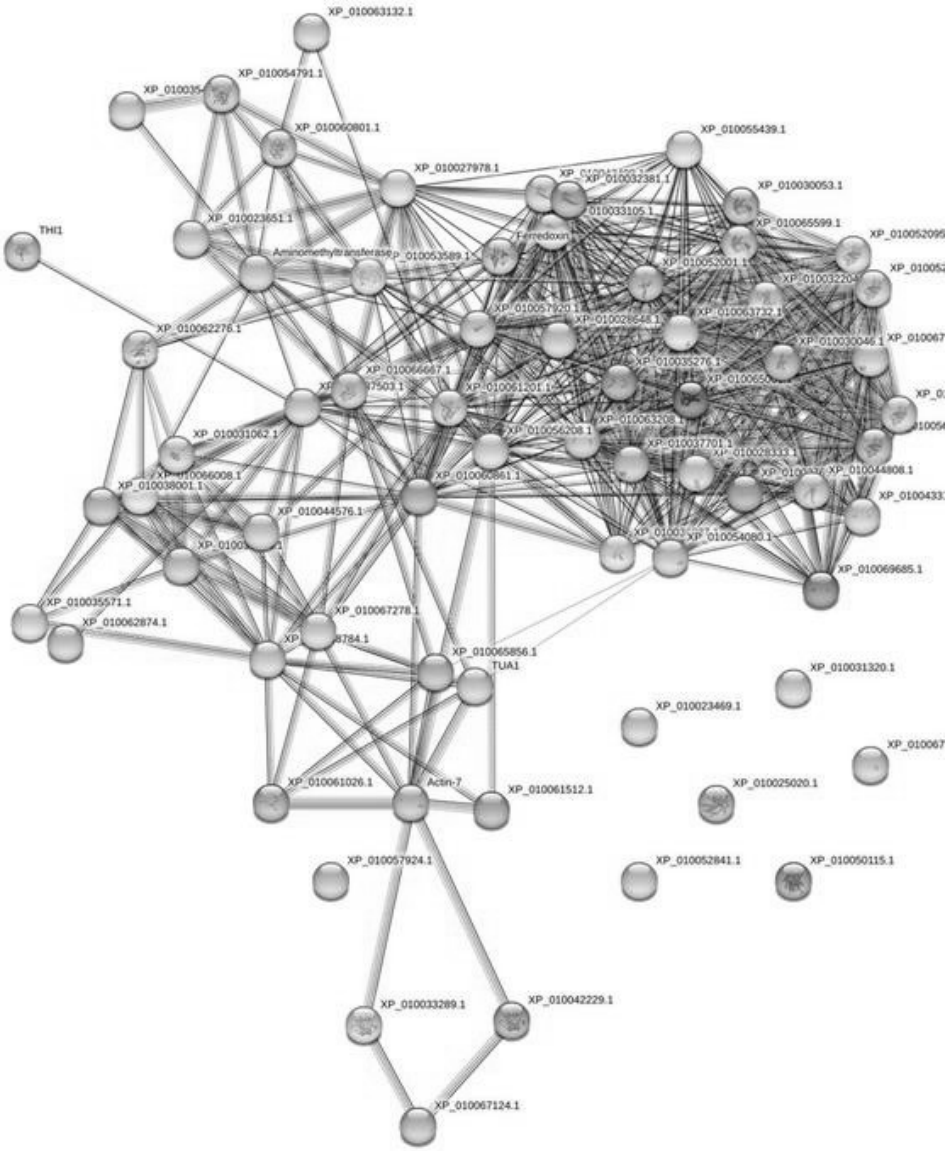

Figure 7 - Schematic representation of the protein interactome. This interactome was built using the 82 genes used for the heatmap, employing STRING (https://string-db.org/) and specific program parameters. The lines represent interactions between proteins, which are seen as circles by their turn. Nodes represent protein interactions produced by a single protein. Colored nodes represent query proteins and first-layer interactors. Empty nodes represent proteins that do not have interactions. Light blue lines indicate known interactions from curated databases, purple lines represent experimental data, green lines represent predicted interactions, and red lines represent predicted gene fusion intersections. Dark blue lines correspond to co-occurrence interactions, yellow lines correspond to proteins co-mentioned in texts in PubMed, and the black lines indicate co-expressed proteins.

3.3.4 Discussion

Comparative transcriptomic analyses between the susceptible *P. guajava* and resistant *P. friedrichstalianium* revealed distinct strategies in response to *Meloidogyne enterolobii* infection. Clustering analyses (HCA and MDS) showed clear separation between the species, highlighting species-specific transcriptional profiles. In *P. guajava*, inoculated and non-inoculated libraries clustered closely, suggesting a limited or less differentiated response to nematode infection. In contrast, *P. friedrichstalianium* exhibited distinct profiles between control and inoculated conditions, reflecting a broader transcriptional reprogramming in response to the nematode.

Differences in the number of expressed contigs support these patterns. In *P. guajava*, inoculation led to an increased number of expressed transcripts, suggesting a broad but potentially less effective defense activation. In *P. friedrichstalianium*, a more restricted but targeted set of transcripts was observed, indicating the activation of specific and efficient defense mechanisms. Dispersion analysis revealed greater transcriptional variation in *P. friedrichstalianium* compared to *P. guajava*, supporting the hypothesis that resistance is associated with a more regulated and coordinated transcriptional response. Differential expression analysis identified 444 transcripts in *P. friedrichstalianium* and 387 in *P. guajava*, highlighting qualitative differences in how each species responds to biotic stress.

Functional enrichment analyses (GO and KEGG) further emphasize this distinction. In *P. friedrichstalianium*, biological processes related to primary metabolism and redox balance were enriched. Pathways such as valine, leucine, and isoleucine degradation, photosynthesis (antenna proteins), carotenoid biosynthesis, and amino sugar and nucleotide sugar metabolism suggest an integration of energy, antioxidant, and metabolic adjustments that support resistance (Sánchez-Bermúdez et al., 2022; Wurtzel, 2019; Chen et al., 2020; Ren et al., 2023). In contrast, *P. guajava* showed enrichment in processes related to gene expression and protein metabolism, with KEGG pathways including protein processing in the endoplasmic reticulum, protein export, phagosome formation, and amino acid biosynthesis. These results indicate that the susceptible species activates stress responses associated with protein folding, synthesis, and modification, which may compromise cellular homeostasis under nematode infection (Chen et al., 2020; Manghwar and Li, 2022).

Differential expression patterns further revealed that genes related to photosynthesis, electron transport, carbon metabolism, and antioxidant responses (e.g., catalase and peroxidase) were upregulated in *P. friedrichstalianium*, whereas many of these genes were downregulated in *P. guajava*. This suggests that maintaining photosynthetic capacity, energy generation, and oxidative stress mitigation are central components of resistance in *P. friedrichstalianium* (Kerchev and Van Breusegem, 2022; Saijo and Loo, 2020; Zhou and Zhang, 2020).

Importantly, the analysis of secondary metabolism highlights that *P. friedrichstalianium* exhibits significant modulation of phenolic compounds, particularly those derived from the shikimate pathway, which are closely associated with oxidative stress responses. Upregulation of hydrolysable tannins, lignans, and terpenes suggests a coordinated strategy to mitigate reactive oxygen species while potentially inhibiting nematode infection, as observed by Costa et al. (2023). In contrast, the susceptible *P. guajava* lacks this targeted phenolic response, indicating that insufficient regulation of oxidative stress-related metabolites may underlie its vulnerability. These findings underscore the central role of phenolic metabolism in plant defense and the integration of chemical and transcriptional responses in resistant species.

Furthermore, studies in guava (*P. guajava*) and the resistant *P. guineense* support the central role of oxidative stress management in nematode defense. Comparative proteomic and histochemical analyses revealed that resistant plants respond to *M. enterolobii* by enhancing antioxidant enzyme activities and synthesizing secondary metabolites, including phenolics, terpenes, and alkaloids, which mitigate reactive oxygen species generated during infection. Upregulation of heat shock proteins and protein disulfide isomerases further integrates oxidative stress mitigation with protein homeostasis, emphasizing that effective resistance relies on coordinated biochemical and cellular adjustments to preserve cellular integrity under biotic stress (Costa et al., 2025b).

The interactome analysis highlighted three main functional hubs in the resistant species: (1) photosynthesis-related proteins, (2) oxidative stress and phenolic metabolism proteins, and (3) cytoskeleton and DNA regulation proteins. These results indicate that *P. friedrichstalianium* coordinates energy production, antioxidant defense,

and structural adjustments as part of an integrated response to *M. enterolobii* (Funkhouser and Aronson, 2007; Ryan et al., 2014).

Overall, these findings suggest that the resistance of *P. friedrichstalianium* involves a targeted and multifaceted transcriptional and metabolic response, whereas the susceptibility of *P. guajava* is associated with a broader but less effective activation of defense pathways. These insights not only enhance our understanding of the molecular mechanisms underlying nematode resistance in *Psidium* spp., but also highlight the crucial role of molecular responses in integrated nematode management, providing valuable information for future breeding programs and the development of biotechnological strategies to improve crop resilience (Costa et al., 2025a).

3.3.5 Conclusion

This study reveals that Psidium species mount systemic transcriptomic responses in leaves following *Meloidogyne enterolobii* infection. In resistant *P. friedrichstalianium*, leaves showed coordinated upregulation of genes related to photosynthesis, carbon metabolism, redox balance, and stress responses, suggesting an integrated defense strategy. In contrast, susceptible *P. guajava* exhibited a broader but less focused transcriptional response. These findings highlight the importance of systemic signaling to aerial tissues in effective nematode resistance and provide insights for developing resistant *Psidium* cultivars. Importantly, this study represents one of the first transcriptomic analyses of *Psidium* species infected by *M. enterolobii*, underscoring its pioneering role in uncovering the molecular mechanisms underlying nematode resistance and establishing a foundation for future research in this area.

References

Aina, O., Bakare, O.O., Fadaka, A.O., Keyster, M., Klein, A (2024). Plant biomarkers as early detection tools in stress management in food crops: a review. Planta, 259, 3, 60. doi: 10.1007/s00425-024-04333-1.

Altendorf, S. (2019). Major tropical fruits market review 2018. Rome: FAO. http://www.fao.org/documents/card/en/c/ca5692en/.

Baillo, E.H., Kimotho, R.N., Zhang, Z., Xu, P. (2019). Transcription Factors Associated

with Abiotic and Biotic Stress Tolerance and Their Potential for Crops Improvement. Genes, 10, 771. doi:10.3390/genes10100771.

Bali, S., Brown, C., Majtahedi, H., Yilma, S., Ingham, R.E., Cimrhakl, L., Quick, R., Sathuvalli, V. (2022). Genomic markers linked to *Meloidogyne chitwoodi* resistance introgressed from *Solanum bulbocastanum* to cultivated potato and their utility in marker-assisted selection. Molecular Breeding, 42, 3. doi.org/10.1007/s11032-022-01285-w.

Castagnone-Sereno, P., and Castillo, P. (2014). *Meloidogyne enterolobii* (Pacara earpod tree root-knot nematode). CABI Compedium. Available online at: https://www.cabi.org/isc/datasheet/33238.

Chen, Q., Yu, F., Xie, Q. (2020). Insights into endoplasmic reticulum-associated degradation in plants. New Phytologist, 226, 345–350. doi: 10.1111/nph.16369.

Costa, S.N. de O., Silva, M.V.T., Ribeiro, J.M., Castro, J.M. da C, Muzitano, M.F., Costa, R.G. da, Oliveira, A.E.A., Fernandes, K.V.S. (2023). Secondary metabolites related to the resistance of *Psidium* spp. against the nematode *Meloidogyne enterolobii*. Heliyon, 9, e17778. doi.org/10.1016/j.heliyon.2023.e17778.

Costa, S.N. de O., Ribeiro, J.M., Castro, J.M. da C, Fernandes, K.V.S. (2025a). Tackling the plant parasitic nematode *Meloidogyne enterolobii*: Challenges and strategies for control in relevant crops. Tropical Plant Pathology, 50, 39, doi.org/10.1007/s40858-025-00734-z

Costa, S.N. de O., Paschoa, R.P. da, Alexandrino, C.R., Cremonez, P.M., Ribeiro, J.M., Castro, Cunha, M da, Silveira, Oliveira, A.E.A., Fernandes, K.V.S. (2025b). *Psidium* defenses against *Meloidogyne enterolobii*: proteomic and microscopic analysis of this plant-predator association. Proteomics, doi.org/10.1002/pmic.70015

Funkhouser, J.D., Aronson, N.N. (2007). Chitinase family GH18: evolutionary insights from the genomic history of a diverse protein family. BMC evolutionary biology, 7, 1-16. doi: 10.1186/1471-2148-7-96.

Gangappa, N.D., Singh, C., Verma, M.K., Thakre, M., Sevanthi, A.M., Singh, R.,

Srivastav, M., Raghunandan, K., Anusha, C., Yadav, V., Nagaraja, A. (2022). Assessing the genetic diversity of guava germplasm characterized by morpho-biochemical traits. Front Nutr. 30,9,1017680. doi: 10.3389/fnut.2022.1017680.

Gasic, K., Hernandez, A., Korban, S.S. (2004). RNA extraction from different apple tissues rich in polyphenols and polysaccharides for cDNA library construction. Plant Mol Biol Rep 22: 437a–437g. DOI:10.1007/BF02772687.

Grabherr, M.G., Haas, B.J., Yassour, M., Levin, J.Z., Thompson, D.A., Amit, I., Adiconis, X., Fan, L., Raychowdhury, R., Zeng, Q., Chen, Z., Mauceli, E., Hacohen, N., Gnirke, A., Rhind, N., di Palma, F., Birren, B.W., Nusbaum, C., Lindblad-Toh, K., Friedman, N., Regev, A. (2011). Full-length transcriptome assembly from RNA-Seq data without a reference genome. Nat Biotechnol., 15, 29, 7, :644-652. doi: 10.1038/nbt.1883.

Jabran, M., Ali, M.A., Zahoor, A., Muhae-Ud-Din, G., Liu, T., Chen, W., Gao, L. (2023). Intelligent reprogramming of wheat for enhancement of fungal and nematode disease resistance using advanced molecular techniques. Frontiers in Plant Science, 14, 1–22. doi.org/10.3389/fpls.2023.1132699.

Kerchev, P.I., Van Breusegem, F. (2022). Improving oxidative stress resilience in plants. Plant J., 109, 2, 359-372. doi: 10.1111/tpj.15493.

Kroll, K.W., Mokaram, N.E., Pelletier, A.R., Frankhouser, D.E., Westphal, M.S., Stump, P.A., Stump, C.L., Bundschuh, R., Blachly, J.S., Yan, P. (2014). Quality Control for RNA-Seq (QuaCRS): An Integrated Quality Control. Cancer Inform., 13, Suppl 3, 7–14. doi: 10.4137/CIN.S14022.

Langdale, J.A. (1994). In situ hybridization. In: Freeling M, Walbot V, editors. The maize handbook. Heidelberg: Springer; 165–179.

La Verde, Dominici, P., Astegno, A. (2018). Towards Understanding Plant Calcium Signaling through Calmodulin-Like Proteins: A Biochemical and Structural Perspective. Int J Mol Sci, 30, 19, 5, 1331. doi: 10.3390/ijms19051331.

Li, X., Hu, Y., Su, M., Zhang, M., Du, J., Zhou, H., Zhang, X., Ye, Z. (2022). Genome-

wide analysis of terpene synthase gene family to explore candidate genes related to disease resistance in *Prunus persica*. Frontiers in Plant Science, 13, 1032838. doi: 10.3389/fpls.2022.1032838.

Lopes, C.M.L., Suassuna, N.D., Cares, J.E., Gomes, A.C.M.M., Perina, F.J., Nascimento, G.F., Mendonça, J.S.F., Moita, A.W., Carneiro, R.M.D.G. (2020.) Marker-assisted selection in *Gossypium* spp. for *Meloidogyne incognita* resistance and histopathological characterization of a near immune line. Euphytica, 216, 2. doi.org/10.1007/s10681-020-2554-7.

Manghwar, H.; Li, J. (2022). Endoplasmic Reticulum Stress and Unfolded Protein Response Signaling in Plants. Int. J. Mol. Sci., 23, 828. https://doi.org/10.3390/ ijms23020828.

Maqsood, A., Wu, H., Kamran, M., Altaf, H., Mustafa, A., Ahmar, S., Hồng, N.T., Tariq, K., He, Q., Chen, J. (2020). Variations in Growth, Physiology, and Antioxidative Defense Responses of Two Tomato (*Solanum lycopersicum* L.) Cultivars after Co-Infection of *Fusarium oxysporum* and *Meloidogyne incognita*. Agronomy, 22. DOI:10.3390/agronomy10020159.

Mohammadi, M.A., Cheng, Y., Aslam, M., Jakada, B.H., Wai, M.H., Ye, K., He, X., Luo, T., Ye, L., Dong, C., Hu, B., Priyadarshani, S.V.G.N., Wang-Pruski, G., Qin, Y. (2021). ROS and Oxidative Response Systems in Plants Under Biotic and Abiotic Stresses: Revisiting the Crucial Role of Phosphite Triggered Plants Defense Response. Front. Microbiol., 12, 631318. doi: 10.3389/fmicb.2021.631318.

Monribot-Villanueva, J.L., Altúzar-Molina, A., Aluja, M., Zamora-Briseño, J.A., Elizalde-Contreras, J.M., Bautista-Valle, M.V., de Los Santos, I.A., Sánchez-Martínez, D.E., Rivera-Reséndiz, F.J., Vázquez-Rosas-Landa, M., Camacho-Vázquez, C., Guerrero-Analco, J.A., Ruiz-May, E. (2022). Integrating proteomics and metabolomics approaches to elucidate the ripening process in white *Psidium guajava*. Food Chem., 15, 367, 130656. doi: 10.1016/j.foodchem.2021.130656.

Olas, J.J., Apelt, F., Annunziata, M.G., John, S., Richard, S.I., Gupta, S., Kragler, F., Balazadeh, S., Mueller-Roeber, B. (2021). Primary carbohydrate metabolism genes

participate in heat-stress memory at the shoot apical meristem of *Arabidopsis thaliana*. Mol Plant. 6, 14, 9, 1508-1524. doi: 10.1016/j.molp.2021.05.024.

Philbrick, A.N., Adhikari, T.B., Louws, F.J., Gorny, A.M. (2020). *Meloidogyne enterolobii*, a Major Threat to Tomato Production: Current Status and Future Prospects for Its Management. Frontiers in Plant Science, 11. https://www.frontiersin.org/journals/plant-science/articles/10.3389/fpls.2020.606395. 10.3389/fpls.2020.606395.

Ren, H., Zhang, Y., Zhong, M., Hussian, J., Tang, Y., Liu, S., Qi, S. (2023). Calcium signaling-mediated transcriptional reprogramming during abiotic stress response in plants. Theor. Appl. Genet. 136, 210. https://doi.org/10.1007/s00122-023-04455-2.

Ribeiro, J.M., Castro, J.M. da, Pinto, M.S.T., Fernandes, K.V.S., Scortecci, K.C., Pedrosa, E.M.R. (2018). Recursos genéticos, biológicos e bioquímicos para o manejo de *Meloidogyne enterolobii* em goiabeira: a contribuição da Embrapa. Petrolina: Embrapa Semiárido. 25 p. (Embrapa Semiárido. Documentos, 286).

Robinson, M.D., Oshlack, A. (2010). A scaling normalization method for differential expression analysis of RNA-seq data. Genome Biol 11, R25. https://doi.org/10.1186/gb-2010-11-3-r25.

Ryan, A., Kaplan, E., N., J.-C., Polycarpou, E., Crescente, V., Lowe, E., Preston, G.M., Sim, E. (2014). Identification of NAD(P) H quinone oxidoreductase activity in azoreductases from P. aeruginosa: azoreductases and NAD (P) H quinone oxidoreductases belong to the same FMN-dependent superfamily of enzymes. PloSone,9, 6, e98551, 2014. doi:10.1371/journal.pone.0098551.

Saijo, Y., Loo, E.P.O. (2020). Plant immunity in signal integration between biotic and abiotic stress responses. New Phytologist, 225, 87–104. doi: 10.1111/nph.15989.

Sánchez-Bermúdez, M., del Pozo, J.C., Pernas, M. (2022). Effects of combined abiotic stresses related to climate change on root growth in crops. Front. Plant Sci. 13. doi: 10.3389/fpls.2022.918537.

Simões, W.L., Andrade, V.P.M., Silva, J.S., Santos, C.A.F., Sousa, J.S.C., Calgaro,

M., Barbosa, K.V.F., Nascimento, B.R. (2023). Fruit production and quality of 'Paluma' guava with nematode-tolerant rootstock irrigated in the semi-arid region. Brazilian Journal of Agricultural and Environmental Engineering. 27, 5, 400-406. doi: dx.doi.org/10.1590/1807-1929/agriambi.v27n5p400-406.

Sikandar A, Jia L, Wu H, Yang S. (2022). Meloidogyne enterolobii risk to agriculture, its present status and future prospective for management. Front Plant Sci. 24, 13, 1093657. doi: 10.3389/fpls.2022.1093657.

Souza, R.R.C. de, Santos, C.A.F., Costa, S.R da (2018). Field resistance to *Meloidogyne enterolobii* in a *Psidium guajava* × *P. guineense* hybrid and its compatibility as guava rootstock. Fruits, 73, 2, 118-124. Doi: 10.17660/th2018/73.2.4.

Su, J., Jiao,Q., Jia, T., Hu, X. (2024). The photosystem-II repair cycle: updates and open questions. Planta, 259, 1, 20, 2024. doi.org/10.1007/s00425-023-04295-w.

Sun J.L., Li J.Y., Wang M.J., Song Z.T., Liu J.X. (2021). Protein Quality Control in Plant Organelles: Current Progress and Future Perspectives. Mol. Plant. 14, 95-114. https://doi.org/10.1016/j.molp.2020.10.011.

Szklarczyk D., Franceschini A., Wyder S., Forslund K., Heller D., Huerta-Cepas J., Simonovic M., Roth A., Santos A., Tsafou K.P., Kuhn M., Bork P., Jensen L.J., von Mering C. (2015). STRING v10: protein-protein interaction networks, integrated over the tree of life. Nucleic Acids Res. 43, D447-452. doi: 10.1093/nar/gku1003.

Thudi, M., Chen, Y., Pang, J., Kalavikatte, D., Bajaj, P., Roorkiwal, M., Chitikineni, A., Ryan, M.H., Lambers, H., Siddique, K.H.M., Varshney, R.M. (2021). Novel genes and genetic loci associated with root morphological traits, phosphorus-acquisition efficiency and phosphorus-use efficiency in chickpea. Front. Plant Sci. 12. doi: 10.3389/fpls.2021.636973.

Tiwari, J.K., Yerasu, S. R., Rai, N., Singh, D.P., Singh, A.K., Karkute, S.G., Singh, P.M., Behera, T.K. (2022). Progress in marker-assisted selection to genomics-assisted breeding in tomato. Critical Reviews in Plant Sciences, 41, 5, 321–350. doi.org/10.1080/07352689.2022.2130361.

Todorov, S.D., Bogsan, C.S. (2016). Tropical fruits-from cultivation to consumption and health benefits: Guava and mango. New York: Nova Science Publishers Inc.

Van der Geer, J., Handgraaf, T., Lupton, R.A. (2020). The art of writing a scientific article. J. Sci. Commun. 163, 51–59. https://doi.org/10.1016/j.sc.2020.00372.

Warmerdam, S., Sterken, M.G., Van Schaik, C., Oortwijn, M.E.P., Lozano-Torres, J.L., Bakker, J., Goverse, A., Smant, G. (2019). Mediator of tolerance to abiotic stress ERF6 regulates susceptibility of *Arabidopsis* to *Meloidogyne incognita*. Mol Plant Pathol. 2019 Jan;20(1):137-152. doi: 10.1111/mpp.12745.

Wurtzel, E.T. (2019). Changing Form and Function through Carotenoids and Synthetic Biology, Plant Physiology, 179, 830–843. doi: 10.1104/pp.18.01122.

Zhang J., Wang, P., Ji, J., Long, H., Wu, X. (2021). Transcriptome analysis reveals the molecular mechanism of yield increases in maize under stable soil water supply. PloS one, v. 16, n. 9, p. e0257756, 2021. doi.org/10.1371/journal.pone.0257756.

Zhou, J.-M., Zhang, Y. (2020). Plant Immunity: Danger Perception and Signaling. Cell, 28, 181, 978-989. doi: 10.1016/j.cell.2020.04.028.

Yadav M., Pandey J., Chakraborty A., Hassan M. I., Kundu J. K., Roy A., Singh, I.K., Singh, A. (2022). A comprehensive analysis of calmodulin-like proteins of *Glycine max* indicates their role in calcium signaling and plant defense against insect attack. Front. Plant Science. 13. doi: 10.3389/fpls.2022.817950

Supplementary materials

A)

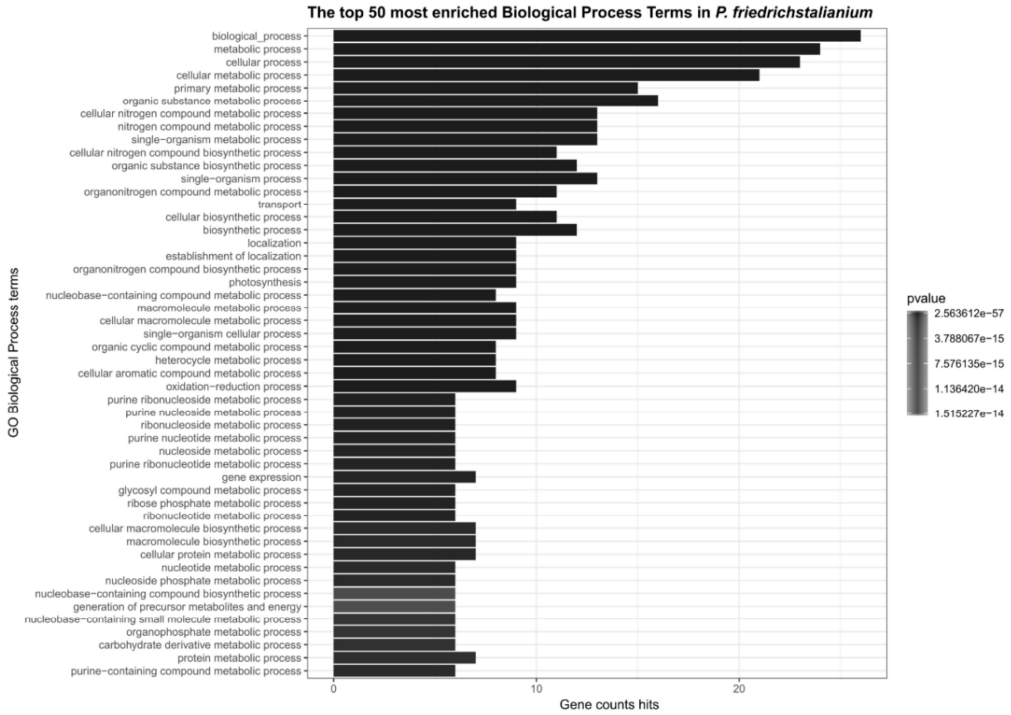

B)

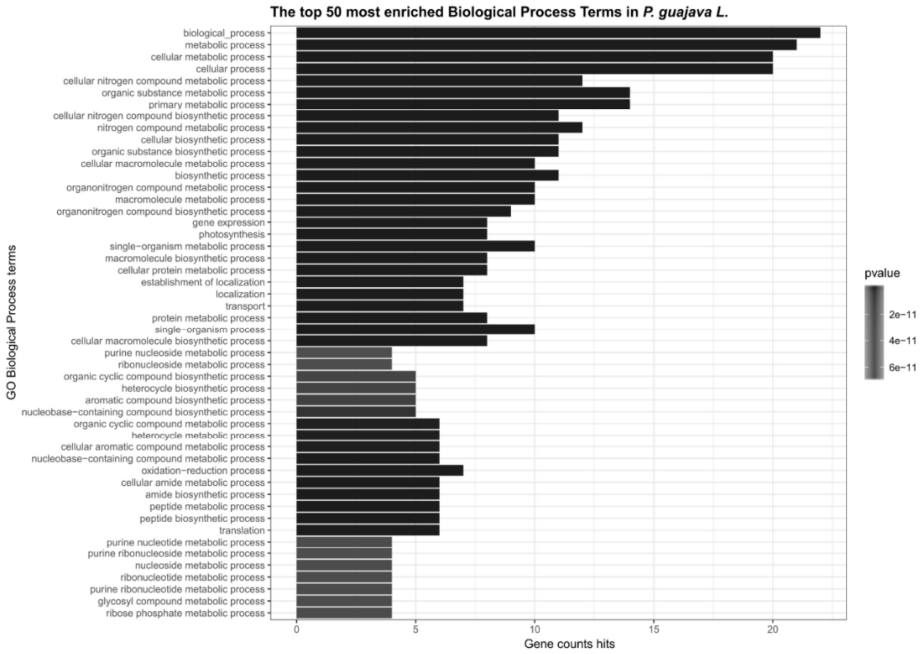

Figure 1S - Gene Ontology terms identified after libraries enrichment. In (a) it was represented for P. *friedrichstalianium* and in (b) for *P. guajava*. The x-axis represents the gene count per hit relative to the term expressed on the y-axis. The color gradient represented in the bars indicate terms with the highest *P*-value (highlighted in blue) and with the lowest *P*-value (highlighted in red). Terms with *P*-value adjusted to ≤0.05.

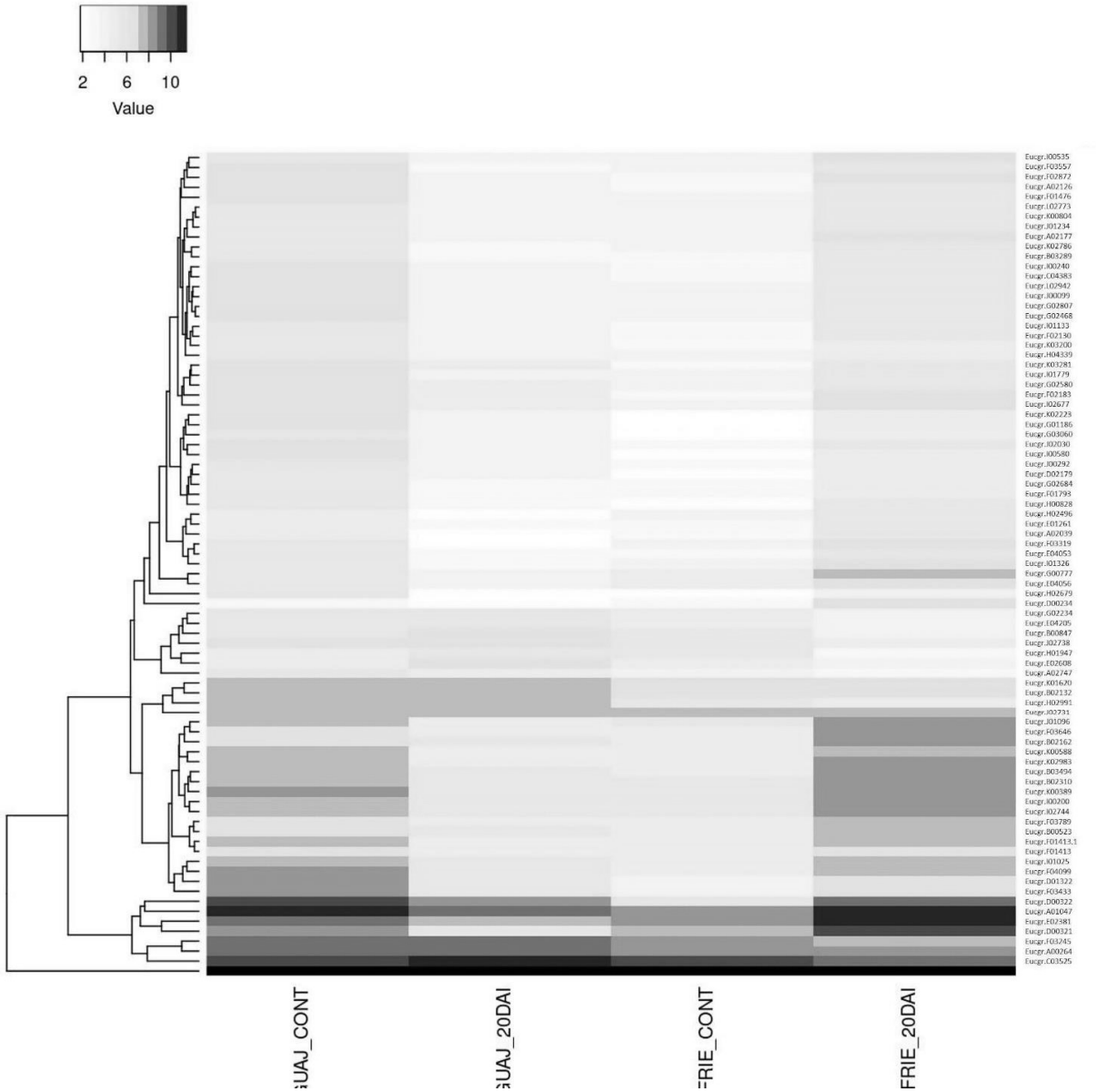

Figure 2S - Heatmap of differentially expressed genes. A heatmap generated from the normalized expression values of the 82 identified genes, with columns representing the analyzed libraries: GUAJ_CONT – *P. guajava* control (not inoculated); GUAJ_20DAI – *P. guajava* inoculated; GUIN_CONT – *P. friedrichsthalianum* control (not inoculated); GUIN_20DAI – *P. friedrichsthalianum* inoculated. Values range from yellow (2) to blue (10).

Table 1S - The annotation of the 82 genes with expression levels above 50 TPM presented in the heatmap, along with their respective protein sequences

Number	Genes Code	Gene Name	Protein sequence
1	Eucgr.I00535	Histone superfamily protein	MARTKQTARKSTGGKAPRKQLATKAARKSAPTTGGVKKPHRYRPGTVALREIRKYQKSTE LLIRKLPFQRLVREIAQDFKTDLRFQSHAVLALQEAAEAYLVGLFEDTNLCAIHAKRVTI MPKDIQLARRIRGERA*
2	Eucgr.F03557	Catalase 2	MDPHKYRPSSAFNTSFWTTNSGAPVWNNNSSLTVGSRGPILLEDYHLVEKLANFDRERIP ERVVHARGASAKGFFEVTHDISQLTCADFLRAPGVQTPVIVRFSTVIHERGSPETLRDPR GFAVKFYTREGNFDLVGNNFPVFFVRDGMKFPDMVHALKPNPKSHIQENWRIVDFFSHHP ESLHMFTFLFDDIGIPQDYRHMEGSGVNTYTLINKAGKVHYVKFHWKPTCGVKNLLEEEA IRVGGSNHSHATQDLYDSIAAGNYPEWKLFIQIIDPDHEDKFDFDPLDVTKTWPEDILPL MPVGRLVLNRNIDNFFAENEQLAFCPSIVVPGVFYSDDKLLQTRIFSYSDTQRHRLGPNY LQLPPNAPKCAHHNNHHEGFMNFMHRDEEINYFPSRYDPVRHAERYPIPTAMLTGKREKT IIEKENNFKQPGERYRSWTPDRQERFICRWVDALSDPRMRSAASGFHTGLRPTNLWVRN*
3	Eucgr.F02872	Glutamine synthase clone r1	MSLLSDLVNLNLSDCTEKIIAEYIWIGGSGMDMRSKARTFPGPVNDPSKLPKWNYDGSST NQAPGEDSEVILYPQAIFKDPFRGGNNILVMCDAYTPGGQPIPTNKRCAAAKIFSHPNVV VEEPWYGLEQEYTLLQKDVKWPLGWPVGGFPGPQGPYYCGAGADKAFGRDIVDAHYKACL YAGINVSGINGEVMPGQWEFQVGPSVGISASDELWVARYILERITEIAGVVLSFDPKPIQ GDWNGAGAHTNYSTKTMRNEGGYEIIKKAIEKLGLRHKEHIAAYGEGNERRLTGRHETAD INTFKWGVANRGASIRVGRDTEKDGKGYFEDRRPASNMDPYVVTSMIAETTILWKP*
4	Eucgr.A02126	Cobalamin-independent synthase family protein	MKKQGTNLDRHCSPSERLPRRTTPKSRQDLPHSLGPDTLFIVTYMLQSTQSLSVAGRMMS AARKAHSQRVGDESYGLNSYLYKEEVKIPHKKKKRKRSTNRHDPQRKTNERGRVGNECGR TWSCEIEERHCQLEPDRFPMSDRSLPLGSPSSNRATLLSLRVSLSLSHSLSLFPREEEEE PVAAPLLSPPREMASHIVGYPRMGPKRELKFALESFWDGKSSAEDLQKVAADLRSSIWKQ MADASIKYIPSNTFAYYDQVLDTTAMLGAVPPRYGWKGGEIGHDVYFSMARGNASVPAME MTKWFDTNYHYIVPELGPDVKFSYASHKAVSEYKEAKALGVNTVPVLVGPVSYLLLSKPA KGVDKNFSLLSLLGKILPVYKEVISELKAAGASWIQFDEPTLVMDLDSHKLQAFTEAYSQ LESSLSGLNVLIETYFADIPAEAYKVLTSLKGVTGFGFDLVRGTKTLDLIKGAFPKGKYL FAGVVDGRNIWANDLAASLSTLNALEGIVGKDKLVVSTSCSLLHTAVDLVNETKLDKEIK SWLAFAAQKVVEVNMLAKALAGQKDEAFFSANATAQASRKTSPRVINQAVQKAAAALKGS DHRRATNVSARLDAQQKKLNLPILPTTTIGSFPQTVELRRVRREYKAKKISEDEYVKAIK EEINKVVKLQEELDIDVLVHGEPERNDMVEYFGEQLSGFAFTVNGWVQSYGSRCVKPPII YGDVSRPKPMTVFWSSMAQSMTARPMKGMLTGPVTILNWSFVRNDQPRFETCYQIALAIK DEVEDLEKAGINVIQIDEAALREGLPLRKSEQAFYLEWAVHSFRITNCGVKDTTQIHTHM CYSHFNDIIHSIIDMDADVITIENSRSDEKLLSVFREGVKYGAGIGPGVYDIHSPRIPST EEIADRVNKMLAVLEKNILWVNPDCGLKTRKYTEVKPALKNMVAAAKVLRTQLASTK*

5	Eucgr.F01476	Phosphoglycerate kinase family protein	MASAAAPTAFSLLSSSASASSSSSSSSTSGSALLHLRSSGLRSSGLRRLGFAAADPFLAA HVASKLRSLRGKGSRGVVSMAKKSVGDLTGPALKGKKVFVRADLNVPLDDNQNITDDTRV RAAVPTIKYLIQNGARVILSSHLGRPKGVTPKYSLAPLVPRLSELLGIQVVKADDCIGPE VEKLVASLPEGGVLLLENVRFYKEEEKNEPEFAKKLASLADLYVNDAFGTAHRAHASTEG VTKFLKPSVAGFLLQKELDYLVGAVSTPKRPFAAIVGGSKVSSKIGVIESLLEKCDILLL GGGMIFTFYKAQGLSVGSSLVEEDKLDLATSLLKKAKAKGVSLLLPTDVVIADKFAPDAN SKIVPASAIPDGWMGLDIGPDSIKTFNDALGTTKTVIWNGPMGVFEFDKFAAGTEAVAKK LAELSAAGVTTIIGGGDSVAAVEKVGVADVMSHISTGGGASLELLEGKELPGVVALDEAT PVPV*
6	Eucgr.L02773	Glycine cleavage t-protein family	MRGGGLWQLGQSIRRQLAQADKKSVARRYFASEADLKKTVLYDFHVTHGGKMVPFAGWSM PIQYKDSIMESTVNCRENGSLFDVSHMCGLSLKGKDCITFLEKLVMGDVAALAPGTGTLS VFTNEKGGAIDDTVITKVKDDHIYLVVNAGCRDKDLAHIEEHMKAFKAKGGDVLWHIHDE RSLLALQGPLAAPVLQHLTKEDLSKIYFSDFRIIDINGASCFLTRTGYTGEDGFEISVPS EHAVDLAKAILEKSEGKVRLTGLGARDSLRLEAGLCLYGNDMEQHITPVEAGLTWAIGKR RRAEGGFLGAETILKQLEEGPKIRRAGFISSGPPARSHSEIQNDKGANIGEVTSGGFSPC LKKNIAMGYVKSGSHKAGTKVKILVRGKAYDGVVTKMPFVPTKYYKPS*
7	Eucgr.K00804	Translation initiation factor sui1 family protein	MSELDVQVPTTFDPFADAKAEDSGAGSKEYVHIRVQQRNGRKSLTTVQGLKKEFSYNKIL KDLKKEFCCNGTVVQDPELGQVIQLQGDQRKNVSTFLVQQAGIVKKERIKIHGF*
8	Eucgr.J01234	Rubisco activase	MATAVPTVGTVNRAPLNLNGSNTGASAPSSAFFGSSLKKMTQKLPKACSPSGGLGVRAMA DDEEKQTDKDKWRGLAYDTSDDQQDITRGKGMVDSVFQAPMGTGTHYAVMSSYDYISTGL RQYDFDNTMGGFYIAPAFMDKLVVHITKNFMTLPNIKVPLILGIWGGKGQGKSFQCELVF AKMGINPIMMSAGELESGNAGEPAKLIRQRYREAADIIKKGKMCCLFINDLDAGAGRMGG TTQYTVNNQMVNATLMNIADNPTNVQLPGMYNKEENPRVPIIVTGNDFSTLYAPLIRDGR MEKFYWAPTREDRIGVCMGIFRTDNIAGEDVVKIVDAFPGQSIDFFGALRARVYDDEVRK WISGVGVETIGKKLVNSKEGPPTFEQPKMSVEKLLEYGNMLVQEQENVKRVQLADKYMSE AALGDANQDSINSGTFYGKAAQQVHVPVPEGCTDPNAANFDPTARSDDGSCLYTF*
9	Eucgr.A02177	Dicarboxylate diiron protein, putative (crd1)	MAAEMALLKPISKFASTPGLAGPGAPSRPRFAAVRMSATAQPAAPKKPAKKANKQAIKET LLAPRFYTTDFDEMEQLFNTEINKNLNQDEFVALLQEFKTDYNQTHFVRNKEFKEAADKM QGPLRQIFVEFLERSCTAEFSGFLLYKELGRRLKKTNPVVAEIFSLMSRDEARHAGFLNK GLSDFNLALDLGFLTKARKYTFFKPKFIFYATYLSEKIGYWRYITIYRHLKENPEYQPYP IFKYFENWCQDENRHGDFFSALMKAQPQFLNDWKAKLWSRFFCLSVYVTMYLNDCQRTAF YEGIGLNTKEFDMHVIIETNRTTARIFPAVLDVENPEFKRKLDRMVEINTKLIAVGETED IPLVKNLKRIPLIAALASELLAAYLMPPIESGSVDFAEFEPRLVY*
10	Eucgr.K02786	Rab gtpase homolog e1b	MANHKGNSPSGTWYTLNEIVKQQMCVPELNYVAPTGAPIGSEEITPRLSLSLLYPLSHSL LSSSSSTHSQALFLSLPKGLPIRRAMALSTAASSKLIYPCPASSSPASSAAAPAAAPAAR ALPSTVAAAAVFRTRLAPAQLSSSFIAPFAPTSGASTGVVPARRGRGAFTVRAARGKFER KKPHVNIGTIGHVDHGKTTLTAALTMALAAMGNSAPKKYDEIDAAPEERARGITINTATV EYETENRHYAHVDCPGHADYVKNMITGAAQMDGAILVVSGADGPMPQTKEHILLAKQVGV

			PNMVVFLNKQDQVDDEELLQLVELEVRELLSSYEFPGDDIPIHSGSALLALEALMANPSI KRGENEWVDKIYELMDSVDSYIPIPQRQTDLPFLLAIEDVFSITGRGTVATGRVERGTVR VGETLDLVGLRETRNTTVTGVEMFQKTLDEAMAGDNVGLLLRGIQKIDIQRGMVLAKPGT ITPHTKFEAIVYVLKKEEGGRHSPFFAGYRPQFYMRTTDVTGRVTSIMNDKDEESKMVMP GDRVKMVVELIMPVACEQGMRFAIREGGKTVGAGVIQSIVE*
11	Eucgr.B03289	Ribosomal protein l18e/l15 superfamily protein	MTTRFKKNRKKRGHVSAGHGRIGKHRKHPGGRGNAGGMHHHRILFDKYHPGYFGKVGMRY FHKLRNKFYCPIVNVEKLWSLVPQDAKDKASGAAAAPVLDVTQFGFFKVLGKGVLPEKQP IVVKAKLVSKIAEKKIKEAGGAVVLTA*
12	Eucgr.I00240	Actin 7	MADAEDIQPLVCDNGTGMVKAGFAGDDAPRAVFPSIVGRPRHTGVMVGMGQKDAYVGDEA QSKRGILTLKYPIEHGIVSNWDDMEKIWHHTFYNELRVAPEEHPVLLTEAPLNPKANREK MTQIMFETFNVPAMYVAIQAVLSLYASGRTTGIVLDSGDGVSHTVPIYEGYALPHAILRL DLAGRDLTDSLMKILTERGYMFTTTAEREIVRDMKEKLAYVALDYEQELETSKSSSSVEK NYELPDGQVITIGAERFRCPEVLFQPSLIGMEAAGIHETTYNSIMKCDVDIRKDLYGNIV LSGGSTMFPGIADRMSKEITALAPSSMKIKVVAPPERKYSVWIGGSILASLSTFQQMWIS KGEYDESGPSIVHRKCF*
13	Eucgr.C04383	Inorganic h pyrophosphatase family protein	MATTILSDLGAEILIPVCAVVGIVFSLVQWLLVSKVKLTPADAAAAPAANNGKNGYTDYL IDEEENINDHSVVLKCAEIQTAISEGATSFLFTEYQYVGVFMVAFAVLIFLFLGSVEGFS MKSQPCTYDATKLCKPALATAVFSTVAFLLGGITSVVSGFLGMKIATYANARTTLEARKG VGKAFITAFRSGAVMGFLLAANGLLVLYIAINLFKIYYGDDWGGLFEAITGYGLGGSSMA LFGRVGGGIYTKAADVGADLVGKVERNIPEDDPRNPAVIADNVGDNVGDIAGMGSDLFGS YAESSCAALVVASISSFGINHELTAMLYPLIVSSVGILVCLVTTLFATDFFEIKAVKEIE PALKKQLIISTVLMTVGIAVVTWISVPSSFTIFNFGTQKVVKNWQLFLCVAVGLWAGLII GFVTEYYTSNAYSPVQDVADSCRTGAATNVIFGLALGYKSVIIPIFAIAVSIFVSFSFAA MYGIAVAALGMLSTIATGLAIDAYGPISDNAGGIAEMAGMSHRIRERTDALDAAGNTTAA IGKGFAIGSAALVSLALFGAFVSRAHIVTVDVLTPKVFIGLIVGAMLPYWFSAMTMKSVG SAALKMVEEVRRQFNTIPGLMEGTAKPDYATCVKISTDASIKEMIPPGALVMLTPLIVGI FFGVETLSGVLAGSLVSGVQIAISASNTGGAWDNAKKYIEAGASEHARTLGPKGSDPHKA AVIGDTIGDPLKDTSGPSLNILIKLMAVESLVFAPFFATHGGLLFKIF*
14	Eucgr.L02942	Adp-ribosylation factor a1f	MGLSFTKLFSRLFAKKEMRILMVGLDAAGKTTILYKLKLGEIVTTIPTIGFNVETVEYKN ISFTVWDVGGQDKIRPLWRHYFQNTQGLIFVVDSNDRDRVVEARDELHRMLNEDELRDAV LLVFANKQDLPNAMNAAEITDKLGLHSLRQRHWYIQSTCATSGEGLYEGLDWLSNNIANK A*
15	Eucgr.J00099	Ribosomal protein l16p/l10e family protein	MWWIFMADEQASSRSGSLARRCAAGSQDAGRSVSRQTSGISVRRVSTVLSSSFIAAPNLL SLQDDRRDVAMGRRPARCYRQIKNKPYPKSRYCRGVPDPKIRIYDVGMKKKGVDEFPFCV HLVSWEKENVSSEALEAARIACNKYMAKFAGKDAFHLRVRVHPFHVLRINKMLSCAGADR LQTGMRGAFGKPQGTCARVAIGQVLLSVRCKDSNSHHAQEALRRAKFKFPGRQKIIVSRK WGFTKFSRADYLKWKSENKIVPDGVNAKVTPWMPWTSGEPSTWKSFLAYNCLGISGVD*
16	Eucgr.G02807	Gtp binding elongation factor tu	MGKEKVHINIVVIGHVDSGKSTTTGHLIYKLGGIDKRVIERFEKEAAEMNKRSFKYAWVL

		family protein	DKLKAERERGITIDIALWKFETTKYYCTVIDAPGHRDFIKNMITGTSQADCAVLIIDSTT GGFEAGISKDGQTREHALLAFTLGVKQMICCCNKMDATTPKYSKARYDEIVKEVSSYLKK VGYNPDKIPFVPISGFEGDNMIERSTNLDWYKGPTLLDALDQISEPKRPTDKPLRLPLQD VYKIGGIGTVPVGRVETGVLKPGMVVTFGPTGLTTEVKSVEMHHEALQEALPGDNVGFNV KNVAVKDLKRGFVASNSKDDPIGNGYAPVLDCHTSHIAVKFSELLTKIDRRSGKELEKEP KFLKNGDAGMVKMIPTKPMVVETFSEYPPLGRFAVRDMRQTVAVGVIKSVEKKDPTGAKV TKSAVKKK*
17	Eucgr.G02468	Eukaryotic elongation factor 5a-1	MSDEEHHFESKADAGASKTYPQQAGTIRKNGYIVIKNRPCKVVEVSTSKTGKHGHAKCHF VGIDIFNGKKLEDIVPSSHNCDVPHVTRTDYQLIDISEDGFLSLLTENGSTKDDLRLPTD DALLGQIKDGFAEGKDLVVTAMCSMGEEQICALKDIGPK*
18	Eucgr.I01133	Ribosomal protein s5 domain 2-like superfamily protein	MAAPIESVQCFGRKKTAVAVTYCKRGRGLIKINGVPIELVEPEILRFKAYEPILLLGRHR FAGVDMRIRVKGGGHTSQIYAIRQSIAKALVAFYQKFVDEQSKKEIKDILVRYDRTLLVA DPRRCEPKKFGGRGARARFQKSYR*
19	Eucgr.F02130	G-box regulating factor 6	MAVPENLGRDQYVYLAKLAEQAERYEEMVEFMHKLVVGWTPAAELTVEERNLLSVAYKNV IGSLRAAWRIVSSIEQKEEGRKNEDHVVLVKEYRSKVENELSDVCASILRLLDTNLVPSA AASESKVFYLKMKGDYHRYLAEFKVGDERKAAAEDTMLAYKAAQDIAQADLASTHPIRLG LALNFSVFYYEILNQSDKACSMAKQAFEEAIAELDTLGEESYKDSTLIMQLLRDNLTLWT SDVQDQLDEP*
20	Eucgr.K03200	Ribosomal protein s12/s23 family protein	MGKTRGMGAGRKLKSHRRRQRWADKSYKKSHLGNEWKKPFAGSSHAKGIVLEKIGIEAKQ PNSAIRKCARVQLIKNGKKIAAFVPNDGCLNYIEENDEVLIAGFGRKGHAVGDIPGVRFK VVKVSGVSLLALFKEKKEKPRS*
21	Eucgr.H04339	Gdp-d-mannose 3\',5\'-epimerase	MGSIDGTDYGAFTYENLEREPYWPSEKLRISITGAGGFIASHIARRLKSEGHYIIASDWK KNEHMTEDMFCHEFHLVDLRVMDNCLKVTKGVDHVFNLAADMGGMGFIQSNHSVIMYNNT MISFNMLEAARINGVKRFFYASSACIYPEFKQLETNVSLKESDAWPAEPQDAYGLEKLAT EELCKHYTKDFGIECRVGRFHNIYGPFGTWKGGREKAPAAFCRKTITSTDKFEMWGDGLQ TRSFTFIDECVEGVLRLTKSDFREPVNIGSDEMVSMNEMAEIVLSFENKKLPIHHIPGPE GVRGRNSDNTLIKEKLGWAPTMKLRDGLRITYFWIKEQIEKEKAQGMDLSIYGSSKVVGT QAPVQLGSLRAADGKE*
22	Eucgr.K03281	Ribosomal protein s10p/s20e family protein	MAYAMKPTKPGLEEPQEQIHKIRITLSSKNVKNLEKVCSDLVRGAKDKRLRVKGPVRMPT KVLHITTRKSPCGEGTNTWDRFELRVHKRVIDLFSSPEVVKQITSITIEPGVEVEVTIAD S*
23	Eucgr.I01779	Adp-ribosylation factor a1b	MGLTFTKLFSRLFAKKEMRILMVGLDAAGKTTILYKLKLGEIVTTIPTIGFNVETVEYKN ISFTVWDVGGQDKIRPLWRHYFQNTQGLIFVVDSNDRDRVVEARDELHRMLNEDELRDAV LLVFANKQDLPNAMNAAEITDKLGLHSLRQRHWYIQSTCATSGEGLYEGLDWLSNNIASK TTILLLLFQA*
24	Eucgr.G02580	Mrna splicing factor, thioredoxin-like u5 snrnp	MFKSDCISDCEKFMVKESITSCIVIRSFCASFLRGGFEGDAEHRHSSVKLWCPLDPSPSP TKDVFSIFAHAHSHSHSPQSERARGREEGRERDVVLVAAPALGMGGGSGHPRRGGARRHH PLRPRLGRHLHAATHFSDARLPSPSPLLCILSLGLGKAAARRSHPIVRSVGSVRAMSYLL

			PHLHSGWAVDQAILAEEERLVVIRFGHDWDETCMQMDEVLASVAETIKNFAVIYLVDITE VPDFNTMYELYDPSTVMFFFRNKHIMIDLGTGNNNKINWALKDKQEFIDIVETVYRGARK GRGLVIAPKDYSTKYRY*
25	Eucgr.F02183	Tubulin/ftsz family protein	MRECISIHIGQAGIQVGNACWELYCLEHGIQPDGQMPGDKTVGGGDDAFNTFFSETGAGK HVPRAVFVDLEPTVIDEVRTGTYRQLFHPEQLISGKEDAANNFARGHYTIGKEIVDLCLD RIRKLADNCTGLQGFLVFNSVGGGTGSGLGSLLLERLSVDYGKKSKLSFTVYPSPQVSTS VVEPYNSVLSTHSLLEHTDVAVLLDNEAIYDICRRSLDIERPTYTNLNRLVSQVISSLTA SLRFDGALNVDVTEFQTNLVPYPRIHFMLSSYAPVISAEKAYHEQLSVAEITNSAFEPSS MMAKCDPRHGKYMACCLMYRGDVVPKDVNAAVATIKTKRTIQFVDWCPTGFKCGINYQPP TVVPGGDLAKVQRAVCMISNSTSVAEVFSRIDHKFDLMYAKRAFVHWYVGEGMEEGEGGC *
26	Eucgr.I02677	Light harvesting complex photosystem ii subunit 6	MAATSSAFVGGLGSSSTFLTGGKRSHELLSAGFGGRAIPAFTPGKLVVAAAAVQPKKSWI PAVRGGGNFIDPEWLDGSLPGDYGFDPLGLGKDPAFLKWYREAELIHGRWAMAAVVGIFV GQAWSGIPWFEAGAAPGAVAPFSFGSLLGTQLLLMGWVESKRWVDFFNPDSQSVEWATPW SRTAENFANATGDQGYPGGKFFDPLGLAGTLKDGEYIPDEEKLARLKLAEIKHARIAMLA MLIFYFEAGQGKTPLGALGL*
27	Eucgr.K02223	Ribulose bisphosphate carboxylase (small chain) family protein	MASSIVSSAAVAAVNRASPAQASMVAPFTGLKSASAFPVTRKSADITSLASNGGRVQCMQ VWPPIGKKKFETLSYLPPLSREELLKEIEYLLRMNWVPCLEFELEKGFVYRDNHKSPGYY DGRYWTMWKLPMFGCTDPLQVLKELDEAIKTYPNAFVRIIGFDNKRQVQCISFIAYKPPG F*
28	Eucgr.G01186	Tubulin alpha-2 chain	MRECISIHIGQAGIQVGNACWELYCLEHGIQPDGQMPSDKTVGGGDDAFNTFFSETGAGK HVPRAVFVDLEPTVIDEVRTGTYRQLFHPEQLISGKEDAANNFARGHYTIGKEIVDLCLD RIRKLADNCTGLQGFLVFNAVGGGTGSGLGSLLLERLSVDYGKKSKLGFTVYPSPQVSTS VVEPYNSVLSTHSLLEHTDVAVLLDNEAIYDICRRSLDIERPTYTNLNRLVSQVISSLTA SLRFDGALNVDVTEFQTNLVPYPRIHFMLSSYAPVISAEKAYHEQLSVAEITNSAFEPSS MMAKCDPRHGKYMACCLMYRGDVVPKDVNAAVATIKTKRTIQFVDWCPTGFKCGINYQPP TVVPGGDLAKVQRAVCMISNSTSVAEVFSRIDHKFDLMYAKRAFVHWYVGEGMEEGEFSE AREDLAALEKDYEEVGAELAEGEDDEGDEY*
29	Eucgr.G03060	Light harvesting complex photosystem ii	MAAASSSYFFGTRIADPKPSLGRFQARFGFGGKKFGFGGKKSPPPKPAPRKLDGERLVWF PGAEPPEWLDGTMVGDRGFDPFGLGKPAEYLQFDLDSLDQNLAKNLAGDVIGVRVEQTEV KPTPFQPYSEVFGLQRFRECELIHGRWAMLGTLGALAVEALTGVAWQDAGKVELVEGSSY LGQPLPFSLTTLIWIEVIVIGYIEFQRNAELDPEKRLYPGGYFDPLGLASDPEKKENLQL AEIKHARLAMIAFLIFGIQAAYTGKGPIAFVATFNK*
30	Eucgr.J02030	Rubisco activase	MAAALSTVGTVNGKPLSFNNSSPAIASSAFLGNSLKKVSSRTTHPKPSSRSLRICAEIDE GKQTEKDKWKGLAYDTSDDQQDITRGKGMVDSLFQAPMGTGTHYAVLSSYEYLSTGLRQY MDNNMDGFYIAPAFMDKLVVHITKNFMTLPNIKVPLILGVWGGKGQGKSFQCELVFSKMG INPIMMSAGELESGNAGEPAKLIRQRYREAADIIKKGKMCCLFINDLDAGAGRMGGTTQY TVNNQMVNATLMNIADNPTNVQLPGMYNKEENPRVPIIVTGNDFSTLYAPLIRDGRMEKF

			YWAPTREDRIGVCTGIFRTDNITGEAIVKLVDCFPGQSIDFFGALRARVYDDEVRKWISG VGVDTIGKKLVNSKEGPPTFEQPKMTLEKLIEYGNMLVQEQENVKRVQLADKYLAEAALG DANQDAVDQGTFYGKAAQQVNVPVPEGCTDPAAANFDPTARSDNGSCQY*
31	Eucgr.I00580	Serine transhydroxymethyltransferase 1	MAMAMALRRLSSSIEKPLRPLINGGGSVCYMASLPNEAVYEKEKNGVTWPKQLNAPLEAV DPEVADIIELEKARQWKGLELIPSENFTSVSVMQAVGSVMTNKYSEGYPGARYYGGNEYI DMAESLCQKRALEAFRLDPAKWGVNVQSLSGSPANFQVYTALLKPHDRIMALDLPHGGHL SHGYQTDTKKISAVSIFFETMPYRLNESTGYIDYDQMEKSATLFRPKLIVAGASAYARLY DYARIRKVCDKQKAILLADMAHISGLVAAGVVPSPFEYADVVTTTTHKSLRGPRGAMIFF RKGVKEINKQGKEVLYDFEDKINQAVFPGLQGGPHNHTITGLAVALKQATTPEYRAYQEQ VLSNCAKFAQTLTEKGYELVSGGTENHLVLVNLKNKGIDGSRVEKVMESVHIAANKNTVP GDVSAMVPGGIRMGTPALTSRGFIEEDFVKVAEFFDAAVGLAVKIKAQTKGTKLKDFLST MQSSPDFQSGIAKLRHDVEEYAKQFPTIGFEKATMKYKN*
32	Eucgr.J00292	Dnaj homologue 2	MFGRAPKKSDNTKYYDVLGVSKNASQDDLKKAYRKAAIKNHPDKGGDPEKFKELAQAYEV LSDPEKREIYDQYGEDALKEGMGGGGGGHDPFDIFQSFFGGSPFGGGGSSRGRRQRRGED VIHPLKVSLEDLYNGTSKKLALSRNVICSKCKGKGSKSGASIKCVGCQGSGMKVSIRHLG PSMIQQMQHPCNECKGTGETINDKDRCPQCKGEKVVQEKKVLEVIVEKGMQNGQKIKFPG EADEAPDTVTGDIVFVLQQKEHPKYKRKGDDLFYEHTLSLTESLCGFQFALSHLDGRQLL IKSQPGEVIKPDQFKAINDEGMPIYPRPFMKGKLYIHFTVEFPDTLSPEQCKALETILPP RSSAQLTDMELDECEETTLHDVNIEEEMRRKQAQAQEAYEEDEDMHGGAQRVQCAQQ*
33	Eucgr.D02179	Single hybrid motif superfamily protein	MALRMWASSTANALRLSSKASLSPAFSLHRCFSSGILDGLKYAPSHEWVKHEGPVASVGI TDHAQDHLGEVVFVDLPEPGGSVSKGGSFGAVESVKATSDINSPISGEIVEVNTKLTETP GLVNSSPYEDGWMIKVKPSDPSELGSLMGPKEYTKFCEEEDAAH*
34	Eucgr.G02684	Ubiquitin e2 variant 1d-4	MTLGSGGSGVVVPRNFRLLEELERGEKGIGDGTVSYGMDDGDDIYMRSWTGTIIGPHNTV HEGRIYQLKLFCDKDYPEKPPTVRFHSRINMTCVNHETGVVEPKKFGLLANWQREYTMED ILTQLKKEMAAPHNRKLVQPPEGTYF*
35	Eucgr.F01793	Glyceraldehyde-3-phosphate dehydrogenase b subunit	MATHAALAPSTLPANAKFSSKSSSHSFPTQCFSKRLEVAEFSGLRAGSCVTYAKNAGEGS FFDAVAAQLTPKTSAPAPAKGETVAKLKVAINGFGRIGRNFLRCWHGRKNSPLDVIVVND SGGVKNASHLLKYDSMLGTFKADVKIVDNETISVDGKPVKVVSNRDPLKLPWAELGIDIV IEGTGVFVDGPGAGKHIQAGAKKVIITAPAKGADIPTYVYGVNETDYSHEVANIISNASC TTNCLAPFVKVLDEKFGIVKGTMTTTHSYTGDQRLLDASHRDLRRARAAALNIVPTSTGA AKAVSLVLPQLKGKLNGIALRVPTPNVSVVDLVVNVEKKGLTAEDVNAAFRDAAEGPLKG ILAVCDDPLVSVDFRCSDVSSTIDSSLSMVMGDDMVKVVAWYDNEWGYSQRVVDLAHLVA VKWPGIEIPGSTGDPLEDFCKKNPADEECKVYEN*
36	Eucgr.H00828	Photosystem i subunit e-2	MASWSMASAASGLVFTPNAPTNGNSSAKNNMVFFAKNNNPSRLVVRAAEEGAAPAATTAA PAAAEASKAKPPPIGPKRGTKVKILRKESYWYNGIGSVVAVDQDPKTRYPVVVRFNKVNY ANVSTNNYALDEIQEI*
37	Eucgr.H02496	Nad(p)-linked oxidoreductase superfamily protein	MNPLWQQKKPREFCKANNVIITAFSPLGARGANWGTNEVMDNESLKEIAKARGKSIAQVC LRWLYEQGVTFVVKSFKKERLKENLGIFDWELT*

38	Eucgr.E01261	Phosphoribulokinase	MAVSTVYTTQSFHSTCSISTPSKTHLGFNQKKQILFYNSGKKVTNRGIAAVPYVIRCSGD TLVIGLAADSGCGKSTFMRRLTSVFGGAAEPPKGGNPDSNTLISDTTTVICLDDYHSLDR TGRKEKGVTALDPRANDFDLMYEQVKAMKEGKAVDKPIYNHVTGLLDPPELIKPPKILVI EGLHPMFDQRVRDLLDFSIYLDISNEVKFAWKIQRDMAERGHSLESIKASIEARKPDFEA YIDPQKQYADAVIEVLPTQLIPGDNEGKILRVRLIMKEGVKYFNPVYLFDEGSTISWIPC GRKLTCSYPGIKFTYGPESYFGHEVSVLEMDGQFDRLDELIYVESHLSNLSTKFYGEVTQ QMLKHSEFPGSNNGTGLFQTIVGLKIRDLYEQITASKAAAPLQATKA*
39	Eucgr.A02039	Photosystem ii subunit p-1	MASTTCFFHHNKLTTPARTPSQRSAPSFKPAQVACRAQKQAAGEEESGAAEVSRRLALTV LIGAAAVGSKVSPADAAYGEAANVFGKPKTNTDFLPYNGNGFTLLIPAKWNPSKEVEYPG QVLRYEDNFDTTSNVSVMVTPTDKKAITDFGSPENFLAEVNYLLGKQAYFGKTDSEGGFE SDAVATANILESSTPEIGGKKYYFVSVLTRTADGDEGGKHQLITASIKDGKLYICKAQAG DKRWFKGARKFVESAASSFSVA*
40	Eucgr.F03319	Thioredoxin m-type 4	MAAVLESLAVPRSSGAASAAALSPVASASSLAPTAGRRRSATFPQASGLRIGPVSVARSL RSPSQRPRRAPAVVCEAQDTAVEVAGVTDATWQSLVLESESPVLVEFWAPWCGPCRMIHP VIDELAKQYAGKLKCYKVNTDESPSVATRYGIRSIPTVMIFKSGEKKDAVIGAVPKSTLT TSIEKFL*
41	Eucgr.E04053	Atpase, f1 complex, gamma subunit protein	MSSSNLTMWASSKPSISDASPLSFRASVGSIFQLPSSGSPSRANPVAPIQCNLRELRDRI DSVKNTQKITEAMKLVAAAKVRRAQEAVVNGRPFSETLVEVLYNINEQLQIEDVDAPLTS VRPVKKVALVVVTGDRGLCGGFNNNIIKKAEARIAELKGLGLDYTVISVGKKGNSYFLRR PYIPVDKFLEGGTLPTAKEAQAIADDVFSLFVSEEVDKVELLYTKFVSLVKSNPVIHTLL PLSPKGEICDLNGNCVDAAEDEFFRLTTKEGKLTVERDVVRTETIDFSPILQFEQDPVQI LDALLPLYLNSQILRALQESLASELAARMSAMSNATDNASELKKSLSMVYNRRRQAKITG EILEIVAGANALT*
42	Eucgr.I01326	Fructose-bisphosphate aldolase 2	MASASLLKSSPVLDKSEFVKGTQTLRTPSLAAVRYHPTTAPSALVVKASAYADELVKTAK TVASPGRGILAMDESNATCGKRLASIGLENTEANRQAYRTLLVSAPGLGQYISGAILFEE TLYQSTTDGRKMVDVLVEQNIVPGIKVDKGLVPLAGSNDESWCQGLDGLASRTAAYYQQG ARFAKWRTVVSIPNGPSALAVKEAAWGLARYAAICQDNGLTPIVEPEILLDGEHGIERTF EVALKVWAEVFYYMAENNVLFEGILLKPSMGHSPASRRVHPQAPPPQDPACRSRNHVLVW WAIRGRSNPEPERDEPVPEPMARVLLLR*
43	Eucgr.G00777	Light harvesting complex photosystem ii subunit 6	MAATSGAVVNGLGSAFLCGGRRSRSLSRAAGFGNEAGSGAGSRNLVVVAAAAKPKKSWIP MAATSGAVVNGLGSAFLCGGRRSRSLSRAAGFGNEAGSGAGSRNLVVVAAAAKPKKSWIP AVKGGGNLIDPEWLDGSLPGDYGFDPLGLGKDPAFLKWYREAELIHGRWAMAAVVGIFVG QAWSGIPWFEAGADPSAIAPFSFGTLLGTQLILMGWVESKRWVDFFNPDSQSVEWATPWS RTAENFANATGDQGYPGGKFFDPLGLAGTIKDGVYIPDVEKLERLKLAEIKHARIAMLAM LTFYFEAGQGKTPLGALGL*
44	Eucgr.E04056	Peroxidase superfamily protein	MGFRALFFFAAIFFSFSTTIIYSAYAEGEAEAEVGSGLVIDFYKDTCPQAEDIIKEQVKL LYKRHKNTAFSWLRNIFHDCAVQSCDASLLLDSTRRDLSEKETDRSFGMRNFRYLDTIKE AVERECPGVVSCADILVLSARDGVVALGGPQIPLKTGRRDGRRSRADVIEEHLPDHNESM

			SVVLERFAKMGIDTPGVVALLGAHSVGRTHCVKLVQRLYPEVDPALNPDHVEHMLYKCPD PIPDPKAVQYVRNDRGTPMIFDNNYYRNILDNKGLLLVDHQLAVDKRTKPYVKKMAKSQN YFFKEFARALTTLSENNPLTGDKGEIRRQCNVANKHH*
45	Eucgr.H02679	Serine hydroxymethyltransferase 4	MDPVTAWGNSPLQAVDPDIHDLIEKEKRRQCRGIELIASENFTSFAVIEALGSALTNKYS EGMPGNRYYGGNEYIDQIENLCRSRALQAYRLDPTSWGVNVQPYSGSPANFAAYTAVLQP HDRIMGLDLPSGGHLTHGYYTSGGKKISATSIYFESLPYKVNSSTGYIDYDKLEEKALDF RPRLIICGGSAYPRDWDYARFRSVADKCGALLLCDMAHISGLVAAQEAANPFEYCDIVTT TTHKSLRGPRAGMIFYRKGPKPAKKGQPADAVYDFEDKINFSVFPSLQGGPHNHQIGALA VALKQAMSPGFKAYAKQVRANAVALGNYLMSKGYKLVTGGTENHLVLWDLRPLGLTGNKV EKLCDLCDITVNKNAVFGDSSALAPGGVRIGTPAMTSRGLVEKDFEQIGEFLHRAVTITL DIQKQHGKLLKDFNKGLVNNKDMETLKADVEKFSGSFDMPGFLMSEMKYKD*
46	Eucgr.D00234	Photosystem i subunit k	MATTVMTSLPQFNGLRPAAPAAPVRSLAAVVQPMRRKGKGALGARCDFIGSPTNLIMVTT TTLMLFAGRFGLAPSANRKATAGLKLEARDSGLQTGDPAGFTLADTLACGSFGHIIGVGV VLGLKNIGAL*
47	Eucgr.G02234	Photosystem ii reaction center protein e	MSGSTRERSFADIIISIRYWVIHSINIPSLFIAGWLFVSTGLAYDVFGSPRPNEYFTESR QGIPLITGHFDPLEQLDEFMRWLAVHGLVVPTVSFLGSISAMQFIQR*
48	Eucgr.E04205	Photosynthetic electron transfer d	MGHNYYGEPAWPNDLLYIFLVVILGTIVCNVGLAVLEPSMIGEPTDPFATPLEILPEWYL FPIFQILHTVPNKLLGTDPHQPLMMI*
49	Eucgr.B00847	Nad(p)h dehydrogenase subunit h	MIVNMGPHHPSMHGVLRLILTLDGEDVIDCEPILGYLHRGMEKIAENRTVIQYLPYVTRW DYLATMFTEAITVNGPEQLGNIQMMHNYFRIGGVAADLPYGWIDKCLDFCDYFLTAGVGI IGPEEAINWGLSGPMLRASGIQWDLRKVDHYECYDELDWEIHWQKEGDSLARYLVRIGEM RESIKLFNKLWRIPGGPYENLETRCFARERDPEWNDFEYRFISKKPSPTFELPKQELYVR VEAPKGELGIF*
50	Eucgr.J02738	Atp synthase subunit beta	FPPGKMPNIYNALVVKGRDTIGQEINVTCEVQQLLGNNRVRAVAMSATDGLMRGMEVIDT GAPLSVPVGGATLGRIFN
51	Eucgr.H01947	Photosystem ii reaction center protein d	MTIALGKFTKDENDLFDIMDDWLRRDGFIFVGWSSLLLFPCTYFALGGWFTEGCNFLTAT AVSTPANSLAHSLLLLWGLEAQGDFTLWCQLGGLWTFVVLQGTFGLIGFMLHQFELARSQ LYFASSFFFQGFHNWTLNPFHMMGVAGVLGATLLCAIHGATVESTLSEDGDGANTFRAFN PTQAEETYSMVTINRFYQSGSEPTCDFVSQEIRVVEDLEFGTFYTKNILLNMEVR*
52	Eucgr.E02608	Unfolded protein binding	MGCRSEHIWIELIVGSRKISNFCWAFILFLGSLGFVLVGSSSYLGKNLISLVPSQQILFF PQGIVMSFYGIAGLFISSYLWCTISWNVGSGYDRFDRKEGIVCIFRWGFPGNNRRIFLRF RMKDIQSIRIEVKEGISARRVLYMEIKGQGAVPLTRTDENLTPREIEQKAAELAYFLRVP IEVF*
53	Eucgr.A02747	Nadh dehydrogenase subunit j	MQEIKKMQGRLSAWLVKHGLVHRSLGFDYQGIETLQIKPEDWHSIAIILYVYGYNYLRSQ CAYDVAPCGLLASVYYLTRIEYGVDQPEEVCIKVFAPRRNPRISSVFWIWKIADFQERES YDMLGNCYDAHPRLKRILMPETWIGWPLHKDYIAPNFYEIQDTHLMIGN*
54	Eucgr.K01620	Nad(p)h dehydrogenase subunit h	MLRASGIQWDLRKVDHYECYDELDWEIHWQKEGDSLARYLVRIGEMRESIKIIQQALEGI PGGPYENLETRCFARERDPEWNDFEYRFISKKPSPTFELPKQELYVRVEAPKGELGIFLI

			GDQSGFPWRWKIRPPGFINLQILPQLVKRMKLADIMTILGSVDIIMGEVDR*
55	Eucgr.B02132	Photosystem ii reaction center protein c	TLGWGVGPGGEVIDTFPYFVFGVLHLISSAVLGFGGIYHALLGPETLEESFPFFGYVWKD RNKMTTILGIHLILL
56	Eucgr.H02991	Atpase, f0 complex, subunit b/b\', bacterial/chloroplast	MRNWHASFDVIPQNNSTEVTRIRKLWSERKICLVRFFSHLISDLLDNRKQRILNTIRNSE ELRGGAIEQLEKARARLRKLEKARARLRKVEMEAEQFRVNGYSEIEQERLNLINSTYKTL EQLENYKNETIHFEQQRAINQVRQRVFQQALQGALGTLNSCLNNELHLRTISANIGMFGA MKEIIFFE*
57	Eucgr.J02731	Atp synthase epsilon chain	MTLNLCVLTPNRIVWDSEVKEIILSTNTGQIGFRKIMIGIADPRLWNLGVGLLSKLNGQL GSFHRLSRVEPWDLTADLKANPREQ*
58	Eucgr.J01096	Photosystem i light harvesting complex gene 1	MAANSLMSCGISTTSFPSVLSSSKSKFAAAVPLPSGASTNAVSRFSMSADWMPGSPRPPY LDGSAPGDFGFDPLRLGEVPENLERFKESELIHCRWAMLAVPGILVPEALGLGNWVQAQE WAAKPGGQATYLGNPVPWGTLPTILAIEFISIAFVEHQRSMEKDPEKKKYPGGAFDPLGY SKDPVKFEELKVKEIKNGRLALLAFVGFCIQQTAYPGTGPLENLATHLADPWHNNIGDIL IPRTVSP*
59	Eucgr.F03646	Photosystem i subunit g	MAAASPAVLSLAAGATSRRHAGGLSPASISFQGLRPLANRATRASSSSSAAAAAPRRSGA VRAELSAPVVISLSTGLSLFLGRFVFFNFQRENVAKQVPEQNGKTHFEAGDVRAQEYVSL LKSNDPVGFNIVDVLAWGSIGHIVAYYILATTSNGYDPKFFG*
60	Eucgr.B02162	Photosystem i subunit e-2	MATLNMASFVLSPSIGSNASSSTARSIAYFPRDANSRSARRLVVRAAEGEAAPPAATTTE APAEGEAKPKAAKPPPIGPKRGTKVKILRRESYWFKDVGSVVAVDQDPKTRYPVVVRFQK VNYANVSTNNYALDEIIEV*
61	Eucgr.K00588	S-adenosylmethionine synthetase 1	METFLFTSESVNEGHPDKLCDQISDAVLDACLEQDPDSKVACETCTKTNMVMVFGEITTK ANVDYEKIVRDTCRSIGFVSDDVLVNIEQQSPDIAQGVHGHLTKRPEEIGAGDQGHMFGY ATDETPELMPLSHVLATKLGARLTEVRKNGTCAWLRPDGKTQVTVEYYNDNGAMVPVRVH TVLISTQHDETVTNDEIAADLKEHVIKPVIPEKYLDERTIFHLNPSGRFVIGGPHGDAGL TGRKIIIDTYGGWGAHGGGAFSGKDPTKVDRSGAYIVRQAAKSIVASGLARRCIVQVSYA IGVPEPLSVFVDTYKTGKIPDKEILKIVKESFDFRPGMISINLDLKRGGSGRFLKTAAYG HFGRDDPDFTWEVVKPLKWEKPQS*
62	Eucgr.K02983	Light harvesting complex photosystem ii	MAAVTTAAAASSFIGTRLPEVPSSGRVQARFGFGAKKAAPKKAAKRTSDRPLWYPGATAP EWLDGSLVGDYGFDPFGLGKPAEYLQFDLDSLDQNLAKNEAGDIIGTRFENSDVKSTPFQ PYTEVFGLQRFRECELIHGRWAMLATLGALTVEWLTGVTWQDAGKVELVEGSSYLGQPLP FSITALIWIEVVVIGYIEFQRNGELDPEKRLYPGGKFFDPLGLAADPEKKATLQLAEIKH ARLAMVAFLGFAVQAAATGKGPLNNWATHLSDPLHTTIIDTFTS*
63	Eucgr.B03494	Photosystem i light harvesting complex gene 2	MASVCASSAIAAVAISSPSGQKNGSSFLTGKRLRVSKYTAPAAAAGRLATVCAVADPDRP LWFPGSTPPPWLDGSLPGDFGFDPLGLGSDPESLRWNQQAELVHCRWAMLGAAGIFIPEF LTKIGILNTPSWYTAGEQEYFTDTTTLFIIELIFIGWAEGRRWADIIKPGCVNTDPIFPN NKLTGTDVGYPGGLWFDPLGWGSGSPEKIKELRTKEIKNGRLAMLAVMGAWFQHIYTGTG PIDNLFAHLADPGHATVFAAFTPK*

64	Eucgr.B02310	Rubisco activase	MAATVSTVGTVNPLSLNSSSSGDSVPRSVFLGSSLKKVNSRFTSPKVSSGSFKVVAEVEE DKQTNKDKWKGLAFDTSDDQQDITRGKGMVDSLFQAPMGTGTHYAIMSSYDYISAGLRQY NLDNNMDGFYIAPAFMDKLVVHITKNFMTLPNIKVPLILGIWGGKGQGKSFQCELVFAKM GINPIMMSAGELESGNAGEPAKLIRQRYREAADIIKKGKMCCLFINDLDAGAGRLGGTTQ YTVNNQMVNATLMNIADNPTNVQLPGMYNKEENPRVPIIVTGNDFSTLYAPLIRDGRMEK FYWAPTREDRIGVCKGIFRSDNIPDEDIVKLVDNFPGQSIDFFGALRARVYDDEVRKWIS GVGVDSIGKKLVNSKEGPPTFEQPKMSLDKLLEYGNMLVQEQENVKRVQLADKYLSDAAL GDANKDAMESGTFFS*
65	Eucgr.K00389	Photosystem i subunit f	MSLTIPTNLSKPIAAPKLSPSKSVRPAATLIRCSSSSPEQGSASTSAASPLQAFSAALAL SSILLSAPQPAAADIAGLTPCKESKQFAKREKQQLKKLESSLKLYAPDSAPALALKATME KTKRRFDNYGKQGLLCGTDGLPHLIVSGDQRHWGEFITPGILFLYIAGWIGWVGRSYLIA IRDEKKPTQKEIIIDVPLASRLVFRGFSWPIAAYRELVNGELIAKDV*
66	Eucgr.I00200	Photosystem i reaction center subunit psi-n, chloroplast, putative / psi-n, putative (psan)	MATMNSSVLACKYAISGTGSSELSSKLGSVAIPGVPGQKLPMIRAQQVRVPESKAAEGRR AALACLAATVFATAVASTSSADAGVIEEYLEKSKVNKELNDKKRLATSGANFARAYTVEF GTCKFPENFTGCQDLAKQKCPSFLMIWRWNAKGRTSTSVAQMSSGNGENLDVFLSLVKATM*
67	Eucgr.I02744	2fe-2s ferredoxin-like superfamily protein	MALAGAALSGTVVSSPFVRMQPVNRLRAFPNVGQALFGVNSGRGRVTAMAAYKVTLLTPE GKVELDVPDDVYILDYAEEQGIDLPYSCRAGSCSSCAGKVVAGSVDQSDGSFLDDDQIEE GWVLTCVAYPKSELTA*
68	Eucgr.F03789	Chlorophyll a-b binding family protein	MAQTMMLMPSVSGHSVDLRTPRLRPTSSSFSRSLLYNPLPSPAASSHRSSPVFALFKSKT KAPPKKVVKEKPKVEDGVFGTSGGIGFTKENELFVGRVAMIGFAASLLGEAITGKGILAQ LNLETGVPIYEAEPLLLFFILFTLLGAIGALGDRGRFVDDSAGIEGAVIPPGKGFLSALG LKEGGPLFGFTKANELFVGRLAQLGFAFSLIGEIITGKGALAQLNIETGVPISEIEPLVL FNVLFFFIAALNPGTGKFLTDEDLED*
69	Eucgr.B00523	Light-harvesting chlorophyll-protein complex i subunit a4	MNCYEIKLQRACKNRHLPPKLLKTPTLIFCSIHTALGLEKKMATVTTQASAAVFRPCSSK TRFLTGSSGKLNREVSIKALPSTSSPASLKVEAKKGEWLPGLASPGYLNGSLPGDNGFDP LGLAEDPENLRWFVQAELVNGRWAMLGVAGMLLPEVFTKIGIINVPAWYDAGKAEYFASS STLFVIEFILFHYVEIRRWQDIKNPGSVNQDPIFKQYSLPPNEVGYPGGIFNPLNFAPTL EAKEKELANGRLAMLAFLGFVVQHNVTGKGPFENLVQHLSDPWHNTIVQTLRGY*
70	Eucgr.F01413.1	Aldolase-type tim barrel family protein	MEITNVNEYQAIAKEKLPKMVYDYYASGAEDQWTLQENQYAFSKILFRPRILIDVSRIDM TTTVLGFKISMPIMVAPTAMQKMAHPEGEYATARAASAAGTIMTLSSWATSSVEEVASTG PGIRFFQLYVYKDRNVVAQLVRRAERAGFKAIALTVDTPRLGRREADIKNRFTLPPFLTL KNFEGLNLGKMDKSDESGLASYVAGQIDRTLSWKDVKWLQTITSLPILVKGVLTAEDARL SIQAGAAGIIVSNHGARQLDYVPATIMALEEVVKAAQGRVPVFLDGGVRRGTDVFKALAL GASGIFIGRPVVFSLAAEGEAGVRKLLPAFSLWTNTFF*
71	Eucgr.F01413	Aldolase-type tim barrel family protein	MEITNVNEYQAIAKEKLPKMVYDYYASGAEDQWTLQENQYAFSKILFRPRILIDVSRIDM TTTVLGFKISMPIMVAPTAMQKMAHPEGEYATARAASAAGTIMTLSSWATSSVEEVASTG PGIRFFQLYVYKDRNVVAQLVRRAERAGFKAIALTVDTPRLGRREADIKNRFTLPPFLTL KNFEGLNLGKMDKSDESGLASYVAGQIDRTLSWKDVKWLQTITSLPILVKGVLTAEDARL

			SIQAGAAGIIVSNHGARQLDYVPATIMALEEVVKAAQGRVPVFLDGGVRRGTDVFKALAL GASGIFIGRPVVFSLAAEGEAGVRKLLPAFSLWTNTFF*
72	Eucgr.I01025	Photosystem ii subunit o-2	MAASLQAAATLMQPTKVGRISSSQLRSSQNVSKTFGLECGAGSRVTCSLQADLKDLAQKC ADATKIAGFALATSALVVSGAGAEGAPKRLTYDEIQSKTYMEVKGTGTANQCPTIDGGLD SFAFKPGKYNAKKICLEPTSFTVKAESVSKNAPPEFQNTKLMTRLTYTLDEIEGPFEVSP DGTVKFEEKDGIDYAAVTVQLPGGERVPFLFTIKQLVASGKPESFSGEFLVPSYRGSSFL DPKGRGGSTGYDNAVALPAGGRGDEEDLTKENIKNASSSTGKITLSVTKTKPETGEVIGV FESVQPSDTDLGAKVPKDVKIQGVWYAQLES*
73	Eucgr.F04099	Light harvesting complex of photosystem ii 5	MASLGVSEMLGNPLNFSSAARSAPTASSPATSKTVALFSRKKPAPPAKAKPVAVSPADEE LAKWYGPDRRIFLPDGLLDRSEIPEYLTGEVPGDYGYDPFGLSKKPENFSKYQAYELIHA RWAMLGAAGFIIPEAFNKFGANCGPEAVWFKTGALLLDGNTLNYFGKNIPINLIFAVIAE VVLVGGAEYYRIINGLDLEDKLHPGGPFDPLGLAKDPDQAAILKVKEIKNGRLAMFAMLG FFLQAYVTGEGPVENLAKHLSDPFGNNLLTVIAGTAERTPTL*
74	Eucgr.D01322	Peroxidase superfamily protein	MASKALIFLALLSFSAVSPRPAIAEINEEDKPGLVMNFYKDTCPQAEDIIKEQVKLLYKR HKNTAFSWLRNIFHDCAVQSCDASLLLDSTRRSLSEKETDRSFGLRNFRYLDTIKEAVER ECPGVVSCADILVLSARDGIVALGGPHFPLKTGRRDGRKSRADVVEQYLPDHNESISVVL DRFAAMGINTPGVVALLGAHSVGRTHCVKLVHRLYPEVDPALNPDHIEHMLHKCPDAIPD PKAVQYVRNDRGTPMVLDNNYYRNILDNKGLLIVDHQLATDKRTKPYVKKMAKSQDYFFK EFARAITILSENNPLTGDQGEIRKQCNVANKHH*
75	Eucgr.F03433	Thiazole biosynthetic enzyme, chloroplast (ara6) (thi1) (thi4)	TTDHDSMPSSNENKNTRIKIHGTTNARKGEKGKREKKLNMGCKRKGERIVVFLACSAHD WESATWCRRHDSPVAHSGPFNSYPLRPPRVPRYFPLRFLIYSPHPITTLRSHPENPPARS PQSSVQEAPPMAAATITSSLSSKPKLSLSSFHGTPLAPAAQSLRLPAPRSSAHSSGISMS AAAANPPPYDLNAFRFDPIKESIVSREMTRRYMMDMITYADTDVVVVGAGSAGLSCAYEL SKNPDVQVAIIEQSVSPGGGAWLGGQLFSAMVVRKPAHRFLDELEIEYDEQDNYVVIKHA ALFTSTIMSKLLARPNVKLFNAVAAEDLIVKNDRVGGVVTNWALVSMNHDTQSCMDPNVM EAKVVVSSCGHDGPFGATGVKRLRSIGMIDSVPGMKALDMNTAEDAIVRLTREIVPGMIV TGMEVAEIDGSPRMGPTFGAMMISGQKAAHLALKALGLPNALDGSYVGSIQPELILAAAD SAEIAEA*
76	Eucgr.D00322	Light-harvesting chlorophyll-protein complex ii subunit b1	MLFIIYKWKPSPLFFFPPIFKAQKFLGGSGTTKRTQETKARIFNSQWKDRYRYPEIRDLD QALHINTPLNSPPSHNISTSKSSKHLGKNSPLGTMAASTMALSSPSFAGKAVKLSPATPD LLGNGRVTMRKAVKPASSGSPWYGPDRAKYLGPFSGEPPSYLTGEFPGDYGWDTAGLSAD PETFAKNRELEVIHCRWAMLGALGCVFPELLARNGVKFGEAVWFKAGAQIFSEGGLDYLG NPSLIHAQSILAIWACQVILMGAVEGYRVAGGPLGEVTDPLYPGGSFDPLGLADDPEAFA ELKVKEIKNGRLAMFSMFGFFVQAIVTGKGPLENLADHLADPVNNNAWAYATNFVPGK*
77	Eucgr.A01047	Photosystem ii light harvesting complex gene 2.2	MATTVIQQSAFAGQTALKQSSELVRKVGNFAGGRATMRRTVKSVPQSIWYGPDRPKYLGP FSEQTPSYLTGEFPGDYGWDTAGLSADPETFAKNRELEVIHCRWAMLGALGCVFPEILQK NGVKFGEAVWFKAGAQIFSEGGLDYLGNPNLIHAQSILAIWACQVVLMGLIEGYRVGGGP LGEGLDPLYPGGAFDPLGLADDPDAFAELKVKEIKNGRLAMFSMFGFFVQAIVTGKGPIE

			NLFDHLADPAANNAWAYATNFVPGK*
78	Eucgr.E02381	Light-harvesting chlorophyll-protein complex ii subunit b1	MAASTMALSSPSLAGKAVQLSPSTPELFGKGRVTMRKTVTKQVSSGSPWYGPDRVKYLGP FSGEPPSYLTGEFPGDYGWDTAGLSADPETFAKNRELEVIHCRWAMLGALGCVFPELLAR NGVKFGEGGLDYLGNPSLIHAQSILAIWACQVILMGAVEGYRVAGGPLGEVTDPLYPGGS FDPLGLADDPEAFAELKVKEIKNGRLAMFSMFGFFVQAIVTGKGPLENLADHLADPVNNN AWAYATNFVPGK*
79	Eucgr.D00321	Light-harvesting chlorophyll-protein complex ii subunit b1	MVSGVHPTSPNNHRQSISTLYFNTRQRSSSQIHSTMAASTMALSSPSLAGQAVKLSPSTP ELLGNGRISMRKAVRKPVSSGSPWYGPDRAKYLGPFSGEPPSYLTGEFPGDYGWDTAGLS ADPETFAKNRELEVIHCRWAMLGALGCVFPELLARNGVKFGEAVWFKAGAQIFSEGGLDY LGNPNLIHAQSILAIWACQVILMGAVEGYRIAGGPLGEVTDPLYPGGSFDPLGLADDPEA FAELKVKEIKNGRLAMFSMFGFFVQAIVTGKGPLENLADHLADPVSNNAWAYATNFVPGK*
80	Eucgr.F03245	Photosystem ii reaction center protein h	MATQTVEGSSRSGPRRTIVGDLLKPLNSEYGKVAHGWGTTPLMGVAMALFAVFLSIILKI YNSSVLLDGISMN*
81	Eucgr.A00264	Photosystem ii reaction center protein b	MPTFFETFPVVLVDGDGIVRADVPFRRAESKYSVEQVGVTVEFYGGELNGVSYSDPAIVK KYARRAQLGEIFELDRATLKSDGVFRSSPRGWFTFGHASFALLFFFGHIWHGARTLFRDV FAGIDPDLDAQVEFGAFQKLGDPTTRRQVV*
82	Eucgr.C03525	Ribulose-bisphosphate carboxylases	MSCREGLMSPQIETKASVGFKVGVKDYKLTYYTPDYETKDTNILAAFRVTPQPGVPPEEA RAVVAAKSSTGTWTIVWTDGLTSLDLYKGRCYHIEPVAGEENQYICYVAYPLELFEEGSV TNMFTSIVGNVFGFKALHALHLEDLRIPPSYTKTFQGPPHGIQVERDKFG*

3.4 Cloning of the catalase protein from tomato using CRISPR technology, responsible for the susceptibility of *Psidium* spp. to the nematode *Meloidogyne enterolobii*

University of California – Davis (UC Davis)
Department of Entomology and Nematology
Supervisor DSc. Shahid Siddique

3.4.1 Introduction

Tomato (*Solanum lycopersicum*), native to Central and South America, is one of the most extensively studied cultivated dicotyledons. Its domestication occurred in stages involving *S. pimpinellifolium* and *S. lycopersicum* var. *cerasiforme*, followed by modern breeding programs aimed at combining desirable agronomic traits. Since the 16th century, tomato has been valued for its flavor, nutritional content, and economic importance (Liu et al., 2022). According to FAO (2020), global production reached 182 million tons across 5.06 million hectares, with Asia accounting for more than one-third of this total.

Given its economic relevance, agronomic traits such as branching, inflorescence architecture, and fruit development have been intensively investigated, as they directly influence productivity. Moreover, tomato is widely employed as a model organism in genetic and molecular studies of disease resistance. However, the species remains susceptible to multiple biotic and abiotic stresses, including more than 200 pathogens that negatively affect fruit yield and quality (Adedayo et al., 2022).

Nematodes represent approximately 80% of belowground biomass and play essential ecological roles in nutrient cycling and soil microbial dynamics. Nevertheless, around 4,100 species are plant parasites, causing diseases of major economic impact. Among them, *Meloidogyne enterolobii* is one of the most aggressive root-knot nematodes, with a broad host range and a high potential for yield losses exceeding 20%. Its recent detection in Europe highlights its growing relevance as a global agricultural threat (Costa et al., 2025).

Root-knot nematode (RKN) infection affects not only root morphology but also crucial physiological processes such as photosynthesis. Photosynthetic efficiency, which can be monitored by chlorophyll content, is a sensitive indicator of biotic stress. Evidence shows that *Meloidogyne* infection significantly reduces chlorophyll

concentration and impairs growth parameters in host plants (Sikandar et al., 2024).

Plants respond to nematode attack through complex immune mechanisms. Defense is initiated by nematode chemotaxis toward the root, mediated by root exudates, which are recognized as nematode-associated molecular patterns (NAMPs). This recognition activates pattern-triggered immunity (PTI), characterized by gene expression, production of reactive oxygen species (ROS), and the establishment of physical barriers. However, nematodes secrete effectors that can suppress PTI, leading to effector-triggered susceptibility (ETS). Resistant plants can detect these effectors through resistance (R) genes, activating effector-triggered immunity (ETI), a faster and more specific response associated with incompatible interactions. Recent studies have identified secreted effectors from root-knot nematodes, including conserved pheromones that regulate nematode development, communication, and immune responses in plants (Costa et al., 2023; Costa et al., 2025).

Advances in molecular biology have fostered innovative strategies for developing resistant cultivars. Among the available tools, CRISPR/Cas9-mediated genome editing stands out due to its precision, efficiency, and broad applicability, overcoming limitations of conventional transgenic approaches. Derived from the adaptive immune systems of bacteria and archaea, CRISPR-Cas enables specific genome modifications through complexes formed between the Cas9 nuclease and a single-guide RNA (sgRNA), which direct accurate DNA cleavage (Sturme et al., 2022; Son, Park, 2022).

CRISPR/Cas applications go beyond loss-of-function mutations, enabling transcriptional activation by catalytically inactive Cas9 (dCas9) fused to transcriptional activators or by insertion of short transcriptional enhancers (STEs) into promoter regions (Yao et al., 2024). These strategies allow fine-tuned regulation of genes of interest, contributing to improved resistance to pathogens and enhanced crop performance.

Genes associated with ROS generation, and regulation have recently attracted attention in plant defense research. For instance, the E3 ligase PIRE was shown to regulate the stability of respiratory burst oxidase homologs (RBOHs), thereby modulating ROS production and playing a central role in tomato leaf defense. Specific editing of *PIRE* enhanced foliar resistance to pathogens without impairing root

interactions, making it a promising target for genetic improvement (Castro et al., 2025).

Managing *M. enterolobii* remains a critical agricultural challenge, particularly in tomato, where conventional sources of resistance have been overcome. Traditional control strategies rely heavily on chemical nematicides, which are costly, environmentally hazardous, and increasingly restricted by regulations. In this context, CRISPR-Cas-mediated genome editing represents a sustainable alternative with the potential to introduce precise modifications into key defense-related genes, conferring stable and durable resistance.

Based on this rationale, the present study focuses on cloning the catalase gene from *S. lycopersicum* using CRISPR/Cas9. This gene, previously associated with susceptibility of *Psidium spp.* to *M. enterolobii*, represents a strategic target for the development of resistant tomato cultivars, with the potential to reduce yield losses, minimize chemical dependence, and advance sustainable agricultural practices.

3.4.2 Materials and methods

3.4.2.1 Target Selection

The target species selected for this study was *Solanum lycopersicum*, based on its ploidy, life cycle, and susceptibility to genetic transformation. Genome editing was designed to be mediated by homology-directed repair (HDR) to introduce precise insertions or substitutions in genes related to resistance against Meloidogyne enterolobii. Strategic genomic regions, including coding sequences (CDS) and promoters, were selected considering potential gene overlaps, regulatory motifs, and chromatin structure to maximize editing efficiency and minimize off-target effects.

3.4.2.2 gRNA and Donor Strand Design

Homologous sequences in tomato were used as input for CRISPR guide RNA (gRNA) design using CRISPR-R 2.0 and Benchling to identify optimal target sites. Two gRNAs targeting the catalase gene were selected based on high predicted on-target efficiency and minimal off-target potential. Forward and reverse oligonucleotide primers for each guide were designed with standard cloning overhangs (ATTG for forward, AAAC for reverse).

Note: Detailed sequences of the target gene, homologous regions, and gRNAs are provided in Supplementary Material 1.

3.4.2.3 gRNA Validation

Oligonucleotide primers were received lyophilized and resuspended in sterile distilled water to 100 μM, then diluted 1:10 to 10 μM working solutions. Forward and reverse primers were annealed by mixing equal volumes and incubating at 94 °C for 20 minutes, followed by gradual cooling to room temperature. Annealed gRNAs were stored at 4 °C until further use.

Plasmid extraction, digestion, and PCR verification were conducted according to standard molecular cloning protocols. Plasmids were purified using the QIAprep Spin Miniprep kit, quantified via NanoDrop, and digested with the appropriate restriction enzyme. Agarose gel electrophoresis was performed to confirm digestion, and uncut DNA fragments were recovered using the Zymoclean Gel DNA Recovery Kit for subsequent ligation.

3.4.2.4 Vector Construction

Vector assembly was performed using T4 DNA ligase. Vector and insert DNAs were combined at a 1:3 molar ratio and incubated overnight at 16 °C. The ligation reaction was heat-inactivated at 65 °C for 10 minutes prior to transformation into chemically competent E. coli DH5α cells.

3.4.2.5 Transformation in *E. coli*

Chemically competent *E. coli* DH5α cells were prepared using the Zymo Research Mix & Go Kit, with minor modifications. Competent cells were incubated with ligation products on ice, followed by heat shock at 42 °C for 30–45 seconds. Cells were recovered in SOC medium at 37 °C for 1 hour with agitation and plated on selective LB agar. Successful transformation was confirmed by colony PCR, plasmid extraction, and sequencing.

LR Clonase reactions were performed for recombination of the pPZP200 and pCR3-EF vectors. Recombined constructs were transformed into E. coli DH5α, selected on spectinomycin-supplemented media, and verified by plasmid extraction,

agarose gel electrophoresis, and sequencing.

3.4.2.6 Transformation in *Agrobacterium tumefaciens*

Electrocompetent *Agrobacterium tumefaciens* strain EHA105 cells were transformed with either LR recombination products or purified plasmids via electroporation (1,500 V). Following transformation, cells were recovered in LB medium at 28 °C for 2 hours with agitation, plated on selective LB agar containing rifampicin and spectinomycin, and incubated at 28 °C for 1–2 days. Verified colonies were propagated in liquid LB with the same antibiotics and stored long-term in 50% glycerol at –80 °C.

Supplementary Material – Detailed Experimental Information

1. Target Gene and Homologous Sequences

Gene of interest: Catalase (*Eucalyptus grandis*)

>A0A059BXE1 A0A059BXE1_EUCGR Catalase OS=Eucalyptus grandis OX=71139 GN=EUGRSUZ_F03557 PE=3 SV=1
MDPHKYRPSSAFNTSFWTTNSGAPVWNNNSSLTVGSRGPILLEDYHLVEKLANFD
RERIPERVVHARGASAKGFFEVTHDISQLTCADFLRAPGVQTPVIVRFSTVIHERGS
PETLRDPRGFAVKFYTREGNFDLVGNNFPVFFVRDGMKFPDMVHALKPNPKSHIQ
ENWRIVDFFSHHPESLHMFTFLFDDIGIPQDYRHMEGSGVNTYTLINKAGKVHYVKF
HWKPTCGVKNLLEEEAIRVGGSNHSHATQDLYDSIAAGNYPEWKLFIQIIDPDHEDK
FDFDPLDVTKTWPEDILPLMPVGRLVLNRNIDNFFAENEQLAFCPSIVVPGVFYSDD
KLLQTRIFSYSDTQRHRLGPNYLQLPPNAPKCAHHNNHHEGFMNFMHRDEEINYFP
SRYDPVRHAERYPIPTAMLTGKREKTIIEKENNFKQPGERYRSWTPDRQERFICRW
VDALSDPRMRSAASGFHTGLRPTNLWVRN

BLAST analysis:
Protein sequence compared across Solanaceae species to identify conserved regions suitable for gRNA design.
Sequence similarity confirmed using NCBI BLAST (https://blast.ncbi.nlm.nih.gov/Blast.cgi).

Tomato homologous sequence:

GACCACCATATTTTTATTTTGGTAAACATGGTGTCAGTCCAAATGTACACGAATT
GAGTAATTAAGATTTTGTGGACTAGTTTTGCACCTGTCTTTGTGTATATATATATA
TATTGTTAGTGCTCTCCCAACAATTGAACTACTCCATAATTTTGTAAATGCTTAAG
TTATAATATAAGTGGAATAAATTATAGTGTTGTGATACTGGAAAAGTTGTTTTGTT

TTTTTAGGCATGGAAGCTCCACCACTATCGTCCGGCACCGGCGAAGCACAGTT
GCCGAGAAGAACCGGAGGCTGGATCACCTTCCCCTTCATCATAGGTCTCTTATA
TATTTGTGTGTCAATCTATGACCATGCATGATATGAAATGTGTAGTATTAAATATT
ATTTGTTTATATATATATGCAGCAACAACAACATGTTTGACCCTAGCATTTGGGG
GTTGGACAAGCAATCTTATTGTGTATCTGATTAAGGAATTTGATATGGAGAGTAT
TGATGCTGCTCAAATATATAATTTGGTTAATGGTGCTGGAAGCTTAATTCCTGTT
GTTGCGGCAATTATTGCTGACTCTTTTCTTGGTTGCTTCTCTATCATATGGATTTC
ATCCATCATCTCATTATTGGTACAAACTAATCTTTGTTTTGTTTCTATCCTAATAAT
ATAATGAGTCTACGCTCTATACTTTTTGGGTGAATACATTATTGTTGTATATGATT
ACATACTTTTTCTATCCAATTTATTATGTGGCACAATGGTGTTTAATTATTTTGTC
GCTTATACGTGTAGGGCACAATCCTTTTAGGTTTAACAGCGACGCTTGATTCTCT
AAGGCCTAAACCTTGTGAAGTTGGTTCAACTTCATGTACCCCTAAACCAAAAGTT
CAATTTGTACTACTCTATGCAGCTATAGTTCTGGCAACTCTGGGGAATGGCGGT
CTCCGATCAACGCTTTCAACAATGGGAGCCAACCAATTTGATAAACAAAAAGAT
GAAGGGATTTTCTTCAATTGGTTCTTTTTCTTCACTTATGGTTCATCTGTAGTAGC
AACAACAGCTATTGTCTATGTTGAAGATAACGTAAGCTGGAAAGCTGGATTTTTC
ATTTGTGTTGCAGCTAATGTACTTGGTTCAGCCATTTTTCTATTGGGGACCAGAT
ATTACACCAATTCTAAGCCAGAAGGGAGTCCTTTCACCAACTTGGCTCGTGTTG
TGGTTGCAAATATTAGGAAAAGGAAAGTGGCAATCTCATTCACTGGGCAACATTT
CTACCACGGACCTAAATCAACAAGTGTTGCGCCTTCAAAAACCTTCCGGTAATAT
ATATTGTATAACTATTACAAAAGATTACTCGTCTCTCTCCCATCTTCTTCCATGTG
TTTGGTATTCCAGATACAAGTAATAAATACATATAAATCTCACTGGTCTTTCTCAC
CAATCTTGCTTGCTTCTCTCTCTATTTTTATGTTAAAAATATAATTATCTAATTAAG
TGTAAAATATGTAAAAAAAAATATTAATTAGTGATAGAATATAATAGTATTTAAAAG
TATAAATGATAATAATGTATAAGATAGTGCACATGTCTTATTGTGTAGATTTTCCA
TATAATCTGGGACTGTAGCGTCACTTTTAAGTGTTTACTATGTCTTTGATCATGT
GCTTGGGTCATCCAGTCACTAATGTTTGTTTTATATTGTCTCAACTCTCAATGAT
GAATTACTATTAAGTAAATCTTGATATTAGTACTGTCTGTCGTGGAGCACTATATA
ATATATTATTAGTTTAGTACTAATAAATACTCTTTAAAAACAGTCTTTACATACTAG
GAATGTTATAATTATATACTATTTCGACGATGACTTTCTTAAGGCTGCTAAGTGAT
TTTTAAAATAAAAGTATCAGAGATTTCACGCCCACTCATGAGTTGTGCTTTTTTAC
TCACTGTTCAAATTGATCTTTTTTGGGGGGGGATTTACACTGATATTACTATTTTG
TCGGCGGATAGGATAGTGATGACACTCAAATTTGGGACTATTAATATCGTGTGA
AAGACTTATATATACTTTCATAATTAGATAATGGACACTTGATTTGCAAACAATTG
ATATACATACGATGTATGCGTTGAGTGTATGTATAATATTTATGTACAATTAGTAC
AAAATATACATTGTGTACTAAAATAGATGTAAATTCGTTTGATAATAAAAGTATTA
GTTTGTTTGTTTTCTTATTGATGCAGGTTTTTGAACCATGCAGCCATTAAAAGTGA
AGGCGATGTTAAACTAGATGGCTCAATAGCTAAGCCATGGAAACTTTGTTCAGT
CCAAGAAATTGAAGATTTCAAATCCTTAATTAAAATTTTACCACTATGGTCAAGTA
GTTTTTTTCTTGGCACAACAATTGGTGTACAAACAAGTTTGTCAATCCTTCAAGC
CTTAGCAATGGATCGTCACATAGGCCCCAATTTCCAAATCCCAGCTGGTTCTATA
TTGGTTTTTGTCATGGTCTCTACTGCTCTATTCCTCGCCCTGTTCGACAAATTTC
TATTTCCTACGTGGAAAAAATTGACTGGTAAATCACTTACGCCTCTCCAAAGAAT
TGGGGTTGGACACTTGATTAGTTTTGTGAGCATGGGTGTCTCAGCCTTAGTTGA
GTCAAAGAGGCTAAATGTAGCAAAATCCAATCAAGGTTCAAAGATTGTGCCTAT
GTCAGTGTTATGGCTTGTGCCGCAATTAGCCATTGTTGGTATTGCAGAGGCATT
TCATTTTCCAGGGCAAGTCACGTTCTATTACCAGGAATTTCCAATAACCTTAAAG
AACATGGCTACCGCGATGATTCAAGTGATTGTAGGGGTGTCATTTTACTTGACC

ACTGCTCTAATTGATGTTGTTAGAAGAACAACTACATGGTTACCAGGTAACATAA
ATAACGGAAGGCTGGACAATGTGTACTGGATATTAGTTGTAGGGGGAATATTGA
ACTTTGGTTACTATGTAACATGTGCTTGGTTTTACAATTATAAAACCATGAAGGAA
GTGGTGGATCATAGTGATTCTCCTTCTCATGAGTGATTAACGGCTCCAAAAGAA
GTCCCGTACCTAGTTATCTATGTAACACTCTGTTTGGATTATGGTTTCATAATGTA
TTGTATTCTACTGTATGGTAAATATAATATTCGGTAAGACCATATTG

2. gRNA and Primer Sequences

Selected gRNAs targeting catalase gene:

- Guide 1: TCGCCGGTGCCGGACGATAGTGG
- Guide 2: TCTCGGCAACTGTGCTTCGCCGG

Overhangs for cloning:

- Forward primers: ATTG + gRNA sequence
- Reverse primers: AAAC + reverse complement of gRNA sequence

Annealing of primers:

- 100 µM stock → 10 µM working solution (1:10 dilution in sterile water)
- Equal volumes of forward and reverse primers mixed, incubated at 94 °C for 20 min, gradual cooling to room temperature

3. Culture Media and Buffers

LB Medium (per liter):

- Tryptone: 10 g
- Yeast extract: 5 g
- NaCl: 10 g
- Agar (for solid medium): 15 g
- pH adjusted to 7.0 with NaOH

SOB Medium (per liter):

- Tryptone: 20 g
- Yeast extract: 5 g
- NaCl: 0.5 g
- KCl: 0.186 g
- $MgSO_4 \cdot 7H_2O$: 2.5 mM

SOC Medium: SOB + 20 mM glucose

Buffers for plasmid extraction (Qiagen):

- P1: 50 mM Tris-HCl, pH 8.0; 10 mM EDTA; RNase A
- P2: 200 mM NaOH, 1% SDS
- N3: 3 M potassium acetate, pH 5.5
- PE: 10 mM Tris-HCl, pH 7.5; 80% ethanol

Competent cell buffers (Zymo Research):

- Wash buffer 1×
- Competent buffer 1×

4. Ligation and Transformation Details

Ligation (T4 DNA Ligase):

- Vector DNA (~50 ng, ~4 kb)
- Insert DNA (~37.5 ng, ~1 kb)
- 1:3 molar ratio vector:insert
- Incubation: 16 °C overnight
- Enzyme inactivation: 65 °C, 10 min

Transformation into *E. coli* DH5α:

- Ice incubation: 30 min with DNA
- Heat shock: 42 °C, 30–45 s
- Recovery: SOC medium, 37 °C, 1 h, 100–200 rpm
- Plating: LB agar + antibiotic

LR Clonase recombination:

- pPZP200 vector: 1 µL
- pCR3-F plasmid: 1 µL
- LR Clonase enzyme: 1 µL

- TE buffer: 3 µL
- Incubation: room temperature, 1 h

Transformation into Agrobacterium tumefaciens EHA105:

- Electrocompetent cells: 100 µL
- DNA: 3 µL
- Electroporation: 1,500 V, ice-cold cuvette
- Recovery: LB medium, 28 °C, 2 h
- Plating: LB agar + rifampicin 100 µg/mL + spectinomycin 50 µg/mL

5. PCR and Agarose Gel Electrophoresis

PCR conditions:

- Initial denaturation: 95 °C, 5 mim
- 32 cycles: 95 °C, 20 s; 50 °C, 30 s; 72 °C, 60 s
- Final extension: 72 °C, 5 min

Master mix (20 µL):

- 2 µL 10× buffer
- 0.5 µL 10 mM dNTPs
- 0.5 µL forward primer (10 mM)
- 0.5 µL reverse primer (10 mM)
- 0.125 µL Taq polymerase
- Nuclease-free water to 20 µL
- Template DNA variable

Agarose gel (1%):

- 1.5 g agarose in 75 mL 1× TAE, microwaved
- Add 1.5 µL GelGreen dye
- Run at 100–110 V, 20–25 min

6. Notes on Troubleshooting

- Large plasmids may reduce transformation efficiency; electroporation may improve results.
- Verify antibiotic activity and DNA quality before transformation.
- Serial dilutions may help optimize colony density.
- Typical issues: “smiley gels”, DNA overload, or contamination affecting band migration.

References

ADEDAYO, A. A.; BABALOLA, O. O.; PRIGENT-COMBARET, C.; CRUZ, C.; STEFAN, M.; KUTU, F.; GLICK, B. R. The application of plant growth-promoting rhizobacteria in *Solanum lycopersicum* production in the agricultural system: a review. **PeerJ**, 2022.

CASTRO, B.; BAIK, S.; LI, T.; TANG, A.; AOUN, N.; BLUNDELL, A. C.; GOMEZ, M.; ZHANG, E.; CHO, M.; LOWE-POWER, T.; SIDDIQUE, S. Gene editing of the E3 ligase PIRE1 fine-tunes reactive oxygen species production for enhanced bacterial disease resistance in tomato. **The Plant Cell**, v. 37, n. 5, p. 1–16, 2025.

COSTA, S. N. DE O.; PASCHOA, R. P. DA; ALEXANDRINO, C. R.; CREMONEZ, P. M.; CASTRO, J. M. R. J. M. DA C. E; CUNHA, M. DA; SILVEIRA, V.; OLIVEIRA, A. E. A.; FERNANDES, K. V. S. *Psidium* defenses against *meloidogyne enterolobii*: proteomic and microscopic analysis of this plant-predator association. **Proteomics**, p. 1–11, 2025.

COSTA, S. N. DE O.; RIBEIRO, J. M.; CASTRO, J. M. DA C. E; FERNANDES, K. V. S. Tackling the plant parasitic nematode *Meloidogyne enterolobii*: Challenges and strategies for control in relevant crops. **Tropical Plant Pathology**, 2025.

COSTA, S. N. DE O.; SILVA, M. V. T. E.; RIBEIRO, J. M.; CASTRO, J. M. DA C. E.; MUZITANO, M. F.; COSTA, R. G. DA; OLIVEIRA, A. E. A.; FERNANDES, K. V. S.

Secondary metabolites related to the resistance of *Psidium* spp. against the nematode Meloidogyne enterolobii. **Heliyon**, v. 9, n. 7, p. 1–10, 2023.

FAO. **Food and Agriculture Organization of the United Nations**. Disponível em: <http://www.fao.org/home/en/>.

GUO, Congting et al. Off-target effects in CRISPR/Cas9 gene editing. Frontiers in Bioengineering and Biotechnology, v. 11, art. 1143157, 9 mar. 2023. DOI: 10.3389/fbioe.2023.1143157.

HASSAN, M.; ZHANG, Y.; YUAN, G.; DE, K.; CHEN, J. Construct design for CRISPR/Cas-based genome editing in plants. **Trends in Plant Science**, v. 26, n. 11, p. 1133–1152, 2021.

LIU, W.; LIU, K.; CHEN, D.; ZHANG, Z.; LI, B.; EL-MOGY, M. M.; TIAN, S.; CHEN, T. *Solanum lycopersicum*, a model plant for the studies in developmental biology, Stress Biology and Food Science. **Foods**, v. 11, n. 2402, 2022.

MOLINARI, H. B. C.; VIEIRA, L. R.; SILVA, N. V. E; PRADO, G. S.; FILHO, J. H. L. **Tecnologia CRISPR na edição genômica de plantas - Biotecnologia aplicada à agricultura**. Brasília, DF: Embrapa Agroenergia, 2020.

SIKANDAR, A.; WU, F.; HE, H.; MUHAMMAD, R.; ULLAH, K.; WU, H. Growth, Physiological, and biochemical variations in tomatoes after infection with different density levels of *Meloidogyne enterolobii* aatika. **Plants**, v. 13, n. 293, p. 1–10, 2024.

SON, Seungmin; PARK, Sang Ryeol. Challenges Facing CRISPR/Cas9-Based Genome Editing in Plants. Frontiers in Plant Science, v. 13, art. 902413, 18 maio 2022. DOI: 10.3389/fpls.2022.902413.

STURME, M. H. J.; BERG, J. P. VAN DER; BOUWMAN, L. M. S.; SCHRIJVER, A. DE; MAAGD, R. A. DE; KLETER, G. A.; WILDE, E. B. Occurrence and nature of off - target modifications by CRISPR-Cas genome editing in plants. **ACS Agricultural Science & Technology**, v. 2, p. 192–201, 2022.

TYAGI, Swati; KUMAR, Robin; KUMAR, Vivak; WON, So Youn; SHUKLA, Pratyoosh. Engineering disease resistant plants through CRISPR-Cas9 technology. GM Crops & Food, v. 12, n. 1, p. 125–144, 2021. DOI: 10.1080/21645698.2020.1831729.

YAO, Q.; SHEN, R.; SHAO, Y.; TIAN, Y.; HAN, P.; ZHANG, X.; ZHU, J.-K.; LU, Y. Efficient and multiplex gene upregulation in plants through CRISPR-Cas-mediated knockin of enhancers. **Molecular Plant**, v. 17, n. 9, p. 1472–1483, 2024.

UNIVERSITY OF CALIFORNIA, DAVIS

BERKELEY • DAVIS • IRVINE • LOS ANGELES • MERCED • RIVERSIDE • SAN DIEGO • SAN FRANCISCO SANTA BARBARA • SANTA CRUZ

DEPARTMENT OF ENTOMOLOGY AND NEMATOLOGY ONE
SHIELDS AVENUE COLLEGE OF AGRICULTURAL AND ENVIRONMENTAL SCIENCES
DAVIS, CA 95616 AGRICULTURAL EXPERIMENT STATION
TEL: (530) 752-0492
FAX: (530) 752-1537

Statement of Internship Period

To Whom It May Concern,

This is to certify that Sara Nállia O. Costa successfully completed an internship under my supervision in the Department of Entomology and Nematology at the University of California, Davis. The internship period extended from 06.01.2024 to 08.31.2024. During this time, Sara contributed to research projects related to plant-parasitic nematodes and gained experience in molecular and bioinformatics methodologies.

If further information is required, please feel free to contact me.

Sincerely,

Shahid Siddique,
Ph.D. Associate
Professor
Department of Entomology and Nematology
University of California, Davis

Shahid Siddique

Digitally signed by Shahid Siddique
Date: 2024.12.10 15:26:22
-08'00'

4. CONSIDERAÇÕES FINAIS

Os resultados deste estudo destacam o potencial das abordagens ômicas como ferramentas integradas e eficazes para a elucidação dos mecanismos de resistência de espécies do gênero *Psidium* ao nematoide-das-galhas *Meloidogyne enterolobii*. A aplicação conjunta de análises microscópicas, histoquímicas, transcriptômicas, proteômicas e metabolômicas possibilitou uma compreensão multiescalar do processo infeccioso, permitindo estabelecer correlações entre alterações estruturais e respostas moleculares e metabólicas específicas.

As análises morfofisiológicas evidenciaram diferenças na formação de galhas e no desenvolvimento radicular entre genótipos resistentes e suscetíveis, sugerindo a atuação de mecanismos anatômicos de defesa. Os estudos histoquímicos revelaram acúmulo diferencial de compostos fenólicos e lignina, associados à formação de barreiras físicas e químicas contra a penetração e migração do patógeno. No nível transcriptômico, foi observada a indução de genes relacionados à defesa, sinalização hormonal e resposta ao estresse oxidativo. A análise proteômica evidenciou proteínas envolvidas na degradação da parede celular do nematoide, no reforço estrutural da parede vegetal e em rotas antioxidantes. Complementarmente, os perfis metabolômicos indicaram acúmulo de metabólitos secundários bioativos, como flavonoides e terpenoides, reconhecidos por sua ação antimicrobiana e antiparasitária.

Entre os mecanismos de resistência identificados, o estresse oxidativo se destacou como resposta inicial crucial à infecção. A rápida produção de espécies reativas de oxigênio (EROs) funcionou como sinalizador para a ativação de processos de defesa, incluindo o reforço da parede celular, a morte celular programada e a indução de vias metabólicas secundárias. A atuação de enzimas antioxidantes, com ênfase na catalase, mostrou-se determinante para a manutenção do equilíbrio redox e para a efetividade da resposta defensiva, configurando-se como alvo promissor em estratégias biotecnológicas.

A identificação de genes, proteínas, metabólitos e vias metabólicas associados às respostas de defesa representa um avanço significativo para programas de melhoramento genético e aplicações em biotecnologia vegetal. A integração desses dados fornece uma visão abrangente dos mecanismos de resistência e subsidia o

desenvolvimento de cultivares de goiabeira mais resistentes a *M. enterolobii*. Tais resultados fortalecem estratégias sustentáveis e cientificamente embasadas para o manejo da cultura, promovendo avanços na interface entre biotecnologia vegetal, nematologia e fitopatologia.

REFERÊNCIAS

BRASIL. Instituto Brasileiro de Geografia e Estatística (IBGE). Tabela 1613: “Área destinada à colheita, área colhida, quantidade produzida, rendimento médio e valor da produção das lavouras permanentes, 1974-2023”. Sidra – Sistema IBGE de Recuperação Automática, Rio de Janeiro, 2023. Disponível em: https://sidra.ibge.gov.br/tabela/1613. Acesso em: 28 jun. 2025.

FOOD AND AGRICULTURE ORGANIZATION OF THE UNITED NATIONS (FAO). The State of Food Security and Nutrition in the World 2023. Rome: FAO, 2023. Disponível em: https://openknowledge.fao.org/items/445c9d27-b396-4126-96c9-50b335364d01. Acesso em: 28 jun. 2025.

GUO, C.; MA, X.; GAO, F.; GUO, Y. Off-target effects in CRISPR/Cas9 gene editing. Frontiers in Bioengineering and Biotechnology, v. 11, p. 1143157, 9 mar. 2023. Disponível em: https://doi.org/10.3389/fbioe.2023.1143157

HUYNH, H. D.; NARGOTRA, P.; WANG, H. D.; SHIEH, C.; LIU, Y.; KUO, C. Bioactive compounds from guava leaves (*Psidium guajava* L .): Characterization, biological activity, synergistic effects, and technological applications. Molecules, v. 30, n. 1278, 2025. Disponível em: https://doi.org/https://doi.org/ 10.3390/molecules30061278

KHAN, M. R.; POORNIMA, K.; SOMVANSHI, V. S.; WALIA, R. K. *Meloidogyne enterolobii*: a threat to guava (*Psidium guajava*) cultivation. Archives of Phytopathology and Plant Protection, v. 55, n. 17, p. 1961–1997, 2022. Disponível em: https://doi.org/10.1080/03235408.2022.2132623

KUMAR, M.; PATEL, M. K.; KUMAR, N.; BAJPAI, A. B.; SIDDIQUE, K. H. M. Metabolomics and molecular approaches reveal drought stress tolerance in plants. International Journal of Molecular Sciences, v. 22, n. 9108, 2021. Disponível em: https://doi.org/https://doi.org/ 10.3390/ijms22179108

LIU, C.; JULLIAN, V.; CHASSAGNE, F. Ethnobotany, phytochemistry, and biological activities of *Psidium guajava* in the treatment of diarrhea: a review. Frontiers in

Pharmacology, v. 15, p. 1–18, 2024. Disponível em: https://doi.org/10.3389/fphar.2024.1459066

MERGNER, J.; KUSTER, B. Plant proteome dynamics. Annual Review ofPlant Biology, v. 73, p. 67–92, 2022. Disponível em: https://doi.org/https://doi.org/10.1146/annurev-arplant-102620- 031308

PARK, H.; KIM, B.; KANG, Y.; KIM, W. Study on chemical composition and biological activity of *Psidium guajava* leaf extracts. Current issues in molecular biology, v. 46, p. 2133–2143, 2024. Disponível em: https://doi.org/10.3390/ cimb46030137

PATEL, M. K.; PANDEY, S.; KUMAR, M.; HAQUE, M. I.; PAL, S.; YADAV, N. S. Plants metabolome study: emerging tools and techniques. Plants, v. 10, n. 2409, p. 1–24, 2021. Disponível em: https://doi.org/https:// doi.org/10.3390/plants10112409

PHILBRICK, A. N.; ADHIKARI, T. B.; LOUWS, F. J.; GORNY, A. M. *Meloidogyne enterolobii*, a major threat to tomato production: current status and future prospects for its management. Frontiers in Plant Science, v. 11, n. November, p. 1–13, 2020. Disponível em: https://doi.org/10.3389/fpls.2020.606395

SALAM, U.; ULLAH, S.; TANG, Z.; ELATEEQ, A. A.; KHAN, Y.; KHAN, J.; KHAN, A.; ALI, S. Plant Metabolomics: An overview of the role of primary and secondary metabolites against different environmental stress factors. Life, v. 13, n. 706, p. 1–25, 2023. Disponível em: https://doi.org/https://doi.org/ 10.3390/life13030706

SCHOLZ, P. et al. Plasticity of the *Arabidopsis* leaf lipidome and proteome in response to pathogen infection and heat stress. Plant Physiology, v. 197, n. 2, p. 1–22, 2025. Disponível em: https://doi.org/10.1093/plphys/kiae274

SEYFFERTH, C.; RENEMA, J.; WENDRICH, J. R.; EEKHOUT, T.; SEURINCK, R.; VANDAMME, N.; BLOB, B.; SAEYS, Y.; HELARIUTTA, Y.; BIRNBAUM, K. D.; RYBEL, B. De. Advances and opportunities in single-cell transcriptomics for plant research. Annual Review of Plant Biology, v. 72, p. 847–866, 2021. Disponível em: https://doi.org/https://doi.org/10.1146/annurev-arplant-081720-010120

SHAW, R.; TIAN, X.; XU, J. Single-cell transcriptome analysis in plants: advances

and challenges. Molecular Plant, v. 14, n. 1, p. 115–126, 2020. Disponível em: https://doi.org/10.1016/j.molp.2020.10.012

SIKANDAR, A.; JIA, L.; WU, H.; YANG, S. *Meloidogyne enterolobii* risk to agriculture, its present status and future prospective for management. Frontiers in Plant Science, v. 13, n. January, p. 1–16, 2023. Disponível em: https://doi.org/10.3389/fpls.2022.1093657

SON, S.; PARK, S. R. Challenges facing CRISPR/Cas9 based genome editing in plants. Frontiers in Plant Science, v. 13, artigo 902413, 2022. Disponível em: https://doi.org/10.3389/fpls.2022.902413

TYAGI, S.; KUMAR, R.; KUMAR, V.; WON, S. Y.; SHUKLA, P. Engineering disease resistant plants through CRISPR-Cas9 technology. GM Crops & Food, v. 12, n. 1, p. 125–144, 2020. Disponível em: https://doi.org/10.1080/21645698.2020.1831729

USMAN, M.; BOKHARI, S. A. M.; FATIMA, B.; RASHID, B.; NADEEM, F.; SARWAR, M. B.; NAWAZ-UL-REHMAN, M. S.; SHAHID, M.; AYUB, C. M. Drought stress mitigating morphological, physiological, biochemical, and molecular responses of guava (*Psidium guajava* l .) cultivars. Frontiers in Plant Science, v. 13, 2022. Disponível em: https://doi.org/10.3389/fpls.2022.878616

YAN, S.; BHAWAL, R.; YIN, Z.; THANNHAUSER, T. W.; ZHANG, S. Recent advances in proteomics and metabolomics in plants. Molecular Horticulture, v. 2, n. 17, p. 1–38, 2022. Disponível em: https://doi.org/10.1186/s43897-022-00038-9

ANEXOS

Secondary metabolites related to the resistance of *Psidium* spp. against the nematode *Meloidogyne enterolobii*

Sara Nállia de Oliveira Costa [a], Marcos Vinicius Toledo e Silva [b], Juliana Martins Ribeiro [c], José Mauro da Cunha e Castro [c], Michelle Frazão Muzitano [b], Rafael Garrett da Costa [d], Antônia Elenir Amâncio Oliveira [a], Kátia Valevski Sales Fernandes [a]

[a] Laboratório de Química e Função de Proteínas e Peptídeos, Universidade Estadual do Norte Fluminense Darcy Ribeiro, Campos dos Goytacazes, Rio de Janeiro, Brazil.
[b] Laboratório de Produtos Bioativos, Universidade Federal do Rio de Janeiro, Macaé, Rio de Janeiro, Brazil.
[c] Empresa Brasileira de Pesquisa Agropecuária Semiárido, Petrolina, Pernambuco, Brazil.
[d] Laboratório de Metabolômica, Universidade Federal do Rio de Janeiro, Rio de Janeiro, Rio de Janeiro, Brazil.

Published in Heliyon (2023) - doi.org/10.1016/j.heliyon.2023.e17778

Abstract

The guava tree (*Psidium guajava*) is a tropical species native to South America and is recognized as the 11th most economically important fruit tree in Brazil. However, the presence of the nematode *Meloidogyne enterolobii* and the fungus *Fusarium solani* in the roots of guava plants leads to the development of root galls, causing significant damage. In contrast, the species *P. guineense* and *P. cattleianum* have been identified as resistant and immune to the nematode, respectively. In this study, the researchers aimed to compare the metabolomic profiles of infected and uninfected roots of P. guajava, *P. cattleianum*, and *P. guineense* using mass spectrometry coupled with liquid chromatography (LC-MS). The goal was to identify secondary metabolites that could potentially be utilized as biochemical resources for nematode control. The findings of the study demonstrated that the plant metabolism of all three species undergoes alterations in response to the phyto-pathogen inoculation. By employing

molecular networks, the researchers identified that the secondary metabolites affected by the infection, whether produced or suppressed, are primarily of a polar chemical nature. Further analysis of the database confirmed the polar nature of the regulated substances after infection, specifically hydrolysable tannins and lignans in *P. guineense* and *P. cattleianum.* Interestingly, a group of non-polar substances belonging to the terpene class was also identified in the resistant and immune species. This suggests that these terpenes may act as inhibitors of *M. enterolobii*, working as repellents or as molecules that can reduce oxidative stress during the infection process, thus enhancing the guava resistance to the nematode. Overall, this study provides valuable insights into the metabolic alterations occurring in different *Psidium* spp. in response to *M. enterolobii* infection. The identification of specific secondary metabolites, particularly terpenes, opens up new possibilities for developing effective strategies to control the nematode and enhance guava resistance.

Keywords: Guava tree; Meloidoginosis; Nematodes; Secondary metabolites.